International

WOCE

Newsletter

Number 34 ISSN 1029-1725 March 1999

IN THIS ISSUE

Published by the WOCE International Project Office at Southampton Oceanography Centre, UK

WOCE and CLIVAR

W. John Gould, Director, WOCE IPO and ICPO, Southampton Oceanography Centre, UK.
john.gould@soc.soton.ac.uk

First let me wish all of you a belated Happy 1999. Since our last issue a notable event has been the International CLIVAR Conference in Paris at the beginning of December. It took place almost exactly 10 years after the equivalent WOCE Conference and in the same UNESCO building in Paris but the world has changed a great deal over the intervening decade and CLIVAR and WOCE are in many ways very different. CLIVAR has a very much wider scientific remit than WOCE and since it is studying the extent to which climate is predictable it has a much more direct link to the non-research world. The general public and politicians are now much more aware of climate issues and their relevance to everyday life. This was perhaps reflected in the fact that although the meetings were of similar size CLIVAR attracted representatives of 63 countries and WOCE 39.

The statements made by countries at the CLIVAR Conference seem to show that ocean measurements – many of them to WOCE standard – will continue to document decadal scale variability in the open ocean and hence to enable us to put the 1990–1997 WOCE period in context. An area in which WOCE and CLIVAR have shared interests is in the matter of data handling. The WOCE data network of DACs and SACs has done an excellent job – a similar structure will be required by CLIVAR. A CLIVAR Data Task Team has been established and will work in the coming months to define CLIVAR's data system requirements and to assess how well these are met by existing (including WOCE) data systems. Their initial conclusions will be discussed at the WOCE/CLIVAR Data Products Committee Meeting in April.

WOCE data inventory and atlases

As we announced last year, a major task for the WOCE IPO and for the Data Information Unit is to compile a comprehensive and accurate inventory of WOCE observations. This is underway and for some parameters (e.g. current meter arrays and one-time hydrography) it is almost complete. In the coming months Penny Holliday in the WOCE IPO and Bert Thompson in the Data Information Unit in Delaware will be tracking down information on missing data sets and attempting to make the final inventory as complete as possible. Please help them if you can by supplying information and data.

Another activity that is now being actively discussed is the production of hard copy atlases of the WHP one-time data sets for each basin. Such atlases will be a tangible and obvious legacy of the biggest ocean survey ever undertaken.

Workshops

Scientific interpretation continues and the next of our WOCE Workshops on Tracers and their use in model validation has just been held in Bremen at the end of February. Almost 90 people attended and it was, by all accounts a stimulating meeting and I'd like to thank Wolfgang Roether, Scott Doney and their organising committee for their hard work. The next issue of the WOCE Newsletter (due for publication in June) will focus on results presented at the workshop. A second announcement for the next WOCE workshop, on the North Atlantic, is printed in this Newsletter.

This Newsletter

This issue of the Newsletter is largely devoted to articles about the use of neutrally buoyant floats. It is a topic close to my heart since I started my research career working for John Swallow – the inventor of the neutrally buoyant float. The early floats, tracked from ships and capable of being followed for only a matter of hours, had limited applications but nevertheless they were used to (accidentally) discover that the deep ocean was not quiescent but was populated by energetic mesoscale eddies. Now, thanks to the development for WOCE of the Autonomous Lagrangian Circulation Explorer (ALACE) and its later profiling (PALACE) version, we are now seriously contemplating a global network of such floats as a central element of the climate component of the Global Ocean Observing System. Float technology has come a long way and, for those who are interested, a concise history of float development can be found on the WOCE Float DAC at http://wfdac.whoi.edu/gould.htm

Finally I'd like to thank those who have returned the reader survey forms. About 35% of readers have responded and almost all of those tell us that they find the Newsletter "Very Useful". That is gratifying (unless, that is, the 65% who have not responded don't read it at all!). The responses are spread quite evenly across our international readership with almost all the larger countries returning between 30 and 40% of the cards. The exception is the USA – our biggest readership country with almost 300 readers from whom only 47 cards (15%) have been returned! We will be making a full analysis of the results over the coming weeks and if there are significant recommendations we will try to implement them. It's not too late to send in your reply if you haven't done so already.

Kinematics and Dynamics of the Deep Western Boundary Current Where it Crosses Under the Gulf Stream

Amy S. Bower and Heather D. Hunt, Woods Hole Oceanographic Institution, USA.
abower@whoi.edu

The Deep Western Boundary Current (DWBC) in the North Atlantic Ocean is the major conduit for the transport of recently ventilated water masses from northern latitudes toward the equator. In recent years, it has become increasingly apparent that there are selected locations along the western boundary where the DWBC interacts strongly with the ocean interior. One such site is located where the DWBC crosses under the Gulf Stream, near 36°N (the "crossover region"). Here the Gulf Stream flows across the continental slope into deep water, and the western limbs of the Northern Recirculation Gyre and the Worthington Gyre converge to form the deep Gulf Stream. The DWBC passes under the separating Gulf Stream between the western boundary and the recirculation gyres, and enters the subtropical regime. Thus two branches of the thermohaline circulation cross each other, setting up the potential for interactions with basin-scale consequences.

Following on the pioneering work of Swallow and Worthington (1961), who experimentally confirmed the existence of the DWBC using neutrally buoyant floats, we have undertaken a major experiment to further investigate the kinematics and dynamics of the DWBC in the crossover region. We deployed 30 RAFOS floats along hydrographic sections upstream (poleward) of the crossover region in 1994 and 1995, and tracked them acoustically for up to two years. Half of the floats were ballasted for the upper chlorofluorocarbon (CFC) maximum associated with Upper Labrador Sea Water (~800 m), and the other half for the deep CFC maximum that identifies Overflow Waters (OW) from the Nordic Seas (~3000 m). In this article, we will focus exclusively on the 3000-m floats. More details on the experiment can be found in Bower and Hunt (1998a, b) and Hunt and Bower (1998).

Fig. 1 shows the trajectories of the 3000-m floats, which were all launched between the 3500 and 4000 m isobaths (lower continental slope) between 55° and 70°W. The floats closely followed the slope equatorward until they reached the crossover region, where there was relatively more eddy motion, and a bifurcation in float pathways. One pathway continued equatorward along the continental slope,

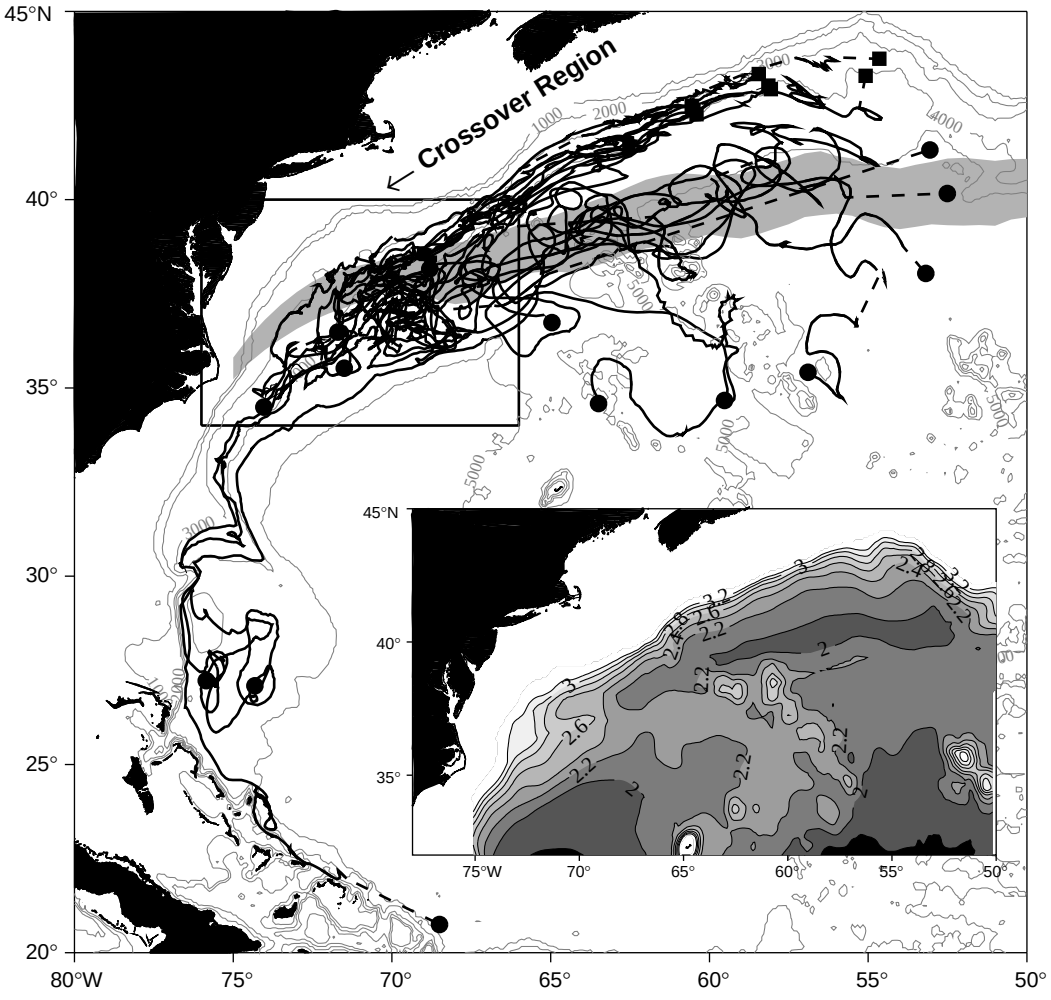

Figure 1. Trajectories of 14 RAFOS floats deployed at ~3000 m in the DWBC and tracked for up to two years. Tracks are superimposed on the meandering envelope of the Gulf Stream (one standard deviation around and eight-year mean path of the Gulf Stream at the surface). Launch and surface positions are indicated by squares and circles respectively. (Inset) Distribution of potential vorticity below the main thermocline showing ridge of high PV extending from the western boundary at about 37°N into the ocean interior. See text for details.

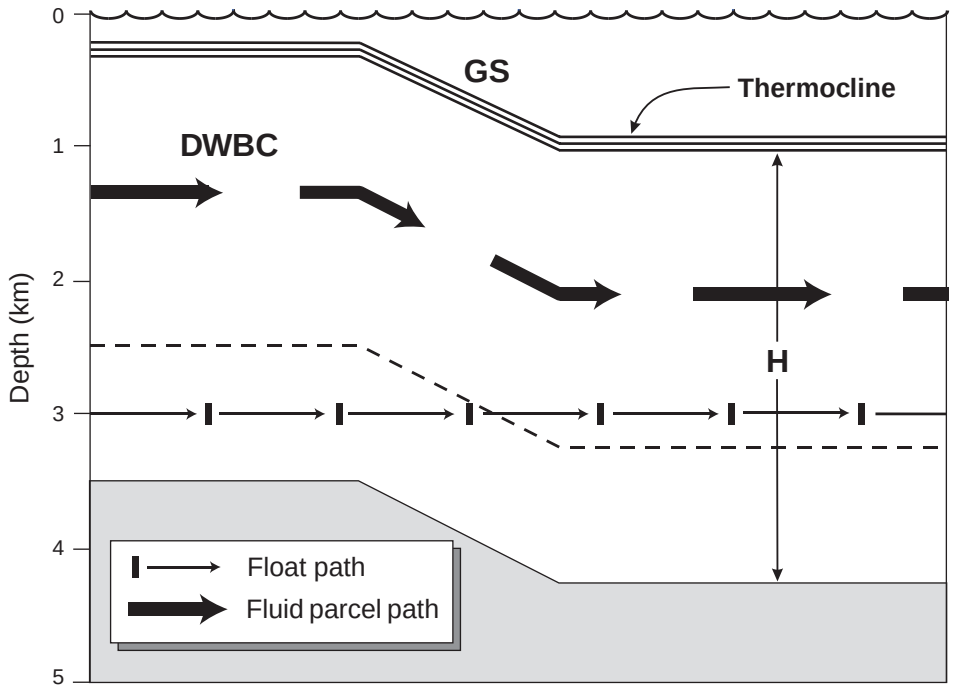

Figure 3. Schematic diagram showing how fluid parcels (bold arrows) and isobaric floats (thin arrows) in the DWBC cross under the Gulf Stream. Fluid parcels and floats in the DWBC flow into deeper water when they encounter the downward sloping main thermocline associated with the Gulf Stream. Note that this is a section along the fluid parcel pathway, not a cross-slope section.

and the other first followed the path of the Gulf Stream toward the east, then turned southward into the interior. At mission's end, about half of the floats were still close to the continental slope, and the other half in the ocean interior south of the Gulf Stream. One float drifted along the continental slope a distance of about 4000 km in two years, from 43° to 21°N, giving a mean along-boundary speed of about 6 cm/s. This represents a "fast track" for the spreading of OW along the western boundary.

The pathways of the DWBC revealed by the floats, including the bifurcation in the crossover region, are consistent with the deep potential vorticity distribution, shown in the Fig. 1 inset. Here we define potential vorticity as f/H, where H is the thickness of the layer bounded by the main thermocline and the sea floor, and the depth of the main thermocline has been taken to be uniform north of the mean Gulf Stream path, slopes down by 700 m over 100 km, and is again constant south of the stream. This represents the shape of the subtropical gyre, and is based on the climatological depth of the thermocline from hydrographic observations. A very similar approach was taken by Hogg and Stommel (1985) in their study of the Northern Recirculation Gyre.

The potential vorticity contours closely follow the bathymetry along the continental slope, except in the crossover region, where a ridge of high potential vorticity extends eastward from the slope due to the deepening thermocline associated with the Gulf Stream. Thus fluid parcels approaching the crossover from the north along the slope can continue equatorward along the slope or turn eastward into the interior while conserving potential vorticity.

Detailed analysis of the individual float tracks and their associated temperature records clearly reveals that the DWBC flows across the isobaths into deeper water as it passes under the Gulf Stream, thus conserving its potential vorticity. Fig. 2a (page 11) shows the track of one float, where daily positions are shown by coloured dots, and the colour indicates float temperature (blue → green → yellow indicates cold → warm). Fig. 2b-d show temperature, bottom depth and speed along the float track. This float approached the crossover region along the 3500–3700 m isobaths. Just as it crossed the path of the Gulf Stream (indicated by the star near where the float path intersects the solid red line), temperature increased abruptly from 2.25 to 2.85°C (Fig. 2b) and bottom depth along the float path increased from 3500 to 4000 m (Fig. 2c) over about 10 days. Subsequent fluctuations in float temperature and bottom depth, of both higher and lower frequencies, are well-correlated. This behaviour was characteristic of all the 3000-m float tracks in the crossover region.

These results are consistent with the two-layer steady model of the crossover introduced by Hogg and Stommel (1985), and are illustrated schematically in Fig. 3. The lower layer flow (DWBC, bold arrows) follows the bathymetry until it hits the downward sloping thermocline associated with the Gulf Stream. To conserve potential vorticity, the fluid parcels flow downslope as they cross under the Gulf Stream. Since the isobaric RAFOS floats are constrained to a pressure surface, they can only follow the horizontal component of fluid parcel motion (thin arrows). The deep isotherms slope down parallel to the thermocline so the float observes increasing temperature as the lower layer fluid parcels cross under the Gulf Stream. Once south of the Gulf Stream, both the float and fluid parcels in the lower layer follow a different, deeper isobath. In the absence of mixing and over the short meridional scales of the crossing, the new isobath will be deeper by the same amount that the thermocline deepens across the Gulf Stream. The total increase in bottom depth along the float track in Fig. 2 (November 1995–March 1996) was ~700 m This is about the same as the typical increase in depth of the main thermocline across the Gulf Stream. These float results thus show that the Gulf Stream has a strong impact on the DWBC in the crossover region, causing fluid parcels to be diverted downslope, and in some cases, into the ocean interior.

References

Bower, A. S., and H. D. Hunt, 1998a: Lagrangian observations of the Deep Western Boundary Current in the North Atlantic Ocean, Part 1, Large-scale pathways and spreading rates. J. Phys. Oceanogr., accepted.

Bower, A. S., and H. D. Hunt, 1998b: Lagrangian observations of the Deep Western Boundary Current in the North Atlantic Ocean, Part 2, The Gulf Stream-Deep Western Boundary Current crossover. J. Phys. Oceanogr., accepted.

Hunt, H. D., and A. S. Bower, 1998. Boundary Current Experiment I & II: RAFOS Float Data Report 1994–1997. Technical Report WHOI-98-06, 106 pp., Woods Hole Oceanographic Institution, MA,USA.

Hogg, N. G., and H. Stommel, 1985: On the relation between the deep circulation and the Gulf Stream. Deep-Sea Res., 32(10A), 1181–1193.

Swallow, J. C., and L. V. Worthington, 1961: An observation of a deep counter current in the Western North Atlantic. Deep-Sea Res., 8, 1–19.

Atlantic Deep Equatorial Jets and the Equatorial CFC Plume

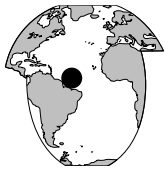

P. L. Richardson and D. M. Fratantoni, Department of Physical Oceanography, Woods Hole Oceanographic Institution, USA. prichardson@whoi.edu

SOFAR floats at a nominal depth of 1800 m were tracked for 3.7 years (1989–1992) in the vicinity of the western boundary and the equator of the Atlantic. Four floats launched near the equator plus two others that drifted southward to the equator in the deep western boundary current revealed swift zonal currents in the equatorial band 3°S–3°N (Fig. 1). Once in this band the floats tended to remain there drifting long distances zonally, except in the west where a direct connection to meridional flows along the boundary were observed.

When grouped together the 1800 m float trajectories revealed mean eastward flowing jets centred at 2°S and 2°N bounding a mean westward flow on the equator (Fig. 2). The equatorial currents (1°S–1°N) changed direction from eastward during the first six months of the experiment to mainly westward for the rest of the experiment. This is in agreement with results of moored current meter records which document long-period fluctuations at the equator (Fischer and Schott, 1997). The eastward jets are around two degrees wide, at least 500 m thick and have mean Lagrangian velocities of 3–5 cm/sec averaged over two degrees of latitude.

Time series of monthly eastward velocity in the jets suggest the presence of an annual cycle as also observed in the equatorial region by Hall et al. (1997) and Thierry et al. (1998). The best evidence for this is in the northern jet (1°N–3°N) where the range in seasonal variation (6.9 cm/sec) is larger than the mean (2.8 ±1.2 cm/sec). The mean Lagrangian velocities could possibly be a result of the Stokes drift of equatorial trapped waves as suggested by model simulations (Thompson and Kawase, 1993; Li et al., 1996).

The southern jet (2°S) coincides with a plume of CFC-rich water which extends from the western boundary across the Atlantic into the Gulf of Guinea. Although some maps of the near-equatorial plume show it centred at the equator (Weiss et al., 1985, 1989; Li et al., 1996) virtually all detailed sections across the equator in the mid-Atlantic reveal that the highest concentration of CFC is centred south of the equator near 2°S and a depth of 1600 m (Fig. 3).

The CFC plume is interpreted to have been advected eastward by the southern jet and to have been

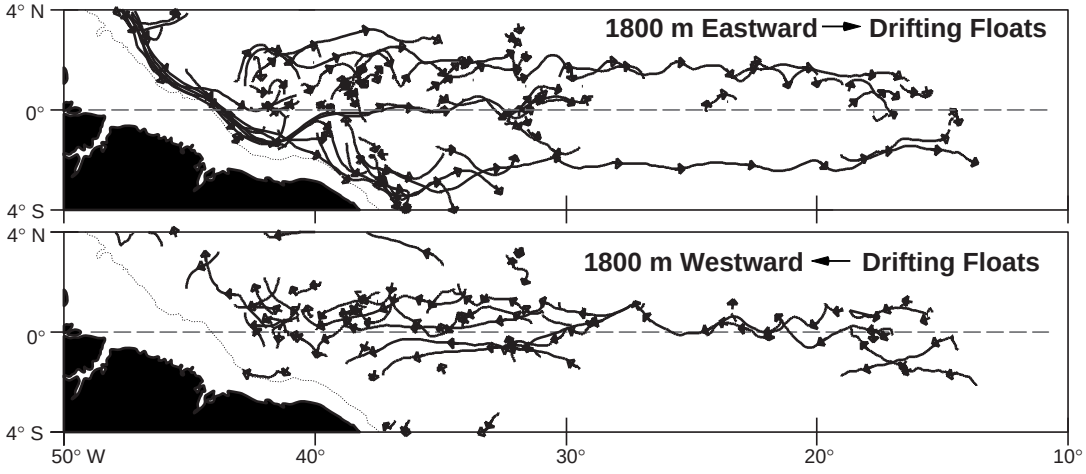

Figure 1. Near-equatorial 1800 m (nominal) float trajectories subdivided into eastward and westward drifting portions. Trajectories reveal eastward currents centred near 2°N and 2°S and westward currents centred near the equator, except for some eastward flow near the equator in the western region during the first six months of the experiment. Four other floats also drifted eastward near 2°S including two SOFAR floats near 800 m, one near 1125 m (Richardson and Fratantoni, 1999), and a RAFOS at 2500 m (Hogg and Owens, 1999). These imply a large ~1700 m vertical scale of the currents near 2°S.

gradually mixed within the equatorial band by exchanges among the series of zonal jets as observed by the floats. Several possible reasons why a CFC-rich plume coincides with the southern jet (2°S) but not the northern one (2°N) include

(1) the deep western boundary current recirculation, located north of the equator and west of the mid-Atlantic Ridge, which carries CFC-rich water away from the northern jet;

(2) the shape of the western boundary which appears to preferentially feed CFC-rich water into the southern jet; and

(3) the height and zonal offset of the mid-Atlantic Ridge which is a more formidable obstacle to the northern jet than to the southern jet (Fig. 3).

A more complete discussion of the results described here is given by Richardson and Fratantoni (1999). The SOFAR float data are available through the WOCE Subsurface Float Data Assembly Center in Woods Hole (http://wfdac.whoi.edu). This experiment was funded by the National Science Foundation grant OCE91-14656.

References

Andrié, C., J.-F. Ternon, M. J. Messias, L. Mémery, and B. Bourlès, 1999: Chlorofluoromethane distributions in the deep equatorial Atlantic during January–March 1993. Deep-Sea Res., in press.

Doney, S. C., J. L. Bullister, and R. Wanninkhof, 1998: Climatic variability in upper ocean ventilation diagnosed using chlorofluorocarbons. Geophys. Res. Lett., in press.

Fischer, J., and F. A. Schott, 1997: Seasonal transport variability of the deep western boundary current in the equatorial Atlantic. J. Geophys. Res., 102 (C13), 27751–27769.

Hall, M. M., M. S. McCartney, and J. A. Whitehead, 1997: Antarctic bottom water flux in the equatorial western Atlantic. J. Phys. Oceanogr., 27, 1903–1926.

Hogg, N. G., and W. B. Owens, 1999: Direct measurement of the deep circulation within the Brazil Basin. Deep-Sea Res., in press.

Li, X., P. Chang, and R. C. Pacanowski, 1996: A wave-induced stirring mechanism in the mid-depth equatorial ocean. J. Mar. Res., 54, 487–520.

Richardson, P. L., and D. M. Fratantoni, 1999: Float trajectories in the deep western boundary current and deep equatorial jets of the tropical Atlantic. Deep-Sea Res., in press.

Thierry, V., H. Mercier, and A. M. Treguier, 1998: Direct observations of low frequency fluctuations in the deep equatorial Atlantic. Ann. Geophys., II, Hydrol., Oceans and Atmos., 16 (suppl. 11), abstract p. C568.

Thompson, L., and W. Kawase, 1993: The nonlinear response of the equatorial ocean to oscillatory forcing. J. Mar. Res., 51, 467–496.

Weiss, R. F., J. L. Bullister, R. H. Gammon, and M. J. Warner, 1985: Atmospheric chlorofluoromethanes in the deep equatorial Atlantic. Nature, 314, 608–610.

Weiss, R. F., J. L. Bullister, F. A. Van Woy, M. J. Warner, P. K. Salameh, and R. H. Gammon, 1991: Transient tracers in the ocean, Tropical Atlantic Study: Chlorofluorocarbon measurements. SIO Reference 91-1, Scripps Institution of Oceanography, La Jolla, CA, USA.

Weiss, R. F., M. J. Warner, K. G. Harrison, and W. M. Smethie, 1989: Deep equatorial Atlantic chlorofluorocarbon distributions. Eos, Trans. AGU, 70, 1132.

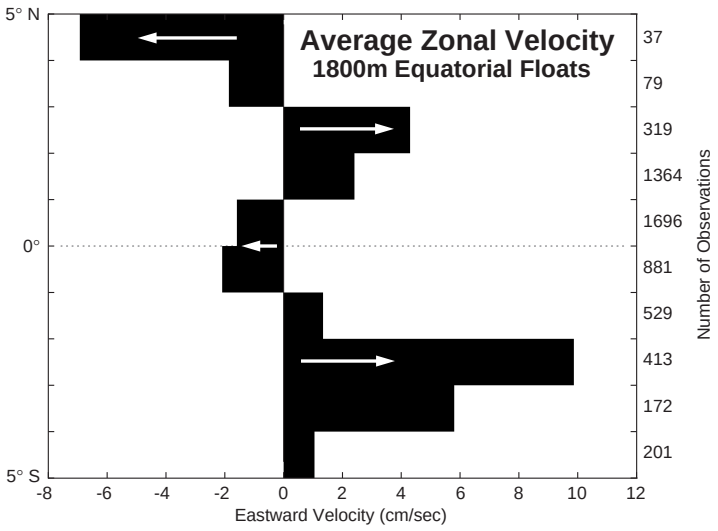

Figure 2. Mean eastward velocity of the near equatorial 1800 m floats in 1° latitude bands east of 40°W. Eastward equatorial jets are centred near 2°N and 2°S with mean westward flow centred on the equator, 1°S–1°N. One float recirculated north-westward causing the westward velocities there. The number of daily velocity observations in each band is listed near the right hand edge. The standard error of the mean velocities between 3°N–3°S is estimated to be ±2.6 cm/sec.

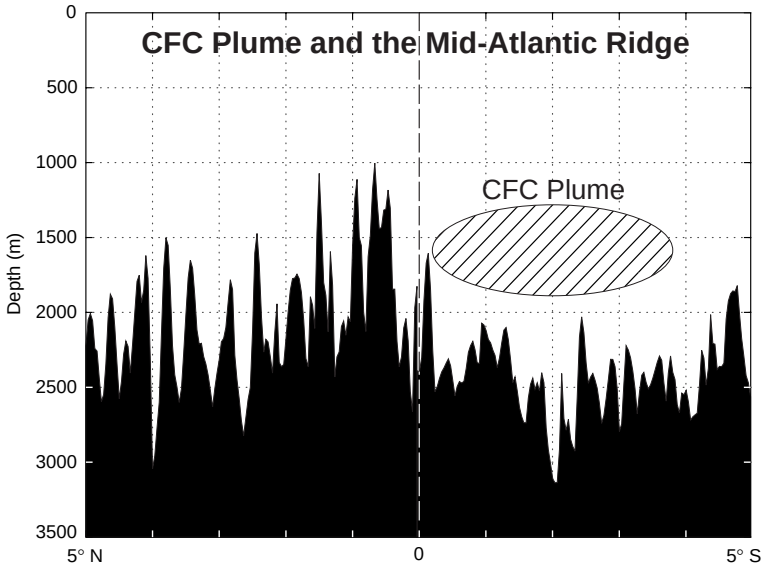

Figure 3. The CFC-plume in the mid-Atlantic is centred south of the equator near 2°S coinciding with the southern jet observed by floats. The limits of the plume shown here are averages of the highest CFC concentrations observed on five sections across the equator between 28°W and 4°W (Weiss et al., 1989, 1991; and pers. comm., Doney et al., 1998; Andrié et al., 1999). The overall thickness and width of the CFC plume are significantly larger than the region of highest CFC concentration shown here. At 25°W the CFC plume extended in depth from 1000 m to 2600 m and in latitude from 6°N to at least 5°S, the southern extent of the section (Doney et al., 1998). The sea floor depth profile shows the crest of the mid-Atlantic Ridge obtained from ETOP02 data. The ridge is roughly 500 m lower south of the equator and under the plume than north of the equator. The ridge crest north of the equator is centred near 31°W and west of the sections used to construct the plume shown here. The ridge crest south of the equator is centred near 12°W and is east of all sections except two at 4°W.

MARVOR Floats Reveal Intermediate Circulation in the Western Equatorial and Tropical South Atlantic (30°S to 5°N)

Michel Ollitrault, Laboratoire de Physique des Océans, IFREMER/Centre de Brest, France.
mollitra@ifremer.fr

At the beginning of the 1990s, the World Ocean Circulation Experiment (WOCE) float programme was undertaken to obtain the first direct current measurement of the general circulation at intermediate depth (around 1000 m). It was anticipated that "space-time" mean currents could be obtained with an accuracy of a few mm/s in the interior (and a few cm/s in boundary currents) with 5 float years of data within each of the thousand ($500\,km \times 500\,km$) square areas covering the world ocean. These estimates relied on assumed EKE values of $O(10\,cm^2\,s^{-2})$ and Lagrangian time scales of O(10 days) for the ocean interior at intermediate depths.

Besides the absolute mean currents at a given level, which permits in turn to convert geostrophic current shears into absolute currents from surface to bottom (via inverse modelling e.g.), float trajectories with a daily sampling can also be used to estimate (Taylor) horizontal diffusivities and to give insight in the (horizontal) mixing processes. While O(200 float years) had already been obtained in the North Atlantic with acoustic subsurface floats, during the pre WOCE years (from 1970 to 1990), it was not practical for the global mapping (which needs 5000 float years at least) to use the acoustic technology (whether the old SOFAR or the new RAFOS), because of financial and logistical unreasonable costs (for example it would have needed several hundreds of RAFOS sound sources).

That is why R. Davis (with D. Webb) developed the ALACE, which is not tracked acoustically, but surfaces regularly (every month e.g.) to be positioned by ARGOS (Davis et al., 1992). Striking new features of the general circulation have been resolved with the O(1000 float years) already gathered by the ALACEs in the Pacific and ACC (where, anyhow, it would be extremely difficult to track floats acoustically since the SOFAR channel outcrops).

With ALACE, however, the details of the water motions between 2 surfacings are lost, which does not allow one to measure the complete mesoscale spectrum (10 to 100 days) and to observe the horizontal mixing processes.

As a contribution to the WOCE float programme, and within the framework of the Deep Basin Experiment (DBE), A. Colin de Verdière and I decided at the end of the 1980s, on the above arguments, to conduct a float experiment named SAMBA in the Western equatorial and tropical South Atlantic with acoustic subsurface floats (to be named MARVOR but not yet developed at that time), near 800 m depth and located daily.

SAMBA (Sub-Antarctic motions in the Brazil basin) aims at obtaining the general circulation of Antarctic Intermediate water as it spreads equatorward in the South Atlantic and finally crosses the equator to leak into the North Atlantic.

MARVOR (which means sea horse in the old Celtic language of Brittany), was developed for this experiment at the beginning of the 1990s by IFREMER and TEKELEC, with the WOCE objectives in mind (Ollitrault et al., 1994). It is a 5-year life long, multi-cycle float (like the ALACE), but with an acoustic receiver (like the RAFOS). At each surfacing, MARVOR transmits the Times of Arrivals (TOAs) recorded during its last cycle at depth, via the system ARGOS, enabling then its tracking. MARVOR doesn't need any ballasting before launch because it actively controls its depth, which permits the float to follow isobars with a good accuracy.

98 MARVORs were launched between February 1994 and December 1997 (and two more in December 1998): these 100 floats initially covered (but unevenly unfortunately) the region between 30°S and 5°N west of the MAR axis (which is situated near 15°W). There are roughly 40 (500x500km) square areas in this region. Since the 100 MARVOR are programmed for a 5 year mission with cycles of 60 or 90-days submerged and 2 or 3 days at surface for data (TOAs, etc....) transmission, the WOCE goals of 5 float years should be reached within each square by the end of the experiment in 2002.

We briefly report here the results obtained at mid-experiment.

189 float years of data have been collected so far. A few floats escaped south of 35°S (not considered here) into the region between 50°S and 35°S (the Argentine Basin) well covered by ALACEs, which complement the WOCE global mapping for the South Atlantic. For their positioning, the SAMBA MARVORs share an array of more than 20 Webb Research Corp. (WRC) sound sources, laid in close co-operation by IfM/Kiel, IFREMER/Brest and WHOI. IfM/Kiel and WHOI have also launched RAFOS floats within the Brazil Basin in intermediate water and North Atlantic deep water respectively. Their data sets will later be combined with the SAMBA set, to meet the objectives of the DBE.

MARVOR technical results

Over a 4-year period and for the 49 MARVORs launched in 1994, Fig. 1 shows the percentage of the floats alive, and the various causes of failure: floats lost for unknown reasons, floats that surfaced prematurely on emergency schedule because of defective control of their hydraulic system so that they sank (deeper than 2750 dbar!), floats that grounded because their surface drift brought them over shoals and they never managed afterwards to reach their target depth (800 dbar). Serious difficulties were encountered with the hydraulic system on several floats.

On the other hand, half of the floats had a perfect behaviour, maintaining their depth to within a few tens of dbar (pressure is measured daily with an accuracy of ±10 dbar). Several modifications made since the beginning of the experiment to resolve this hydraulic problem have reduced the corresponding failure rate by a factor of 2 approximately.

Temperature is also measured daily with a platinum resistance thermometer with an accuracy of ±0.03°C (without any problems).

To obtain a good tracking accuracy, the speeds of sound between the float and the various sound sources, and the clock drifts of both the float and sources are needed (a 1 s error on time of propagation corresponds to a 1.5 km error on distance; a $5\,m\,s^{-1}$ error on speed of sound corresponds to a 1 s error on time at a 500 km distance). Since the float internal time is transmitted during surfacings and compared to UTC provided by ARGOS system, its clock drift is effectively monitored to a ±0.1 s accuracy (over the 2- or 3-month submerged periods, float clocks have perfect linear drifts).

This permits a precise tracking using least square minimisation over distances to the several sound sources listened, with a typical accuracy better than 5 km (sound source clock drifts are estimated in an inverse fashion and mean speeds of sound come from ray tracing through the Levitus climatological field).

Raw positions estimated daily, are finally filtered to suppress periods of less than 3 days and velocities are obtained after a cubic spline fit, yielding $O(1\,cm\,s^{-1})$ error on "instantaneous" velocities (there is generally only a few hundred of metres error on the displacement between 2 positions a few days apart (Ollitrault et al., 1995).

SAMBA scientific results

123 float-years of processed trajectories in the [750, 950] dbar interval are shown (red or green) in Fig. 2 (page 12), while the first 9 months of the 49 MARVORs launched in December 1997 are shown (pink) as submerged displacements over 90 days as they are not yet processed). Selected trajectories in green highlight the Intermediate (depth) Western Boundary Current (IWBC) flowing northward along the Brazilian continental slope. To complement the MARVOR trajectories in the Western Equatorial Atlantic 12.5 float-years of SOFAR data (Richardson and Schmitz, 1993) collected from February 1989 to February 1990 near 800-900 dbar have been added (yellow on Fig. 2).

Space-time averages of float velocities (Fig. 3) were obtained within 1° by 2° (latitude by longitude) areas to adapt to the predominantly zonal motions revealed by the floats. On the western boundary, however, averages were obtained over areas (generally 1° by 1°) matched to the continental slope bathymetry.

The Intermediate Western Boundary Current

South of the Vitoria-Trindade seamount chain (a topographic barrier stretching eastward at 21°S), the mean westward flow, which must probably be the return current of the South Atlantic subtropical anticyclonic gyre (this should be confirmed by the on-going KAPEX float experiment taking place in the Cape Basin east of the MAR) bifurcates near 27–28°S at the western boundary, to form a south-westward flow closing in the west the anticyclonic gyre circuit and a comparatively very narrow IWBC flowing northward, stuck to the continental slope, which transports AAIW from the subtropical gyre to the equatorial region: all the floats launched near 22.5°S, 33°W were later entrained within the IWBC, whereas only half for those launched near 26.5°S, 36°W. Contrary to Wüst's scheme (1995) no mean northward flow is observed on the western boundary between the confluence zone (near 40°S) and this so-called "Santos-Rio" bifurcation (Boebel et al,, 1997).

The presence of the northward-flowing IWBC is observed permanently and continuously from 27°S to 2°S. Mean speeds are of the order of $25\,cm\,s^{-1}$ (daily speeds may reach $50\,cm\,s^{-1}$) and the jet width is about 30 km, implying a 4 Sv transport if we assume a 500 m thickness (600 to 1100 dbar) for intermediate water. Under favourable conditions a water particle using the IWBC conveyor, and starting at 27°S may reach the equator in O(1 year)! The journey will not usually be so fast because of the frequent recirculations observed south of 21°S and of the unstable character of the IWBC jets pouring out through the holes of the Vitoria Trindade (20°S) chain into the tropical region north of it.

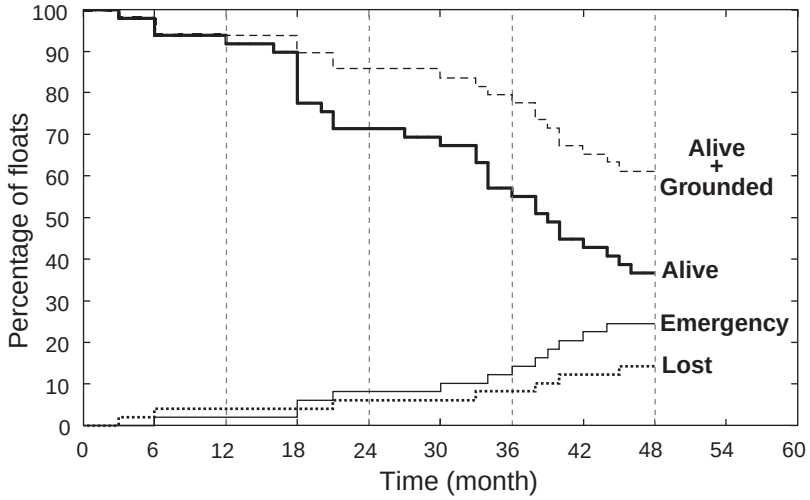

Figure 1. Survival and failure rates of the 49 MARVORs deployed in 1994. After 4 years, 37% of the floats are still alive and working well, 24% have surfaced on emergency, 24% have grounded and 15% were lost (for unknown reasons).

The tropical/subequatorial region

In the tropical/subequatorial region (between 5°S and 21°S) floats in the IWBC are often detrained into the interior, showing how intermediate water of subtropical origin may be injected into the tropical interior (there are also some exchanges along 21°S and east of 35°W between eastward flowing floats at 19–20°S and westward flowing floats at 21–22°S).

The western tropical interior of the Brazil Basin is a region of weak mean currents (mean speed is less than $1\,cm\,s^{-1}$, east of 35°W). With the data at hand (75 years) no cyclonic gyre (as shown by Reid, 1989, for example) has yet been seen although the error on the mean is $O(5\,mm\,s^{-1})$. Rather there is a diffusive regime with homogeneous turbulence (EKE is $10-15\,cm^2\,s^{-2}$ in the middle of the basin).

A band of high EKE ($\geq 50\,cm^2\,s^{-2}$) is present all along the western boundary, from the Santos-Rio bifurcation to 5°S and is clearly related to the recirculations and entrainments/detrainments into/out of the IWBC. It seems correlated as well with bottom topography or roughness (see the Fig. 6 of the poster presented at Halifax by O. Boebel, P. Richardson and myself, available on the web at woceipo/wconf/posters).

Taking advantage of the absence of a mean flow in the tropical region, the isotropic horizontal diffusivity over the 600 km diameter region centred at 16°S, 30°W is estimated at $600\,m^2\,s^{-1}$ with a Lagrangian time scale of 5.5 days. Zonal motions however are more diffusive than meridional ones, and isotropic diffusion is probably not relevant. It is difficult to estimate correctly this anisotropy, even with the 13.6 float-years that we have, which may be due in part to the down-gradient flux of floats eastward where their concentration vanishes (Davis, 1991).

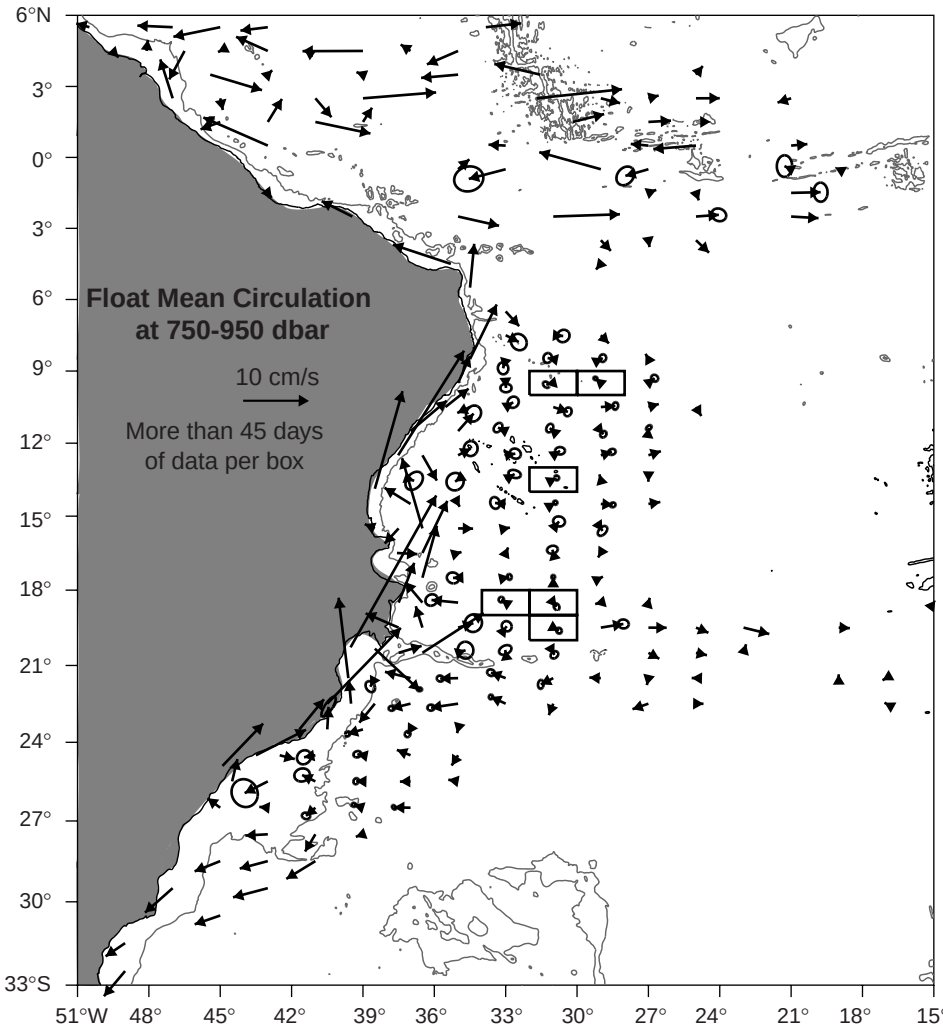

Figure 3. Space-time averages and estimated errors of 750–950 dbar float velocities. Averaging areas are 1° latitude by 2° longitude except at the western boundary where they are generally 1° squares. The centre of the averaging area is at the base of the vector. Only vectors obtained with more than 45 float days are given. Error ellipses (axes are $\sqrt{2}$ times standard deviations of averaging error along the principal axes, thus probability is 0.63) are given only if more than 180 float days, and averaging areas are shown only if more than 720 float days (for these, averaging error is of a few mm/s).

Approaching the equatorial zone, the floats turned westward at the "Nordeste" corner (5°S, 35°W) of South America. Thus the route of intermediate water seems to occur wholly within the IWBC north of Cape São Roque, possibly merging with the overlying westward flowing North Brazil UnderCurrent (NBUC).

Western Equatorial Atlantic

Before flowing northward into the North Atlantic, intermediate water circulates through an equatorial current system of swift zonal jets. Although only data between 750 and 950 dbar is used in this study, there will be some inappropriate vertical averaging in the float mean circulation, because equatorial currents do show vertical shears (see the Pegasus profile on Fig. 7 in Richardson and Schmitz, 1993).

The Southern Intermediate Counter Current (SICC) flowing eastward near 2°S–3°S is well resolved between 37°W and 17°W, and stands out as a permanent feature.

In contrast, the Northern Intermediate Counter Current (NICC) flowing eastward is only marginally resolved near 2°N–3°N, because of seasonal reversals.

Although the mean currents indicate a coherent symmetrical circulation scheme with a westward Equatorial Intermediate Current (EIC), not enough data is available to resolve the seasonal and interannual fluctuations which are important.

Only one MARVOR crossed the equator northward at the western boundary. It seems more likely that Intermediate Water reaching 2–3°S within the IWBC/NBUC turns eastward within the SICC. We may conjecture it may be entrained afterwards within the EIC, east of 25°W to finally come back near the western boundary before escaping in the North Atlantic, unless it recirculates once more via the NICC-EIC or SICC-EIC loops. Definitely more data is needed to describe the equatorial transfer of AAIW to the North Atlantic.

References

Boebel, O., C. Schmid, and W. Zenk, 1997: Flow and recirculation of Antarctic Intermediate Water across the Rio Grande Rise. J. Geophys. Res., 102(C9), 20967–20986.

Davis, R. E., 1991: Observing the general circulation with floats. Deep-Sea Res., 38(suppl. 1), 531–571.

Davis, R. E., D. C. Webb, L. A. Regier, and J. Dufour, 1992: The autonomous Lagrangian circulation explorer (ALACE). J. Atmos. Oceanic Technol., 9(3), 264–285.

Ollitrault, M., G. Loaëc, and C. Dumortier, 1994: MARVOR: a multi-cycle RAFOS float. Sea Technol., 35(2), 39–44.

Ollitrault, M., Y. Auffret, N. Cortès, C. Hémon, P. Jégou, S. Le Reste, G. Loaëc, and J. P. Rannou, 1995: The SAMBA experiment, Vol. 1, SAMBA 1 Lagrangian and CTD data. Repères Ocean, 12, IFREMER, 488 pp.

Reid, J. L., 1989: On the total geostrophic circulation of the South Atlantic Ocean: Flow patterns, tracers and transports. Prog. Oceanogr., 23, 149–244.

Richardson, P. L., and W. J. Schmitz, 1993: Deep cross-equatorial flow in the Atlantic measured with SOFAR floats. J. Geophys. Res., 98(C5), 8371-8387.

Wüst, G., 1935: Schichtung und Zirkulation des Atlantischen Ozeans. Die Stratosphäre. Wiss. Erg. Deut. Atl. Exp. Meteor, 1925–1927, 6.

Float Observations Showing the Equatorial Crossing of Antarctic Intermediate Water in the Western Pacific

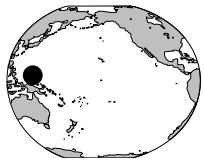

Walter Zenk, Gerold Siedler (presently at Instituto Canario de Ciencias Marinas, Spain), and Jürgen Holfort, Institut für Meereskunde, Kiel, Germany; and Olaf Boebel, University of Cape Town, South Africa. wzenk@ifm.uni-kiel.de

The German research vessel Sonne operated in the western tropical Pacific from 10 October–19 November 1996. The areas of investigation covered the East Mariana Basin and the Caroline Basins (Siedler and Zenk, 1997). Among the topics of study was the spreading of the Antarctic Intermediate Water (AAIW) at about 800 m depth in the Bismarck Sea and along the equator west of 150°E (Fig. 1).

The flow path of this low-salinity and oxygen-rich watermass in the Salomon and Bismarck Seas has been well documented by Tsuchiya (1991) on the basis of the Western Equatorial Pacific Ocean Studies (WEPOCS). The AAIW is entrained into the subtropical gyre in the eastern Pacific after being formed at the Antarctic Convergence Zone and is then advected eastward with the Antarctic Circumpolar Current. It circulates anticyclonically and on its westward path reaches the eastern approaches of Australia north of New Zealand. From the Coral Sea it spreads northward into the Solomon Sea, avoiding the shallow Torres Strait. AAIW reaches the Bismarck Sea through Vitiaz Strait separating New Britain from New Guinea. An additional, though smaller portion of AAIW may enter the Bismarck Sea through St. George's Channel between New Britain and New Ireland (Lindstrom et al., 1990).

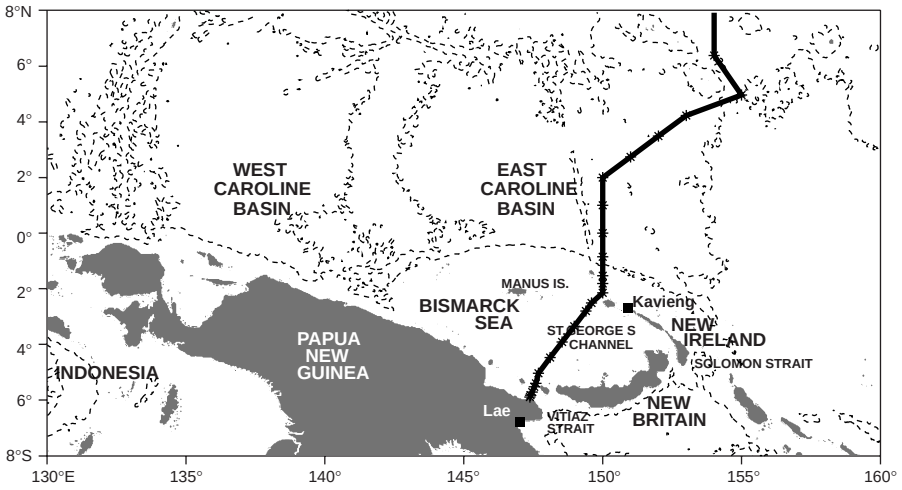

Figure 1. Map of the western equatorial Pacific with the 3500 m isobath showing the prime deep sea basins. FS Sonne operated in the region from October–November 1996. Position of the CTD section in Fig. 2 is shown by the thick line.

Further results from WEPOCS have revealed the permanent existence of the New Guinea Coastal Undercurrent (Tsuchiya et al., 1989). Although the upper core of this intermediate western boundary current advects high-salinity water (S>35.5) at only 200 m depth, its downward extension reaches well into AAIW range at 800 m (S <1.50).

Fig. 2 shows the salinity distribution along 150°E from the

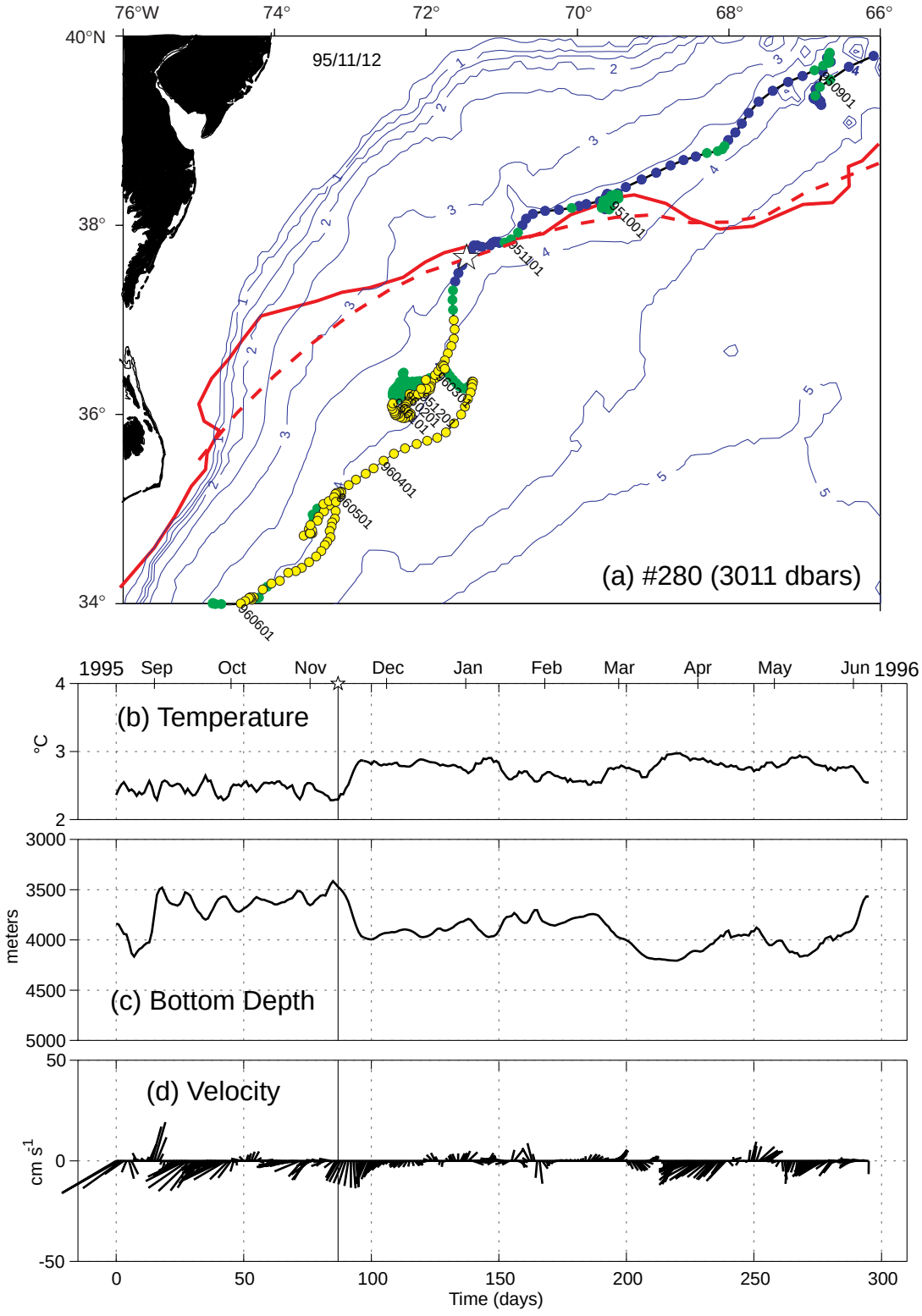

Bower and Hunt, page 3, *Figure 2. (a) Track of representative 3000-m RAFOS float in the crossover region, with simultaneous records of (b) temperature, (c) bottom depth and (d) speed along the float track. Colour coding along float track indicates temperature (blue → yellow indicates cold → warm). The location where the float began to cross under the Gulf Stream is indicated by a star in (a), and by vertical lines in (b-d). Solid red line indicates Gulf Stream path at the time of the float crossing, and the dashed red line the long-term mean path of the Gulf Stream.*

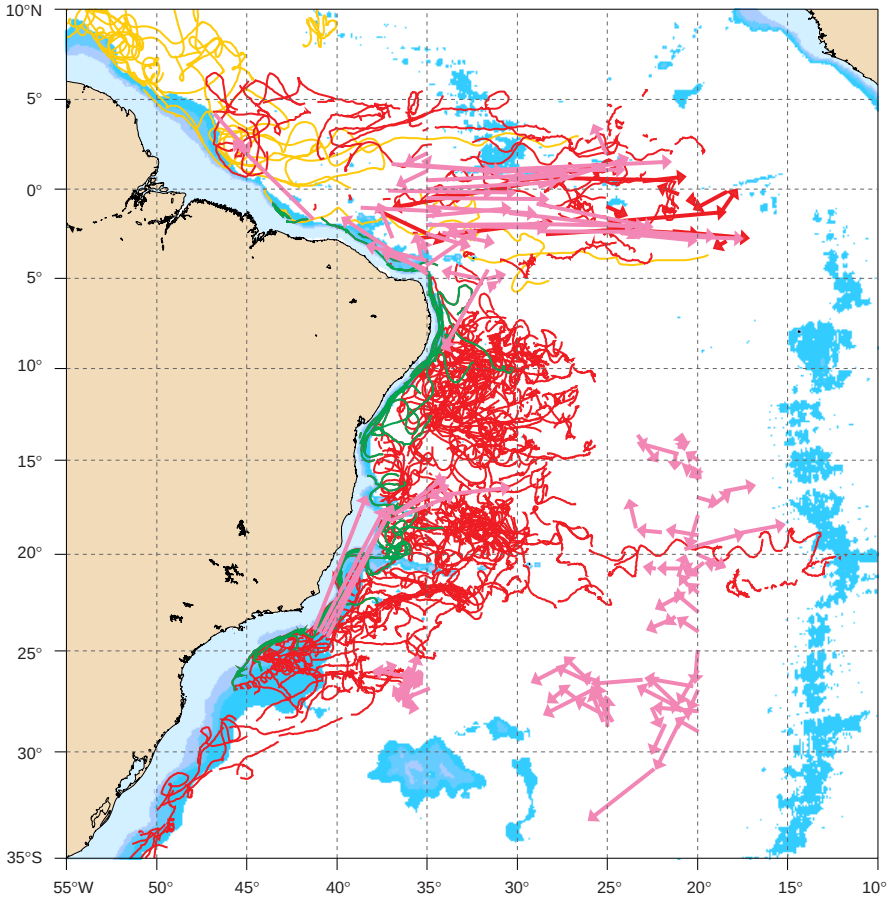

Ollitrault, page 7, *Figure 2. Trajectories (red or green) of 49 MARVORs launched in 1994 in intermediate water near 800 m totalling 122.5 float years. 90-day submerged displacements (pink) of 49 MARVORs launched in 1997 (44 years of data have been obtained but tracking of these floats have not yet been done). Trajectories (yellow) of 13 SOFARs near 800–900 m totalling 12.5 float years from Richardson and Schmitz, 1993.*

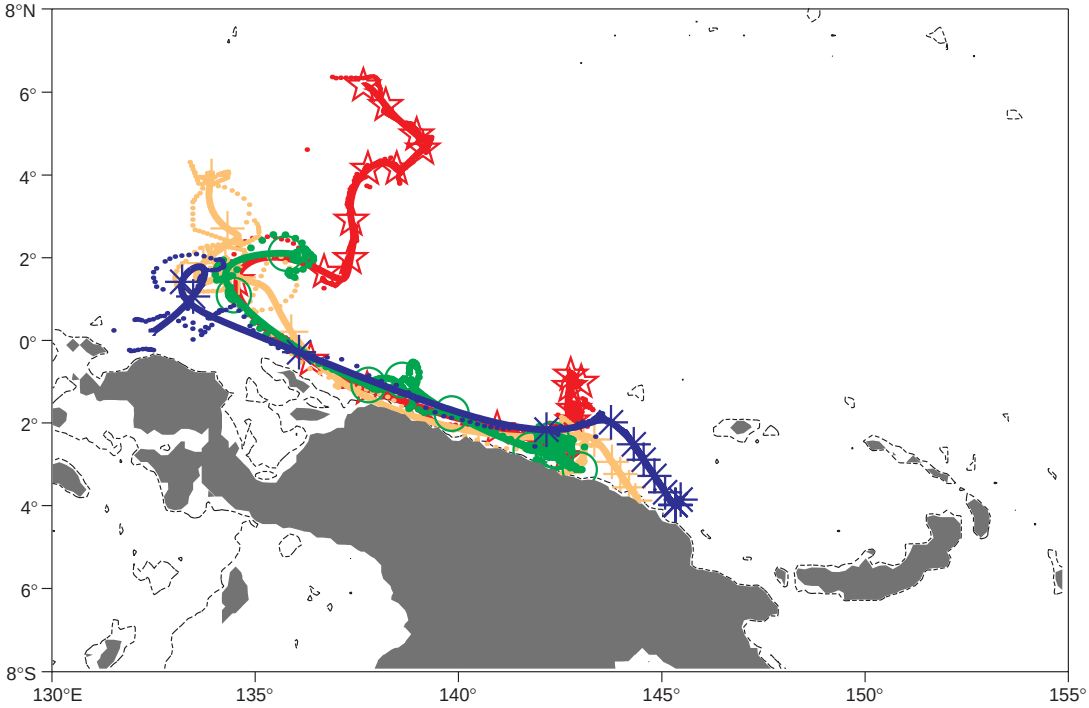

Zenk et al, page 10, *Figure 4 . Low-passed filtered trajectories of four RAFOS floats (blue asterisks = float #188, red stars = #191, green circles = #189 and yellow pluses = 190).released between 143°E and 145°E north of the coast of Papua-New Guinea. Large markers are set at 30 day intervals, smaller markers give unfiltered positions in daily intervals. Also shown is the 200 m isobath. All four floats were advected by the deep New Guinea Coastal Undercurrent up to 135°E, where they crossed the equator. North of the equator a more eddy-intensified region was observed.*

SONNE section in November 1996. On the southern side we recognise the two salinity extrema of the coastal undercurrent system between 200 and 900 m. The low-salinity core at 10°N originates from the North Pacific Intermediate Water. Concurrent Doppler observations of the coastal undercurrent from the Sonne cruise show narrow bands of O(<20 km) width with speed values exceeding 80 cm s^{-1} at the western exit of the Vitiaz Strait. While the indicated current flows parallel to the slope off Papua-New Guinea at 200 m depth, its core widens by a factor of 2 and the speed decreases in the central Bismarck Sea (Siedler and Zenk, 1997).

A key subject of our work in the tropical Pacific deals with the connection of the deep-reaching New Guinea Coastal Undercurrent and the equatorial current system. The fate of the AAIW core, while passing the equator, is highly questionable. Does it overshoot the equator and then reflect eastward to become an integral part of the equatorial current system? What is its impact on the Indonesian Throughflow? Will the deepest part of the New Guinea Coastal Undercurrent end up in the Mindanao Undercurrent, i.e. in a deep source region of the Kuroshio (Lucas et al., 1996)?

To answer such questions the Sonne cruise 113 contained a Lagrangian observational component. Four sound sources were moored from November 1996 to January 1998. They enabled the necessary insonification for 20 RAFOS floats which were launched in the East Mariana and the Caroline Basins. In Fig. 3 we show a displacement diagram as it was obtained at the end of the experiment in the spring of 1998. With an exception at 2°N all floats which were launched along 143°E drifted westward towards the Philippine Basin. Their mean speed at the 800 m level amounts to O(2.0) cm s^{-1}. The 2°N float (#193) apparently was caught by the deep reaching eastward flowing Northern South Equatorial Countercurrent. It surfaced 4020 km farther east from its launch point after a mission length of 538 days, corresponding to a mean speed of 8.7 cm s^{-1}.

In Fig. 4 (page 12) we display preliminary trajectories from the southern floats which were seeded along 143°E in the western Bismarck Sea between 1° and 3°S. Initially they all stalled for several weeks during winter 1996/97. Superimposed on their initial stagnation phase was a feeble southerly drift. Slowly approaching the continental slope the floats' advection merged with the deep New Guinea Coastal Undercurrent. According to recent WOCE current meter observations in the Vitiaz Strait (Murray et al., 1995) we had expected a more persistent drift at our float seeding sites. However, the lateral scale of

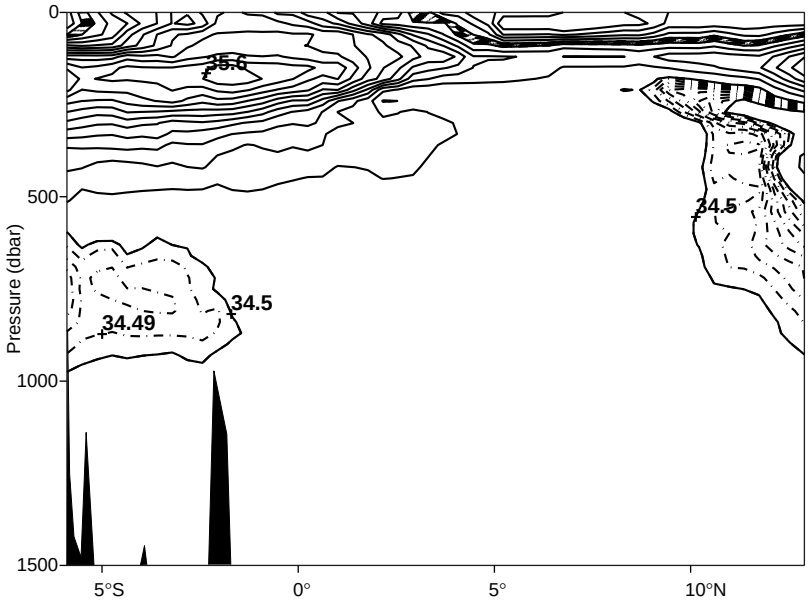

Figure 2. Salinity section along a nominal longitude of 150°E. Contour interval is 0.1 for solid lines. Salinities between 34.4 and 34.5 are contoured every 0.01 with dash-dotted lines. Two modes of intermediate waters are visible. South of the equator Antarctic Intermediate Water at about 800 dbar leans upon the northern slope of New Guinea. The salinity minimum between 300–700 dbar north of 9°N represents North Pacific Intermediate Water.

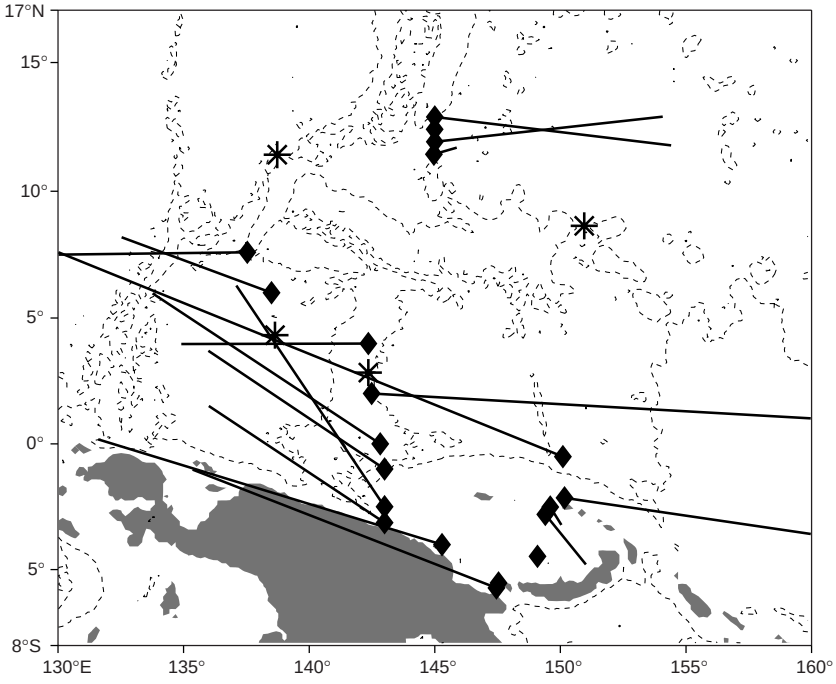

Figure 3. Map of the western equatorial Pacific with the 3500 m isobath showing the displacement vectors of the 20 RAFOS floats launched during Sonne cruise 133. Launch positions are marked with diamonds. Positions of the four sound sources are marked by asterisks.

the undercurrent appears to be more confined to the immediate slope region then the hydrography in Fig. 2 suggests. All four floats swiftly crossed the equator without any sign of reversal towards the east. Such a uniform easterly displacement was observed at about 2°N after the equator had been crossed. Float #189 stopped its mission in a region which potentially could have been occupied by the Northern Subsurface Equatorial Countercurrent. Its two companions #190 and #191 drifted slightly northward and were finally advected towards the western side of the Caroline Basins.

It was the purpose of this note to inform the WOCE/AIMS community about our modest Lagrangian data set from the tropical western Pacific. Based on direct current observations, it demonstrates on an eddy-resolving scale the equatorial crossing of Antarctic Intermediate Water in the Pacific. We look forward to joint analyses with other investigators with current observations from this exciting area. The region might play a key role in preconditioning of the Indonesian Throughflow with its global impact.

Acknowledgement

This work has been funded by a grant from Bundesministerium für Bildung, Wissenschaft, Forschung und Technologie, Bonn (Fkz GO113A).

References

Lindstrom, E., J. Butt, R. Lukas, and S. Godfrey, 1990: The flow through Vitiaz Strait and St. George's Channel, Papua New Guinea. In: The physical oceanography of Sea Straits, L. J. Pratt (ed.), pp. 171–189, Kluwer.

Lucas, R., Y. Yamagata, and J. P. McCreary, 1996: Pacific low-latitude western boundary currents and the Indonesian throughflow. J. Geophys. Res., 101(C5), 12209–12216.

Murray, S., E. Lindstrom, J. Kindle, and E. Weeks, 1995: Transport through the Vitiaz Strait. WOCE Notes, 7, 21–23.

Siedler, G., and W. Zenk, 1997: Untersuchungen zu den tiefen Wassermassen und planktologische Beobachtungen im tropischen Westpazifik während der Sonne-Fahrt Nr. 113 (TROPAC). 288, 129 pp., Ber. Inst. Meeresk., Kiel, Germany.

Tsuchiya, M., 1991: Flow path of Antarctic Intermediate Water in the western equatorial South Pacific. Deep-Sea Res., 38(suppl.), S273–S279.

Tsuchiya, M., R. Lukas, R. A. Fine, E. Firing, and E. Lindstrom, 1989: Source waters of the Pacific Equatorial Undercurrent. Prog. Oceanogr., 23, 101–147.

First Float Trajectories from KAPEX

Olaf Boebel and Johann Lutjeharms, University of Cape Town, South Africa; and Tom Rossby, University of Rhode Island, USA. oboebel@physci.uct.ac.za

From a global perspective, the import of saline and warm water from the Indian Ocean into the South Atlantic is of major importance since it is believed to be a key factor for the conditioning of the North Atlantic for deep convective overturning at high latitudes (Gordon et al., 1992). The Indian Ocean inflow within the SE Atlantic is thought to follow partly the Benguela Current (Fig. 1), which feeds into the South Equatorial Current and to finally cross the equator to the North (Garzoli and Gordon, 1996; Garzoli et al., 1996). However, the upper flow patterns seem to differ significantly from the flow at intermediate depth which is oriented more zonally than near the surface (Boebel et al., 1997b). This results in major uncertainties regarding the cross-equatorial transport of intermediate water of Indian Ocean origin. Does it flow north to the equator and contribute directly to the export of heat from the South Atlantic into the North Atlantic, or is it entrained into the subtropical gyre and, at least partly, re-expelled into the Indian Ocean within the eastward continuation of the South Atlantic Current? Or, as a third alternative, does it indirectly flow north by modifying the properties of South Atlantic Intermediate Water, which flows north to the equator in a narrow intermediate western boundary current?

These issues depend upon the dynamics and structure of the inter-ocean exchange between the Indian and Atlantic Oceans which has long been a matter of considerable debate (Gordon et al., 1992; Rintoul, 1991). While the import of Indian Ocean surface waters into the Atlantic through Agulhas Rings and to a lesser extent Agulhas filaments is well documented by satellite infra-red images and satellite altimetry (Lutjeharms, 1996), the inter-ocean fluxes at intermediate and greater depths remain much less understood. This is largely due to the substantial temporal and spatial variability of the flow field at the Agulhas Retroflection which, combined with remoteness of the region, hamper the collection of high-resolution, quasi-synoptic hydrographic data to adequate depth. Similarly, the conditions that trigger the spawning of Agulhas Rings have yet to be understood. Crucial aspects such as the

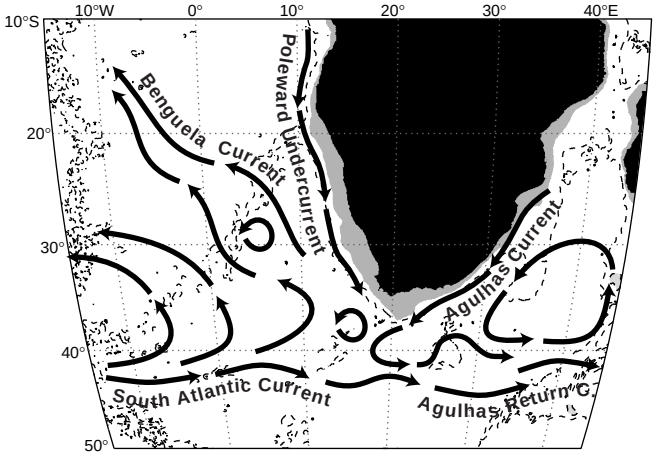

Figure 1. Map of area and major current systems on a McBryde-Thomas flat-polar parabolic projection. The continent is black and the area up to 1000 m lightly shaded. The 3000 m isobath is indicated by a dashed line.

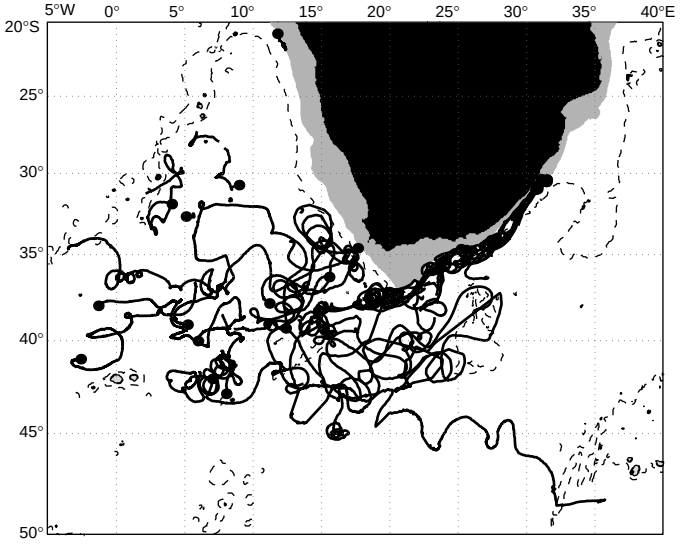

Figure 2. Currently available RAFOS float trajectories. Topography as in Fig. 1 but on a Mercator projection.

evolution of the velocity and density structure along the Agulhas Current (AC), the downstream propagation of large meanders, called Natal Pulses (Lutjeharms, 1996), and the interaction of the current with the shelf have yet to be studied, particularly at depths below the upper layer.

To address these questions, an international co-operative programme, KAPEX (Kap der guten Hoffnung Experimente), was organised to deploy and acoustically track a total of 124 RAFOS floats in order to observe pathways, speed and transport of the thermocline and intermediate depth layers. The floats are ballasted for intermediate depths and have been launched in the major currents of the area namely the Agulhas, Benguela and South Atlantic Current (Fig. 1). Float missions cover the period between March 1997 and November 1999, with some float missions lasting as long as 2 years. Floats launched into the South Atlantic Current (SAC) at various locations near 40°S are intended to reveal the expected bifurcation of the SAC into a northward branch and the eastward continuation along and south of the Agulhas Return Current. Along 30°S a line of floats across the Benguela Current (BC) are expected to depict the downstream fate of intermediate water: do they follow the near-surface flow directly to the equator or do they turn west as part of the Subtropical Gyre? Finally, to study the intermediate component of the Agulhas Current and its fate in the Agulhas Retroflection, floats were launched into this western boundary current on two occasions upstream of the Agulhas Retroflection region.

First trajectories

By now, 21 of a total of 47 floats launched in the Agulhas experiment have surfaced with only one no-show. From a total of 35 floats launched into the South Atlantic Current and its vicinity 25 floats surfaced with 2 no-shows and 8 are due in early 1999. Most of the floats (29 of 30) of the Benguela experiment are not due before the summer of 1999. We are hence approximately half way through the experimental phase of KAPEX. In this note we give a first report on the data obtained to date. Fig. 2 shows all currently available trajectories, with the respective launch positions indicated by dots at the beginning of each. More detailed studies will be presented by members of the KAPEX science team[1] in May 1999 at the 31st International Liege Colloquium.

In the plot (Fig. 2) the Agulhas Current is revealed by the tracks of 17 trajectories along the 1000 m isobath. Even west of 20°E, where the Agulhas Current detaches from the Agulhas Bank and the shelf, a clear boundary between Agulhas and Atlantic waters in the Cape Basin is distinct. This boundary apparently reaches from the tip of the Agulhas Bank to the eastern outposts of the Agulhas Ridge. Viewed from the South Atlantic Current, the Agulhas Ridge might act as a wedge, leading to the bifurcation of SAC water into an north-eastward branch that feeds into the Cape Basin and an eastward continuation of the SAC into the Indian Ocean. However, strong mesoscale activity has thus far precluded clear evidence for such a separation scheme. One float, for example, was launched just off Cape Town and, flowing south-westward around the Agulhas Ridge and then east with the Agulhas Return Current, drifted against the expected mean flow field of the region.

The Agulhas Current

While the cruises[2] focusing on the Benguela and South Atlantic Current were already described in detail in earlier publications (Boebel et al., 1998; Boebel et al., 1997a), the float deployments in the Agulhas Current occurred later. Hence we use this opportunity for a brief description of the two Agulhas Current launch cruises. The first deployment took place on 4 December 1997. To launch the floats a local oil spill combat vessel, SA Kuswag V, was chartered and used offshore of Port Elizabeth. Designed for coastal missions it lacks many of the navigational luxuries of dedicated research vessels, particularly a deep reaching echo sounder. We hence relied on a XBT sections to position the floats relative to the Current. The XBT section was taken while the vessel headed offshore and the floats where subsequently launched on the way back. The 17 floats were launched in groups of 9, 4 and 4 at three sites of differing lateral position. Launch sites were characterised as follows: where the 10°C isotherm reached 400 m, 300 m and 200 m. All three sites were probably on the cyclonic side of the current. The isopycnal RAFOS floats were ballasted for 2 density surfaces, namely $26.8\sigma_\theta$ and $27.2\sigma_\theta$. The shallower level is representative of the upper thermocline whereas the lower level was chosen to trace the

1 The KAPEX science team consists of: Olaf Boebel (UCT, South Africa), Chris Duncombe Rae (SFRI, South Africa), Silvia Garzoli (NOAA/AOML, USA), Johann Lutjeharms (UCT, South Africa), Phil Richardson (WHOI, USA), Tom Rossby (URI, USA), Claudia Schmid (NOAA/AOML, USA) and Walter Zenk (IfM-Kiel, Germany)

2 For a detailed description of the cruises and the KAPEX project please access http://triton.sea.uct.ac.za.

fate of Antarctic Intermediate and Red Sea Water. The floats listened for sound sources and sampled pressure, temperature and, as a novelty, oxygen twice a day at 12 h intervals.

Approximately 6 months later, on 13 June 1998, the second series of 15 floats were launched from SA Kuswag I, a sister vessel of SA Kuswag V. The floats were again launched in 3 groups of 5 floats, with launch sites defined by the 10°C isotherm at 600 m, 450 m and 350 m. Again, all 3 launch positions were believed to be on the current's cyclonic side. The launch sites were located somewhat south of Durban along a line perpendicular to the shelf break near 31°S, in close vicinity of the WOCE I5 (Beal and Bryden, 1997) and other hydrographic sections (Beal and Bryden, 1998; Toole and Warren, 1993). A third and final series of 15 floats was launched 2 days later on 15 June 1998. This time the launch sites were located about 100 km to the northeast of the previous ones, right off Durban. The launch sites of the three floats groups were defined by the 10°C isotherm at 700 m, 620 m and 520 m and, due to the lesser slope of the shelf, located much farther offshore than on the previous occasion. With the current centre at intermediate depth roughly defined by the location where the 10°C isotherm reaches 750 m, the launch position at 700 m was believed to be close to the maximum velocity core, whereas the positions at 620 m and 520 m are on the current's cyclonic side. Similar to the first set of floats launched off Port Elizabeth, half of the Durban floats were ballasted for the $26.8\sigma_\theta$ and the other half for the $27.2\sigma_\theta$ level.

The trajectories of 10 Durban floats are depicted in Fig. 3. These floats had been ballasted for the deeper $27.2\sigma_\theta$ level and drifted around 800 m depth. However, the depth of the $27.2\sigma_\theta$ level depends strongly on the cross-stream position and floats drift at 500–600 m depth closer to shore and at 1100-1200 m depth farther offshore. The resulting isopycnal slope of 500 m in 50 km is compatible with the sloping ratio of 1:100 as observed by Beal and Bryden (1996) in hydrographic data during the Agulhas Current Experiment (ACE).

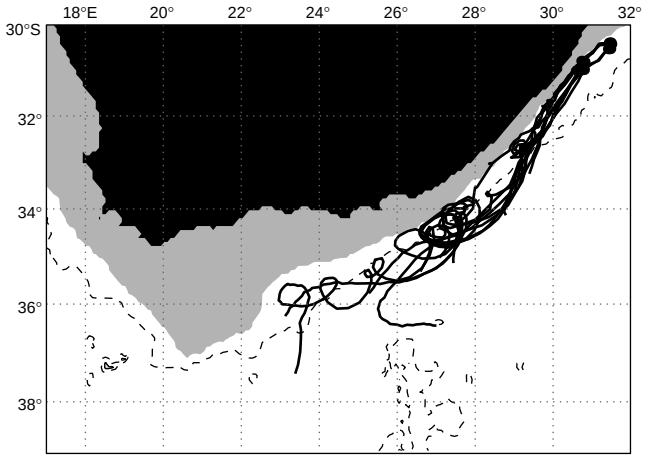

Figure 3. Summary plot of "Durban" float trajectories. Topography as in Fig. 2.

Float velocities observed near 31°S at 800 to 1000 m depth are around 60 to 80 cm s^{-1} southwestward along the shelf. Some of the floats were located very close to the 1000 m isobath while others floated at about 25 km farther offshore. On this occasion we could not observe an inshore countercurrent as reported by Beal and Bryden (Beal and Bryden, 1997). Even though the countercurrent might have existed at greater depth during the passage of the floats, the high velocities observed by the floats suggest that the zero velocity isoline lies at least 200 m deeper than the float observations. This estimate assumes a similar geostrophic shear as depicted by Beal and Bryden in their lowered ADCP section (Beal and Bryden, 1998).

Farther downstream however, the floats get repeatedly trapped in cyclonic recirculations on the inshore side of the current. The size of the 3 cyclonic loops observed increases with downstream distance, culminating in a ~100 km loop near 34.5°S (Fig. 4, page 21). Southwestward velocities, probably near the maximum velocity core of the AC, range between 60 to 80 cm s^{-1}, whereas the "inshore" (near the 1000 m isobath) countercurrent flows north-eastward at 40 to 60 cm s^{-1}. For single floats, the speed difference between successive along- and counter current segments amount to 20 cm s^{-1} in most cases.

A possible explanation of this flow pattern is the development of meanders that contain cyclonic circulations between mender crests as they propagate downstream. In a crude model, if the cell advects southwestward at 10 cm s^{-1} (the phase speed), the superposition of this feature with the Agulhas Current would lead to a particle speed difference of 20 cm s^{-1} across the cell. An independent estimate of the meander's phase speed can be derived from the translation of the estimated centre of rotation (Fig. 4), which yields 12 cm s^{-1} between yeardays 178 and 190 of 1998. A second confirmation of this value can be obtained from satellite infrared imagery, where in fact a cell of cooler water is observed in SST images at this very location and advected at about 10 cm s^{-1}. The meander could have been triggered by a Natal Pulse (Lutjeharms, 1996) that originates further upstream, but further analysis is needed. The increasing perturbation of the laminar along-current flow indicates a growing instability with downstream distance.

Similar repeated cyclonic recirculations at intervals of 50 to 100 km (Fig. 5) are depicted by the group of floats launched off Port Elizabeth half a year earlier. At the $27.2\sigma_\theta$ level, the group of 4 floats measured along stream velocities of around 80 cm s^{-1}, while the particle velocity is below 10 cm s^{-1} during the cusp-like trajectory segments. These values apply to the point where the float trajectories detach from the continental shelf at the tip of the Agulhas Bank. Here the cyclonic loops instantly become larger and more circular, with diameters ranging from 20 to 80 km and along current speeds reduced to about 50 cm s^{-1}. The floats move together on a nearly westward course, with a slight southward component leading them to the easternmost outposts of the Agulhas Ridge. There topographic steering appears to deflect the thrust of the current to the south, where mesoscale cyclonic motion prevails. The floats

reach their westernmost position near 13.5°E, which is near the extreme position of the Agulhas Current Retroflection surface expression (Lutjeharms, 1996).

Apparently, most of the floats remain trapped within the cyclonic part of the current. This is probably a manifestation of the strong potential vorticity front observed between 400 m and 1400 m (Beal and Bryden, 1998) near the current core. Bower and Lozier (1994) found analogous results for the Gulf Stream where the front however extends and sharpens towards the surface. This continuation appears absent in the case of the AC, since, in addition to the hydrographic evidence provided by Beal and Bryden (1998), a group of 3 shallow floats set at the $26.8\sigma_\theta$ level exhibit trajectories crossing the current, which leads to an early expulsion of these floats from the current core (Fig. 2, trajectories that leave the AC to the south between 20°E and 25°E). Based on satellite altimetry, this site was recently suggested by Matano et al. (1998) as the location of an early retroflection of the AC to occur during austral summer.

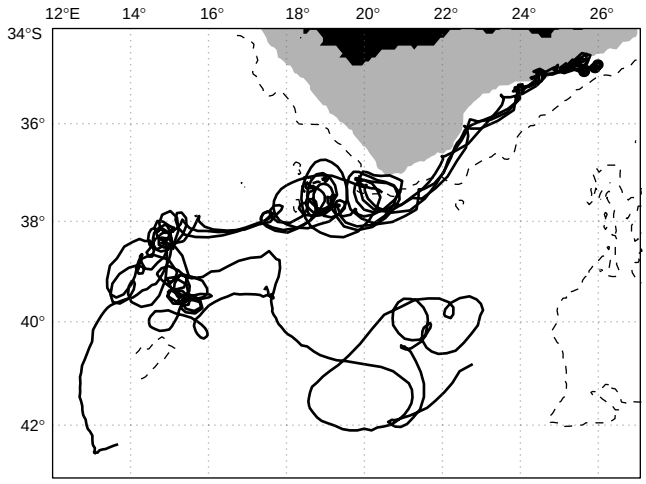

Figure 5. "Port Elizabeth" float trajectories at ($27.2\sigma_\theta$). Topography as in Fig. 2.

Acknowledgement

We would like to extend our thanks to all officers and crews of vessels participating in KAPEX, which are, in alphabetical order, SA Kuswag I, SA Kuswag V, RV Seward Johnson and RV Polarstern. Technical and scientific contributions from I. Ansorge, S. Becker, R. Berger, P. Bouchard, D. Carlsen, J. Fontaine, S. Fontana, J. Kemp and M. Nielsen and C. Wooding are greatly appreciated. Support from the National Science Foundation, USA, the Foundation for Research Development, RSA, and the Alfred Wegener Institut, Germany, is gratefully acknowledged. Olaf Boebel acknowledges his support from the German Alexander von Humboldt Foundation.

References

Beal, L., and H. Bryden, 1996: The water masses, velocity structure and volume transport of the Agulhas Current at 31°S. Int. WOCE Newsl., 22, 20–27.

Beal, L. M., and H. L. Bryden, 1997: Observations of an Agulhas Undercurrent. Deep-Sea Res., I, 44(9–10), 1715-1724.

Beal, L. M., and H. L. Bryden, 1998: The velocity and vorticity structure of the Agulhas Current at 32°S. J. Geophys. Res., submitted.

Boebel, O., C. Duncombe Rae, S. Garzoli, J. Lutjeharms, P. Richardson, T. Rossby, C. Schmid, and W. Zenk, 1998: Float experiment studies interocean exchanges at the tip of Africa. Eos, Trans. AGU, 79(1), 1, 6–8.

Boebel, O., C. Schmid, and M. Jochum, 1997a: Deployment of RAFOS floats in the Cape Basin. Int. WOCE Newsl., 28, 30–33.

Boebel, O., C. Schmid, and W. Zenk, 1997b: Flow and recirculation of Antarctic Intermediate Water across the Rio Grande Rise. J. Geophys. Res., 102(C9), 20967–20986.

Bower, A. S., and S. M. Lozier, 1994: A closer look at particle exchange in the Gulf Stream. J. Phys. Oceanogr., 24, 1399–1418.

Garzoli, S. L., and A. L. Gordon, 1996: Origins and variability of the Benguela Current. J. Geophys. Res., 101(C1), 897–906.

Garzoli, S. L., A. L. Gordon, V. Kamenkovich, S. Pillsbury, and C. Duncombe Rae, 1996: Variability and sources of the south eastern Atlantic circulation. J. Mar. Res., 54, 1039–1071.

Gordon, A. L., R. F. Weiss, W. M. Smethie, and M. J. Warner, 1992: Thermocline and intermediate water communication between the South Atlantic and Indian Ocean. J. Geophys. Res., 97(C5), 7223–7240.

Lutjeharms, J. R. E., 1996: The exchange of water between the South Indian and South Atlantic Oceans. In: The South Atlantic: Present and past circulation, G. Wefer, W. H. Berger, G. Siedler, and D. Webb (eds.), pp. 122–162, Springer-Verlag, Berlin-Heidelberg, Germany.

Matano, R. P., C. G. Simionato, W. P. de Ruijter, P. J. van Leeuween, P. T. Strub, D. B. Chelton, and M. G. Schlax, 1998: Seasonal variability of the Agulhas Retroflection region. Geophys. Res. Lett., 25(33), 4361–4364.

Rintoul, S. R., 1991: South Atlantic interbasin exchange. J. Geophys. Res., 96, 2675–2692.

Toole, J. M., and B. A. Warren, 1993: A hydrographic section across the subtropical South Indian Ocean. Deep-Sea Res., I, 40(10), 1973–2019.

North Indian Ocean Eddies From TOPEX Altimeter

Available on request...

An atlas of the North Indian Ocean eddies from TOPEX altimeter derived sea surface height has been published by the Indian Space Research Organisation, Bangalore.

The authors are: **M.M. Ali, Rashmi Sharma**, Oceanic Science Division, Meteorology and Oceanography Group, Space Applications Centre, Ahmedabad 380 053, India and **Robert Cheney**, Laboratory for Satellite Altimetry, NOAA/NESDIS, Silver Spring, MD 20910, USA.

The Atlas contains colour plates of the 10-day averaged SSH every 10 days from 1993 to 1997, 5-year averages for the same dates and SSH RMS variations on a monthly basis for the 5-year period.

Contact the Indian authors for further information and a copy of the Atlas.

Summary of Meddies Tracked by Floats

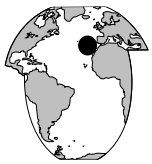

P. L. Richardson and A. S. Bower, Woods Hole Oceanographic Institution, USA; and W. Zenk, Institut für Meereskunde, Kiel, Germany. prichardson@whoi.edu

The Mediterranean salt tongue is one of the most prominent hydrographic features of the mid-depth Atlantic. The salty water originates in the Mediterranean Sea, overflows the Strait of Gibraltar, cascades down the continental slope and equilibrates at depths of 500–1500 m in the northern Gulf of Cadiz as a westward flowing boundary current called the Mediterranean Undercurrent. The undercurrent flows around Cape St. Vincent at the south-western corner of the Iberian Peninsula and continues northward along the continental slope as an eastern boundary current. Large segments of the undercurrent separate from the boundary in the form of 20–100 km diameter lenses of warm, salty Mediterranean Water. These Mediterranean Water eddies (Meddies) rotate anticyclonically (clockwise) with azimuthal velocities up to 30 cm/sec. Compared to background water in the Canary Basin Meddy salinity and temperature anomalies reach 1 psu and 4°C. Due to the difficulty in observing these subsurface, eddies, knowledge of where they form, and their life histories has remained rudimentary until very recently.

Several experiments using freely drifting subsurface RAFOS floats have obtained new information about the formation and trajectories of Meddies. Acoustic tracking of the floats provided at least one and usually two or three positions, temperatures and pressures each day, sufficient to measure the swirl velocity and temperature of a Meddy. During 1993–1994 49 RAFOS floats were launched in the Undercurrent south of Portugal to study the spreading pathways of Mediterranean Water and the formation of Meddies (Bower et al., 1997). These floats plus 36 others launched directly into Meddies provide trajectories that document the formation of 9 Meddies and the translation of 27 Meddies. Although some subsets of the float observations have been published (Armi et al., 1989; Richardson et al., 1989; Zenk et al., 1992; Pingree and LeCann, 1993; Schultz Tokos et al., 1994; Pingree, 1995; Käse and Zenk, 1996; Bower et al., 1997; Richardson and Tychensky, 1998) the grouping together of all the float

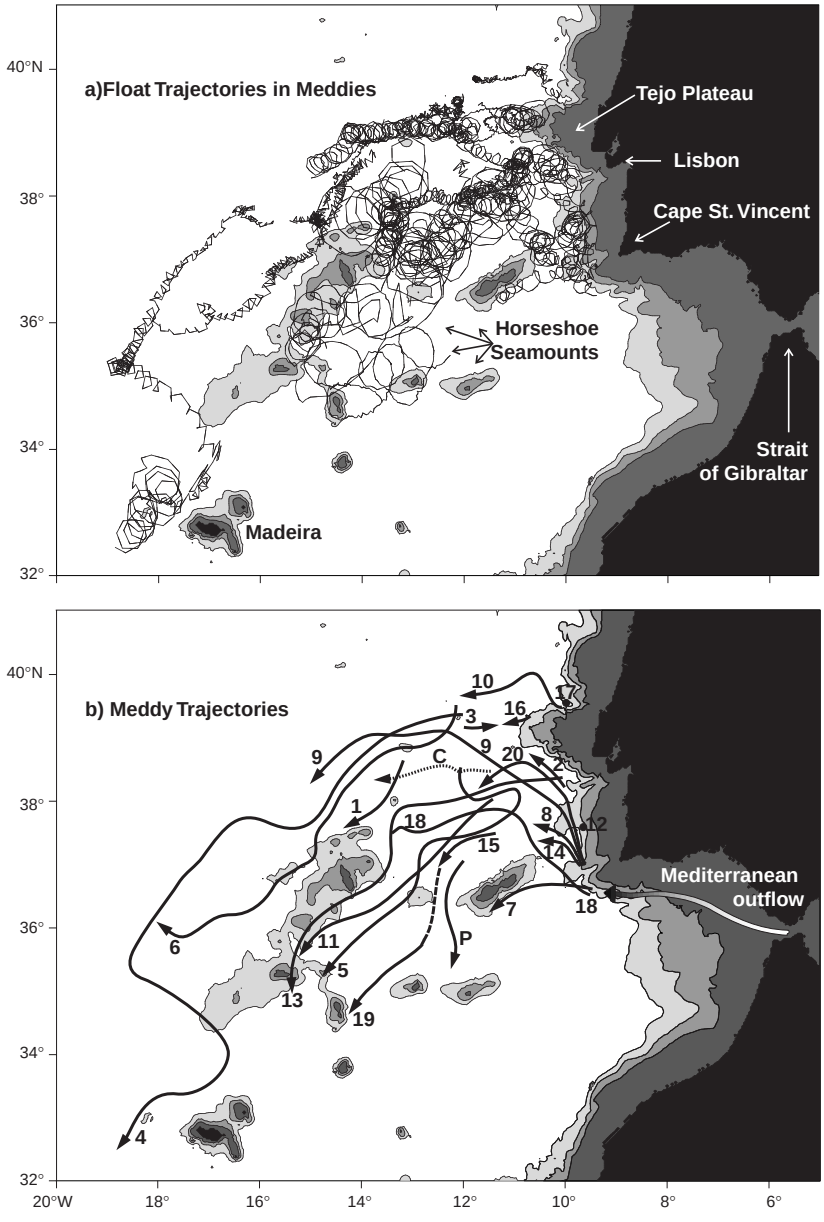

Figure 1. (a) Trajectories of floats looping clockwise in 20 Meddies in the Iberian Basin. These floats remained in the Meddies for the longest period of time. Other floats that also looped in the Meddies are not shown in order to avoid clutter. Note the numerous seamounts in the Horseshoe Seamount Chain south-west of Cape St. Vincent, many of which reach up to the depth of Meddies.

(b) Trajectories of the same Meddies in (a), obtained by subjectively smoothing the float tracks to emphasise large scale patterns. Eighteen Meddy trajectories were obtained from the translation of looping floats, and two Meddies (12 and 16) were stationary during the period of observation. An additional Meddy (P) was tracked with surface drifters by Pingree and LeCann (1993). Five Meddies (4, 5, 6, 9, 13) were continuously tracked for roughly a year, two (4, 6) for a year and a half. The trajectory of a coherent cyclone (C) is shown by a dotted line. The coastline and 1000, 2000 and 3000 m isobaths are superimposed.

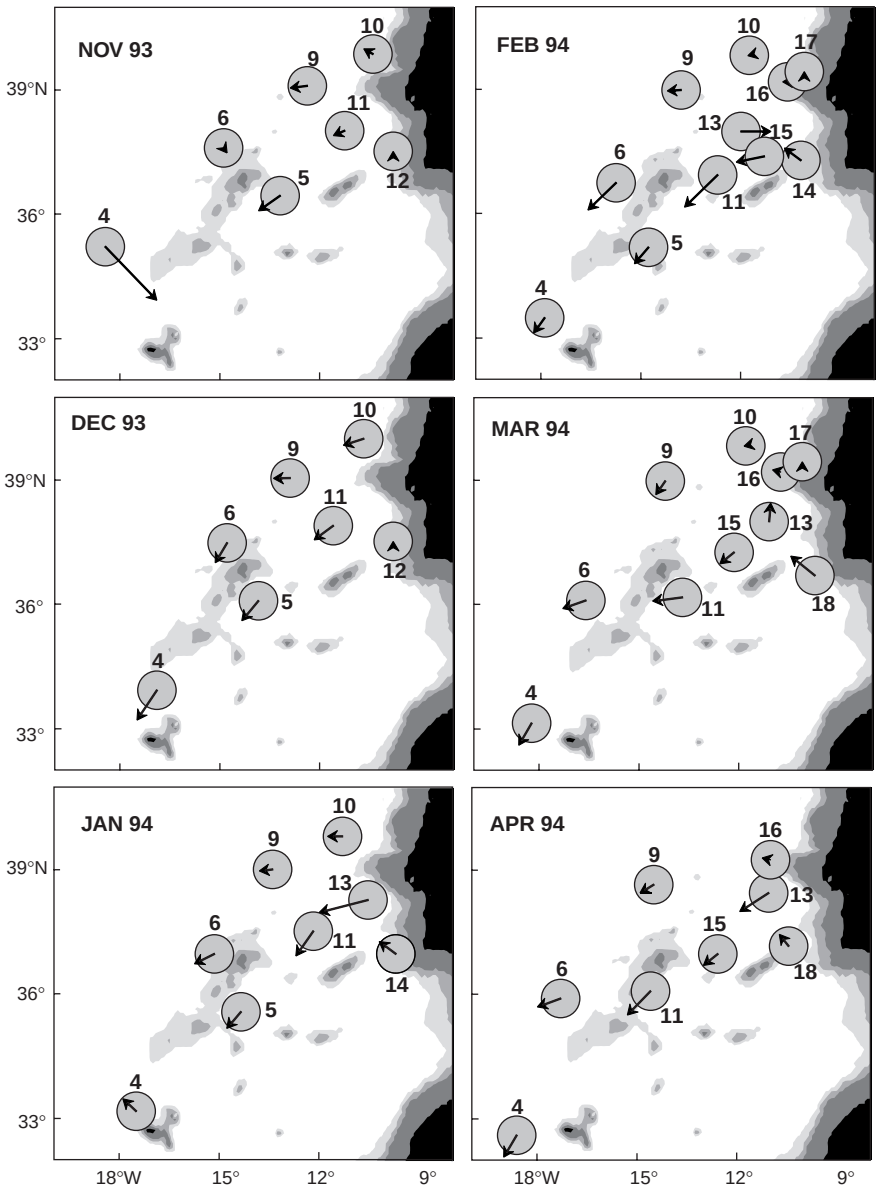

Figure 2. Summary of Meddies observed by looping floats in the Iberian Basin November 1993–April 1994. Meddies are indicated schematically by 100 km diameter circles. Some Meddies such as 12, 14, and 17 near the eastern boundary were probably smaller than 100 km as implied by the circle which overlaps the 1000 m depth contour. The velocity of each Meddy between positions one month apart is shown by vectors.

trajectories is new and enables us to describe the long term pathways and life histories of Meddies in much better detail than previously possible.

Twenty Meddies were tracked with RAFOS floats in the Iberian Basin between May 1991 and February 1995. Fig. 1a shows the trajectories of the RAFOS floats that were trapped in each Meddy for the longest period of time, Fig. 1b shows the subjectively smoothed Meddy trajectories and Fig. 2 shows a summary of all Meddies during a six month period of intensive observations. Six Meddies (7, 8, 9, 14, 18, 20) were observed to form near Cape St. Vincent, at the south-western corner of the Iberian Peninsula, and three Meddies (10, 16, 17) formed in the vicinity of the Tejo Plateau west of Lisbon (Bower et al., 1997; Fig. 1b). The formation events were observed by floats which had been launched in the Mediterranean Undercurrent south of Portugal and began to loop anticyclonically with periods and temperatures typical of previously documented Meddies. Based on the number of floats launched in the Undercurrent and that ended up in Meddies, Bower et al. (1997) estimated that about 10 Meddies form per year near Cape St. Vincent and seven near the Tejo Plateau, a total of 17 per year.

Meddies observed near the eastern boundary tended to translate initially in a northward or north-westward direction, while those farther offshore tended to drift south-westward (Fig. 1b). The mean speed of the poleward undercurrent measured by floats is similar to the mean translation speed of Meddies near the slope, evidence that the Meddies are advected northward by this current. The mean velocity of all the Meddies from start to end and weighted by number of days tracked was 2.0 cm/sec towards 227°T (south-westward). Three Meddies (3, 16, 17) stagnated for a month or two in the vicinity of the Tejo Plateau and did not translate significant distances, at least while they were being tracked by floats. Some Meddies appeared to alternate periods of relatively fast translation with periods of stagnation (see Käse and Zenk, 1996).

Major obstructions to the south-westward translation of Meddies away from the eastern boundary are the Horseshoe Seamounts, a curved line of seamounts in the form of a large (~500 km) horseshoe located south-west of Cape St. Vincent (Fig. 1, Fig. 3). At least nine of these seamounts rise above the mid-depth (1100 m) of a Meddy and five seamounts rise up to within a few hundred metres of the sea surface.

Roughly 69% of the Iberian Basin Meddies are inferred to collide with the Horseshoe Seamounts, sometimes fatally: the other 31% of the Meddies pass northward around the seamounts and into the Canary Basin. Four of the seven Meddies tracked there collided with the Great Meteor Seamounts, three fatally. Overall, an estimated 90% of the Meddies collided with major seamounts after a mean lifetime of around 1.7 years. Although some of these

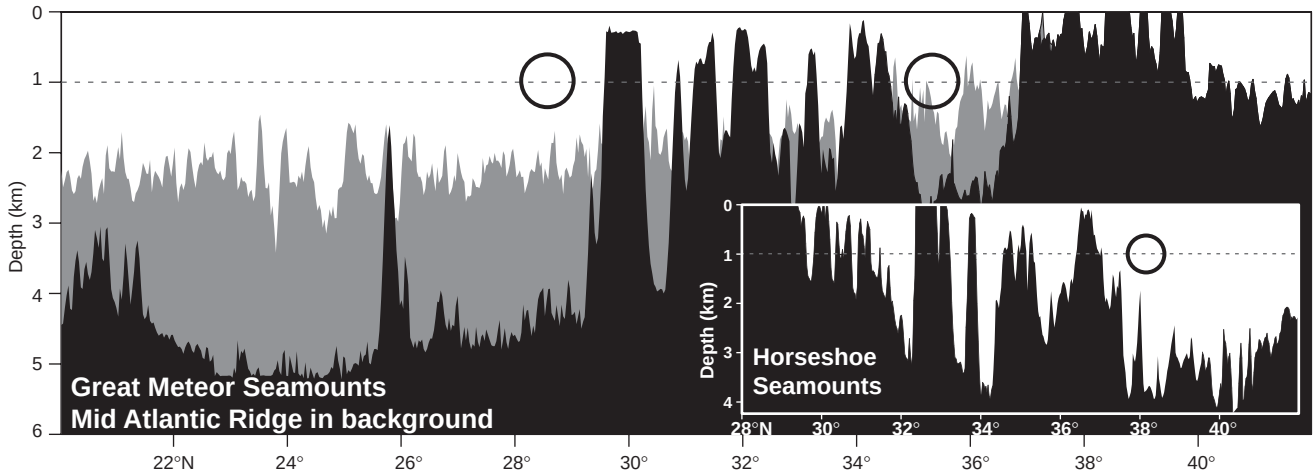

Figure 3. North-south bottom depth profiles showing (a) the Horseshoe Seamounts, and (b) the Great Meteor Seamounts and the Azores (black), and the mid-Atlantic Ridge (grey). These are major obstacles faced by a Meddy translating westward in the Atlantic. Typical Meddies are shown schematically to be 800 m in vertical extent and 100 km in diameter. The Meddies are shown centred where they could possibly translate westward without colliding with seamounts. Depth profiles were created by plotting the shallowest depth at each latitude using ETOP02 data in meridional swaths in the Iberian Basin 11 °W–17 °W (Horseshoe Seamounts), in the Canary Basin 25 °W–32 °W (Great Meteor Seamounts), and along the mid-Atlantic Ridge 32 °W–45 °W.

Meddies could have survived for a long time after colliding with smaller seamounts, we think the usual fate in a collision with a major seamount is an accelerated Meddy decay and a much shorter life than the estimated 5-year (or more) lifetime of Meddies that do not collide with seamounts.

The mean lifetime of a newly formed Meddy was crudely estimated to be 1.7 years by combining the ratios of Meddies that hit seamounts with the times to collision. Since warm salty remnants of Meddies (less warm and salty than typical Meddies) could possibly continue undetected after the collisions, the mean lifetime of 1.7 years could underestimate the total lifetime including Meddy remnants. This estimate coupled with the estimated 17 Meddies which form each year (Bower et al., 1997) suggests that at least 29 Meddies coexist in the North Atlantic.

Eight floats originally looping in the cores of four Meddies that collided with seamounts were dispersed into the background water where the looping stopped. This was interpreted to be measurements of the break-up of the Meddies and the dispersal of their warm salty core waters. The decrease in temperature measured by floats looping in Meddies especially the cold spikes observed during collisions is interpreted to be the entrainment of colder background water into the cores of Meddies where it is rapidly mixed with warmer Meddy water. Therefore the floats measured two processes – the detrainment or dispersal of what was originally Meddy core water into background water and the entrainment into the Meddy of background water where it rapidly mixed with Meddy water. Some decrease of temperature was observed by floats after they had stopped looping implying that pieces or blobs of Meddy water too small or weak to rotate had been dispersed into background water where their temperature and salinity anomalies decayed. The large number of Meddy collisions with seamounts and the resulting disruption of Meddies is to disperse large amounts of the warm salinity Mediterranean water carried by Meddies into the vicinity of the Horseshoe and Great Meteor Seamounts. This dispersal of Meddy water is considered to be important in maintaining the high salinities located in the vicinity of the Horseshoe Seamounts.

References

Armi, L. D., D. Hebert, N. Oakey, J. F. Price, P. L. Richardson, H. T. Rossby, and B. Ruddick, 1989: Two years in the life of a Mediterranean salt lens. J. Phys. Oceanogr., 19, 354–370.

Bower, A. S., L. Armi, and I. Ambar, 1997: Lagrangian observations of Meddy formation during A Mediterranean Undercurrent Seeding Experiment. J. Phys. Oceanogr., 27, 2545–2575.

Käse, R. H., and W. Zenk, 1996. Structure of the Mediterranean water and Meddy characteristics in the northeastern Atlantic. In: The Warmwatersphere of the North Atlantic Ocean, W. Krauss (ed.), pp. 365–395, Gebrüder Borntraeger, Berlin, Germany.

Pingree, R. D., 1995: The droguing of Meddy Pinball and seeding with ALACE floats. J. Mar. Biol. Assoc. UK, 75, 235–252.

Pingree, R. D., and B. LeCann, 1993: A shallow Meddy (a Smeddy) from the secondary Mediterranean salinity maximum. J. Geophys. Res., 98 (C11), 20169–20185.

Richardson, P. L., and A. Tychensky, 1998: Meddy trajectories in the Canary Basin measured during the SEMAPHORE Experiment, 1993–1995. J. Geophys. Res., 103(C11), 25029–25045.

Richardson, P. L., D. Walsh, L. Armi, M. Schröder, and J. F. Price, 1989: Tracking three Meddies with SOFAR floats. J. Phys. Oceanogr., 19, 371–383.

Schultz Tokos, K. L., H.-H. Hinrichsen, and W. Zenk, 1994: Merging and migration of two Meddies. J. Phys. Oceanogr., 24, 2129–2141.

Zenk, W., K. Schultz Tokos, and O. Boebel, 1992: New observations of Meddy movement south of the Tejo Plateau. Geophys. Res. Lett., 19, 2389–2392.

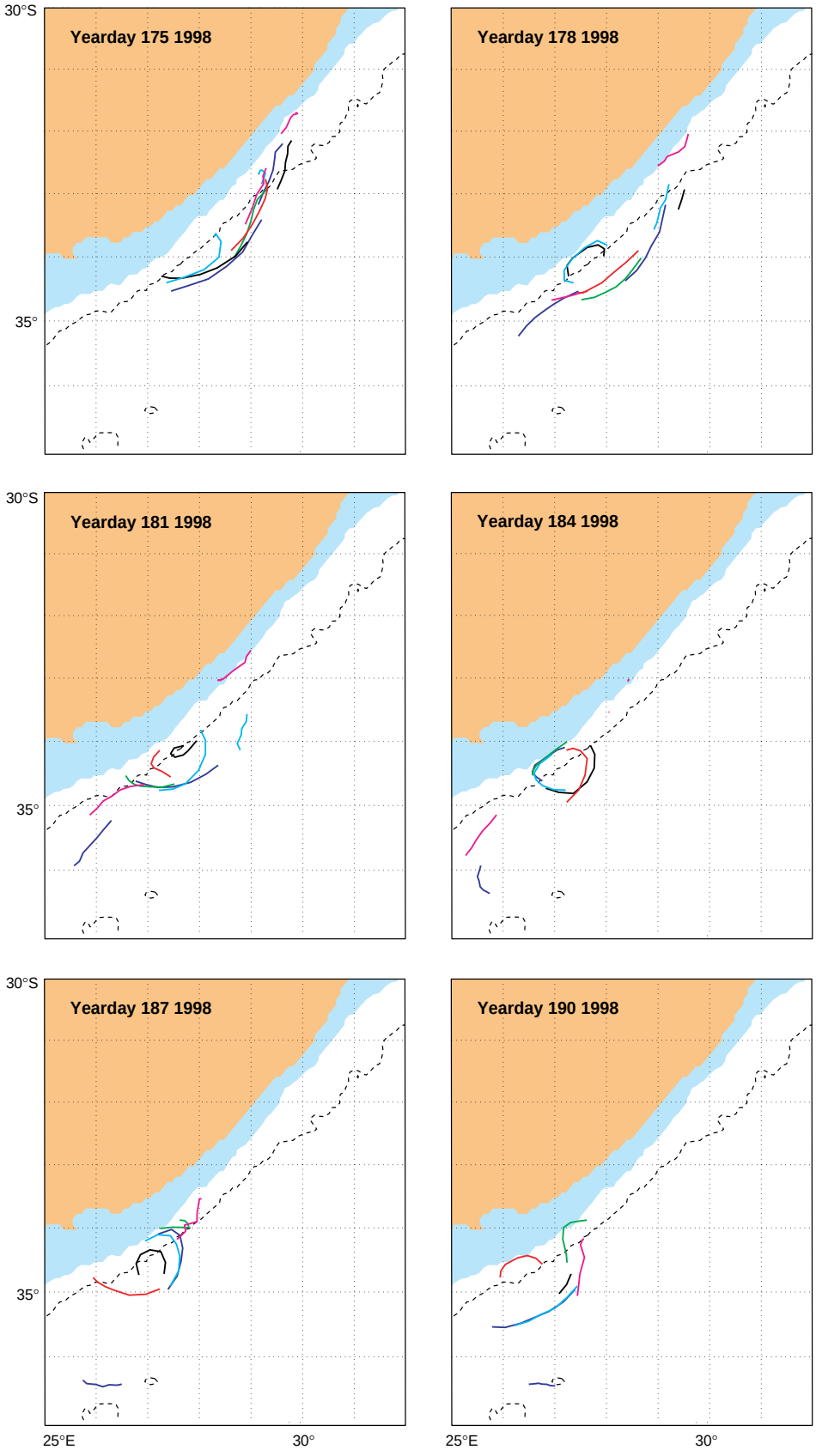

Boebel et al., page 14, *Figure 4. Trajectory segments of 3 days length of deep (27.2σ_θ) "Durban" floats on a Mercator map. The continent is light brown and the area up to 1000 m light blue. The 3000 m isobath is indicated by a dashed line.*

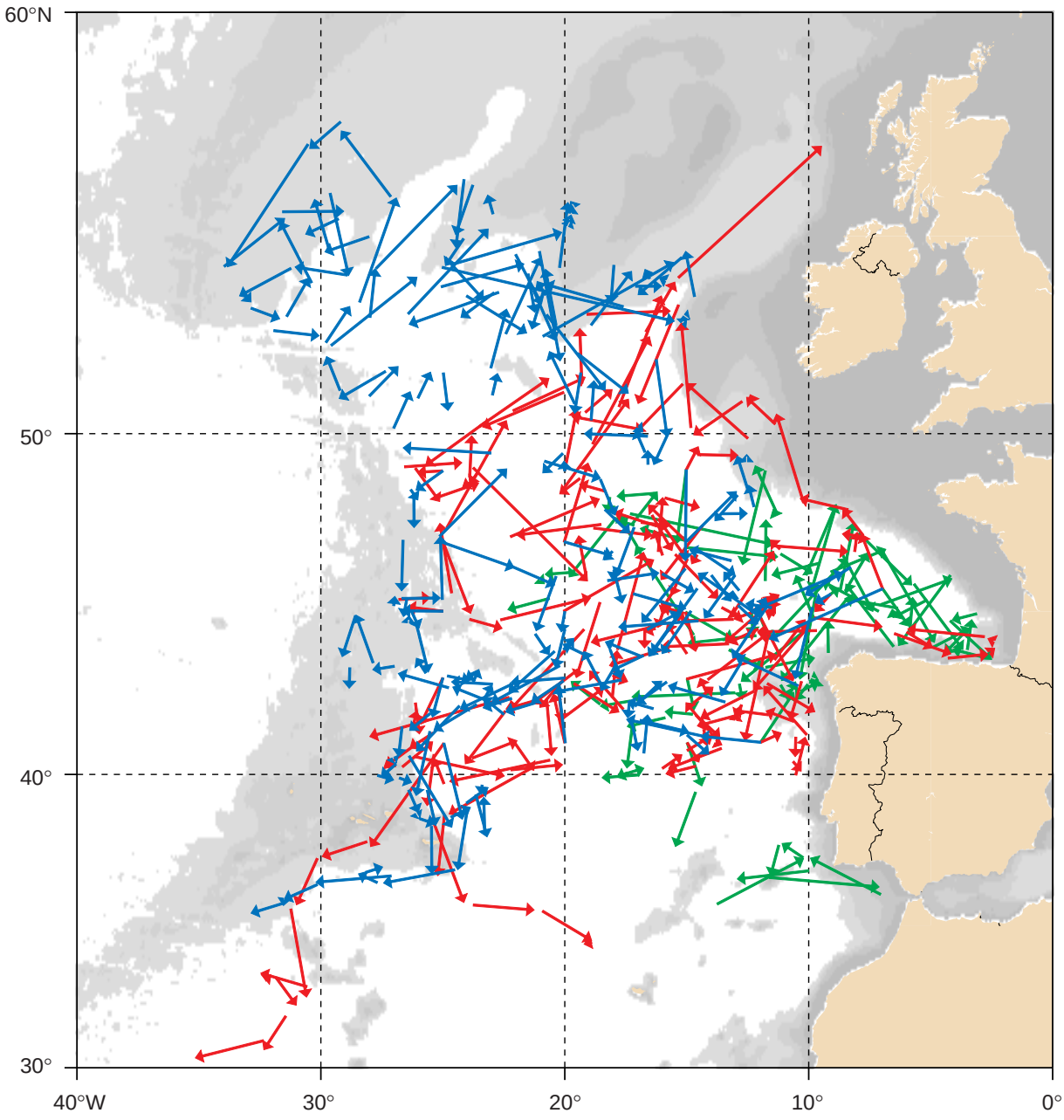

Le Cann et al., page 25, *Figure 2. 3-month displacement vectors for ARCANE/EUROFLOAT floats (green: nominal pressure depth P = 450 dbars; red: P = 1000 dbars; blue: 2000 dbars≥P≥1500 dbars).*

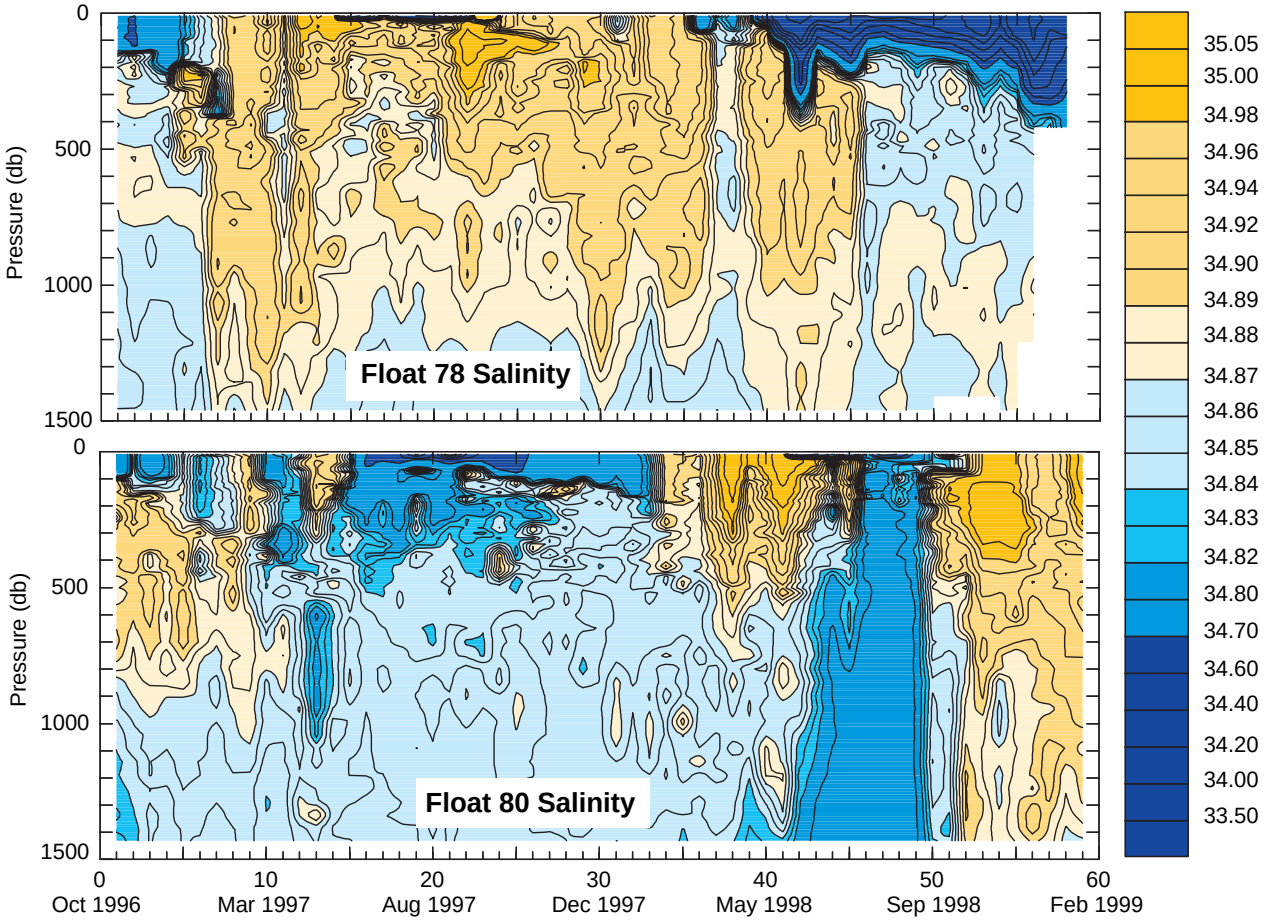

Above: Bacon et al., page 28, *Figure 2. Contoured time series of salinity measurements for floats 78 and 80. The dates on the lower panel are also applicable to the upper panel.*

Right: Müller and Ikeda, page 30, *Figure 1. Recovery of the mooring K1/351.*

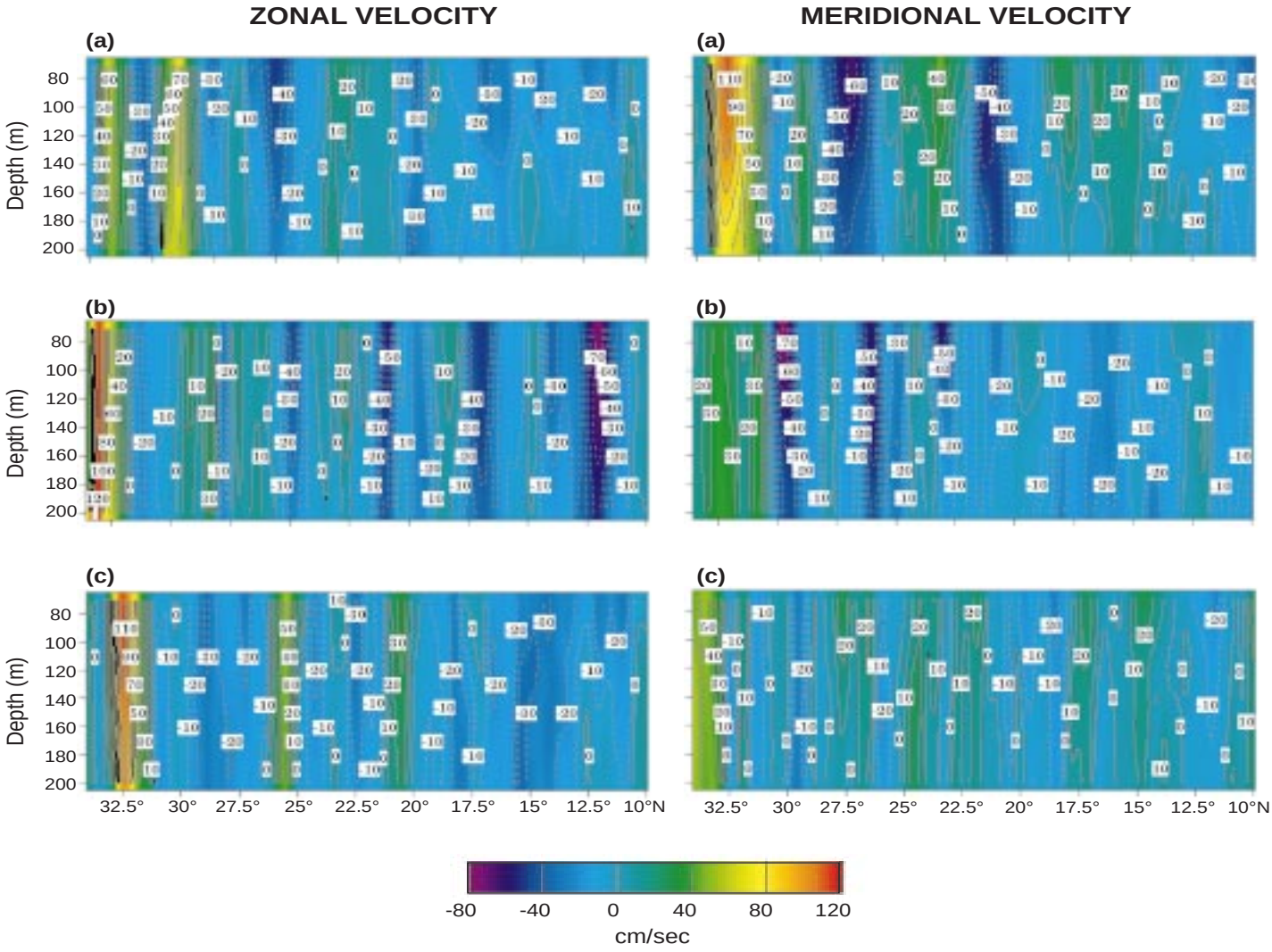

Kaneko et al., page 31, *Figure 2. Sections of the zonal component of velocity for (a) the first cruise, and (b) the outward and (c) the return trip of the second cruise.*

Kaneko et al., page 31, *Figure 3. Sections of the meridional component of velocity for (a) the first cruise, and (b) the outward and (c) the return trip of the second cruise.*

Lagrangian Observations in the Intergyre North-East Atlantic during the ARCANE and EUROFLOAT Projects: Early Results

Bernard Le Cann and Kevin Speer, Laboratoire de Physique des Océans, IFREMER/Centre de Brest, France; Alain Serpette and Jérôme Paillet, Centre Militaire d'Océanographie, Service Hydrographique et Océanographique de la Marine, France; and Thierry Reynaud, LPO, France. treynaud@ifremer.fr

In late 1996, 43 MARVOR acoustic floats, of ALFOS type, have been deployed in the intergyre region of the North-East Atlantic (NEA) in the framework of the ARCANE and EUROFLOAT projects. The three major upper and mid-depth water masses of the area were targeted: North Atlantic Central Water (NACW) at 450 dbars, Mediterranean Water (MW) at 1000 dbars, both ARCANE, and Labrador Sea Water (LSW) at 1750 dbars, from EUROFLOAT.

The scientific objectives of the ARCANE/EUROFLOAT experiments are:

- to determine the mean Lagrangian circulation in the intergyre region at the NACW, MW and LSW levels.
- to evaluate the mixing and dispersion of these water masses.

The fate of the northern part of the MW plume, the intrusion of LSW in the area and the adjustment of the upper layer eastward geostrophic flow at the eastern boundary are of particular interest.

We present here some preliminary results, notably 2-year long displacements showing the general circulation in the area and some sample trajectories showing the role of topography, like the Mid-Atlantic Ridge and the Continental Slope, in this circulation.

Scientific questions

Saunders (1982) describes the mean circulation in the intergyre region of the Eastern North Atlantic (30°N to 50°N) as:

- Southward flow in the upper layers (above ~500 m),
- Northward flow north of 40°N, between ~500 m and ~1000 m,
- Southward flow below ~1000 m.

The amplitude of the circulation is rather weak, of order 1 cm/s. Recent inverse modelling by Paillet and Mercier (1997) broadly confirms this analysis, except that no clear meridional flow is found in the middle layer, away from the continental slope. Long term current meter data (Müller and Siedler, 1992; Gould, 1983; Arhan et al., 1989) are somewhat supportive of this circulation. Schopp and Arhan (1986) have suggested that the wind-induced upwelling in the subpolar gyre is responsible for the northern MW plume. The MW itself has been suggested as a dynamical cause, through flow generated by mixing or double diffusion (Schopp, 1987; Spall, 1999). Mixing tends to stretch water columns locally and permits a

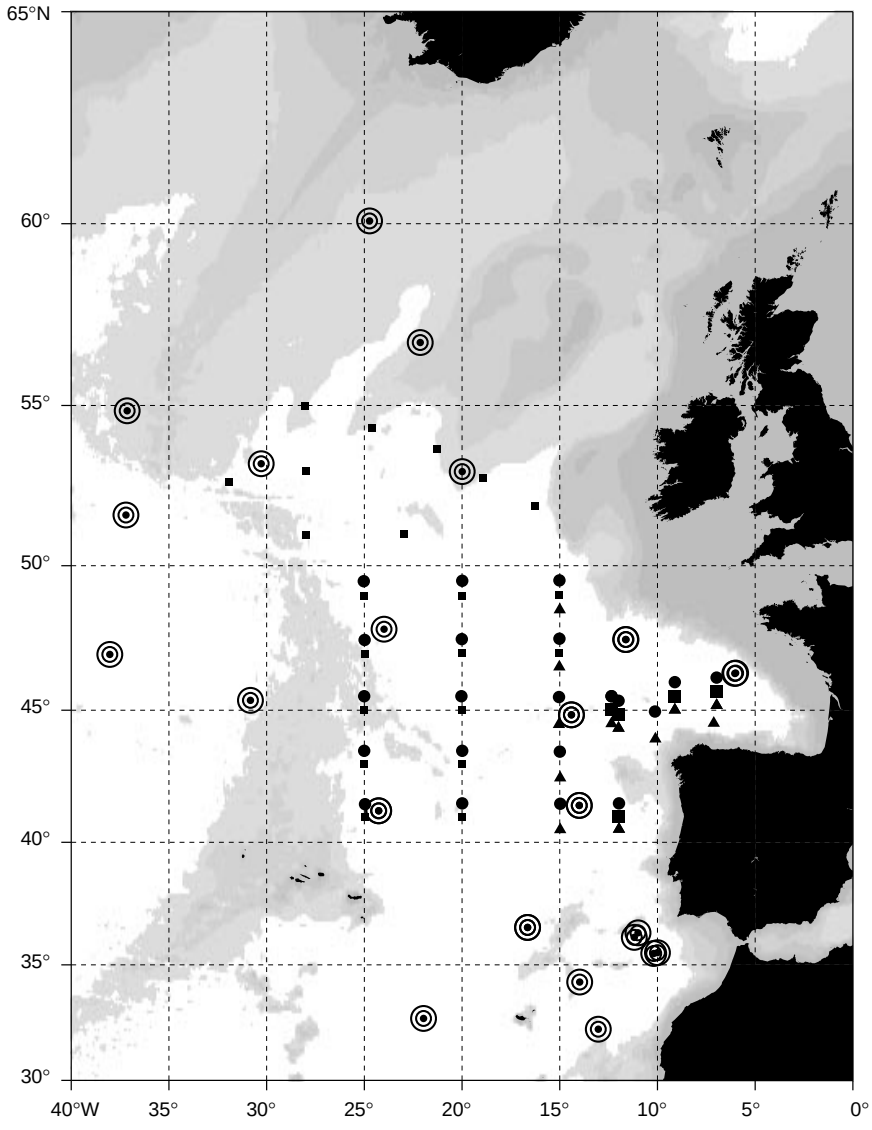

Figure 1. Acoustic network in the North-East Atlantic (concentric circles) and deployment locations for the ARCANE/EUROFLOAT multi-cycle floats. (Nominal depth: triangles: 450 dbars; dots: 1000 dbars; large squares: 1500 dbars; small squares: 1750 dbars). In order to improve the figure, the latitude of the launch positions have been shifted by 0.5°. Consequently the 450 dbars/1000 dbars floats deployment positions are located northward southward of that presented on the figure.

diapycnal velocity to arise, thereby inducing vorticity and meridional flow. The MW outflow from Gibraltar tends to follow the continental slope northward. This current gets unstable, generating Meddies which propagate warm and salty anomalies into interior ocean. One of the objectives of ARCANE is to investigate the northern Meddy population.

Very little long-term Lagrangian data exist in the intergyre region of the NEA. Some near surface drifting buoy trajectories were analysed by Pingree (1993) and the TOURBILLON experiment provided a few month-long trajectories which suggest a surprisingly short 2 day Lagrangian time scale, and a 15–30 km spatial correlation scale as analysed by Mercier and Colin de Verdière (1985).

Experimental Projects: ARCANE and EUROFLOAT

In 1996, two projects to answer these scientific questions were initiated as joint projects:

- One is ARCANE (Actions de Recherche sur la Circulation dans l'Atlantique Nord-Est), co-ordinated between the LPO (Laboratoire de Physique de Océans, Brest) and the CMO (Centre Militaire d'Océanographie, Brest), with WHOI (Woods Hole Oceanographic Institution/US) and IH (Instituto Hidrografico/Portugal) as international partners. We shall speak only of the oceanic Lagrangian part of this project, which also involves other float deployments on the slope, hydrology ($CTDO_2$, tracers) and current meter measurements.
- The second one is EUROFLOAT, a European-funded Lagrangian project (coordinator: J. Gould/SOC) which involves the LPO, SOC, IfM/Kiel and AINCO InterOcean from Madrid as partners. We shall speak only of the floats deployed north of 40°N.

An acoustic network was set up as an international cooperation: The French operator is SHOM (Service Hydrographique et Océanographique de la Marine) and the network is also contributed by Amy Bower (WHOI), Tom Rossby (URI), Walter Zenk (IfM/Kiel) and Isabel Ambar (FCUL/Lisbon). The sources are of WRC type. A schematic of the network is represented on Fig. 1.

The ARCANE/EUROFLOAT floats were deployed on a loose grid, as seen on Fig. 1. After more than two years at sea, most of the floats are still operating, and we hope for a mean 3 year long life.

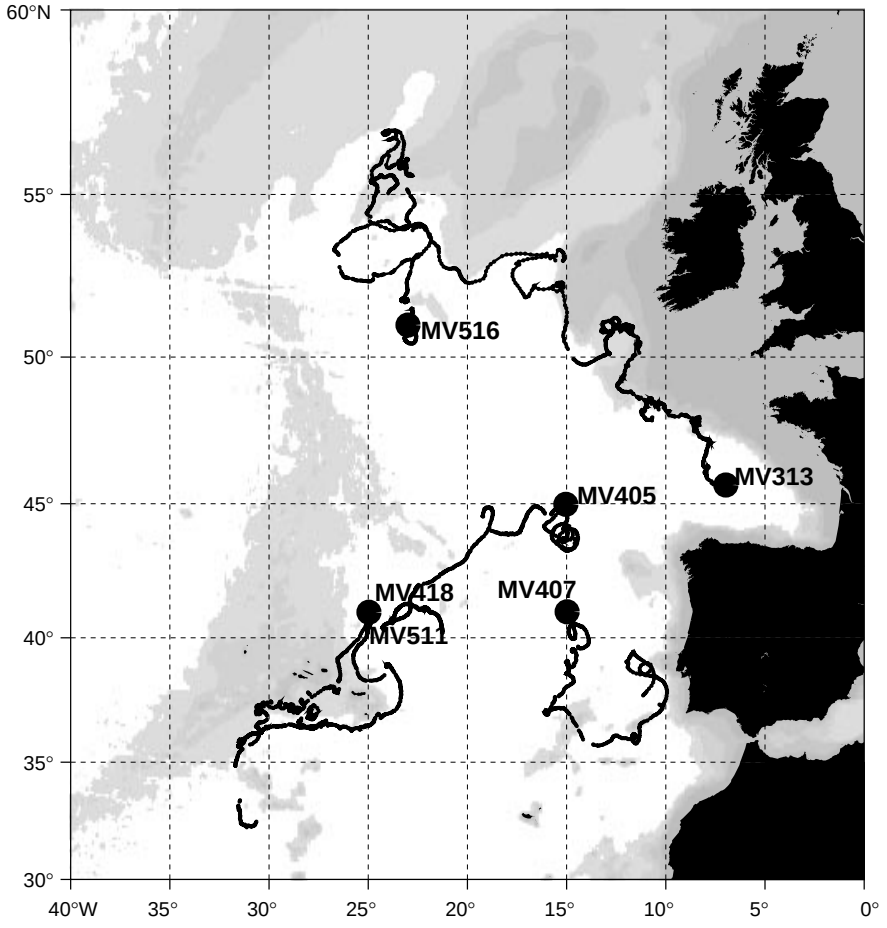

Figure 3. Six sample trajectories of ARCANE/EUROFLOAT floats. Dots indicate the deployment location in autumn 1996. Nominal float depths are 450 dbars (MV 407), 1000 dbars (MV 313, MV 405 and MV 418) and 1750 dbars (MV 511 and MV 516). Gaps in trajectories are due to the surfacing procedure or to bad acoustic tracking. Shaded regions indicate depths shallower than 3000m.

Technical information about the floats and processing can be found in Ollitrault et al. (1995 and references therein). Briefly, the MARVOR is a multi-cycle RAFOS type float. It dives to the prescribed nominal depth by activating an external bladder. It then actively controls its depth. The underwater cycle duration is set to 90 days. The floats are programmed to listen to the acoustic network every 24 hours. They precisely date the Time Of Arrival (TOA) of the signals from the acoustic beacons. The floats also record pressure and temperature every day. After 90 days underwater, the floats activate their external bladder and surface to transmit their data (TOA, pressure and temperature) through the Argos system. After transmission, the floats return to their nominal depth. The surfacing/Argos transmission/diving procedure takes less than 3 days.

A 3-year duration was asked for the programme, on the basis of the error on the anticipated weak mean velocity in the area: $\delta U = < u'^2 >^{1/2} (T/F)^{1/2}$, where $< u'^2 >^{1/2}$ is a typical velocity variability (O(5 cm/s), T is a typical integral Lagrangian time-scale (O(10 days)) and F is the number of float-days. To achieve a 0.5 cm/s accuracy at the

resolution of deployment (assuming a confinement of the floats), which is the order of magnitude of the mean flow, one typically needs a F = 2 years duration.

There are three major problems which have affected about one fourth of the floats:

- Non-stabilisation, due to faulty hydraulics.
- Various electronics failures (major clock drift, black out,…)
- Float stranding (due to windage during the surface period).

That means that three quarters of the floats have experienced no major problem after two years at sea.

First results

More than one year of data has been processed and shows mean speeds of 1–5 cm/s throughout the region, and a variance of about 10 cm^2 s^2 overall. 3-month displacements are presented on Fig. 2 (page 22). There is a tendency for southward flow in the southern part of the domain to be statistically significant, but elsewhere the mean flow is not well defined. Longer flights occur in the northern inter-gyre region while more compact eddying occurs to the south.

A few sample trajectories are presented on Fig. 3:

- The two floats deployed at 41°N, 25°W (MV 418 at 1000 dbars, MV 511 at 1750 dbars) were strongly affected by the Mid-Atlantic Ridge topography. The 1000 dbars float went through the Azores Archipelago and was then caught in a local anticyclonic vortex, near the Azores Plateau. The 1750 dbars float passed round the Azores to join the MAR again (Speer et al., 1999).
- MV 405, at 1000 dbars, after some eddying motions, followed the Azores-Biscay Rise. These trajectories are also roughly coincident with the edge of the anomaly of salinity, depicting the extent of the MW plume, as described by Richardson, 1993. This seems to imply a role of the topography in shaping the MW plume.
- MV 313 was deployed in the Bay of Biscay and entered the continental slope to be caught in a slow boundary current, up to 53°N. Boundary currents are not yet well sampled but indications are of substantial exchange with the interior, so that a continuous current along the slope, carrying Mediterranean Water to the Norwegian Sea, is unlikely, despite the fact that a mean flow appears at fixed locations along the boundary.
- MV 516 (1750 db) moves north and enters the energetic North Atlantic Current zone. Floats in this zone interact with the Rockall Bank, in this case moving south along the eastern boundary to meet MV 313 from below.

A strong Meddy was found at a surprisingly northerly position and is described elsewhere (Paillet et al., submitted). This suggests more northerly formation sites than presently reported.

Conclusions

ARCANE and EUROFLOAT are on-going experiments and more data is still coming in. Other float data are starting to be processed, like the more conventional one-shot RAFOS floats deployed near the continental slope. These data, together with those of partner projects in WOCE and ACCE, will help improve our understanding of the upper and mid-depth circulation in the mid-latitude Eastern North Atlantic, separate interior from eastern boundary processes, and perhaps illuminate the key mechanisms of heat and salt transport.

Acknowledgements

Technical preparation, float deployment and data processing are collective activities and careful, and sometimes tedious, work is needed from many individuals. We particularly acknowledge the work done by Norbert Cortès, Loic Gourmelen, Gérard Loaëc, Yves Auffret, Olivier Péden and J. P. Girardot. The floats were deployed from the BO D'Entrecasteaux and the NO Thalassa. We thank all the people involved in the cruises at sea, and the officers and crew from these two vessels. ARCANE is funded by IFREMER and SHOM. EUROFLOAT is funded by the European Union (project No. MAS2-CT94-0/02). Further information could be found on http://www.ifremer.fr/lpo/arcane and on http://www.ifremer.fr/lpo/eurofloat.

References

Arhan, M., A. Colin de Verdière, and H. Mercier, 1989: Direct observations of the mean circulation at 48°N in the Atlantic. J. Phys. Oceanogr., 19, 161–181.

Gould, W. J., 1983: The North-east Atlantic Ocean. In: Eddies in Marine Science, A. R. Robinson (ed.), pp 145–157, Springer-Verlag, Berlin, Germany.

Mercier, H., and A. Colin de Verdière, 1985: Space and time scales of mesoscale motions in the eastern North Atlantic. J. Phys. Oceanogr., 15, 171–183.

Müller, T. J. and G. Siedler, 1992: Multi-year current time series in the eastern North Atlantic. J. Mar. Res., 50, 63–98.

Ollitrault M., Y. Auffret, N. Cortès, C. Hémon, P. Jégou, S. Le Reste, G. Loaec, and J. P. Rannou, 1995: The SAMBA Experiment, Volume 1, SAMBA I and CTD data. Repères Océan, 12.

Paillet, J., and H. Mercier, 1997: An inverse model of the eastern North Atlantic general circulation and thermocline ventilation. Deep-Sea Res., 44(8), 1293–1328.

Paillet, J., B. Le Cann, A. Serpette, Y. G. Morel, and X. J. Carton, 1999: Real-time follow-up of a northern Meddy in 1997–1998. Submitted.

Pingree, R. D., 1993: Flow of surface waters to the west of the British Isles and in the Bay of Biscay. Deep-Sea Res., II, 40, 1/2, 369–388.

Richardson, P. L., 1993: A census of eddies observed in North Atlantic SOFAR float data. Prog. Oceanogr., 31, 1–50.

Saunders, P. M., 1982: Circulation in the Eastern Atlantic. J. Mar. Res., 40(suppl.), 641–651.

Schopp, R., 1987: Large-scale circulation at mid-depth in the Eastern North Atlantic: Processes study. PhD thesis, 156 pp., UBO.

Schopp, R., and M. Arhan, 1986: A ventilated mid-depth circulation model for the eastern North Atlantic. J. Phys. Oceanogr., 16, 344–357.

Speer, K., J. Gould, and J. LaCasce, 1999: Year-long float trajectories in the Labrador Sea Water of the eastern North Atlantic Ocean. Deep-Sea Res., in press.

Spall, M., 1999: A simple model of the large-scale circulation of Mediterranean Water and Labrador Sea Water. Deep-Sea Res., accepted.

Profiling ALACE Float Salinity Measurements

Sheldon Bacon, Luca Centurioni, and W. John Gould, Southampton Oceanography Centre, UK. sheldon.bacon@soc.soton.ac.uk

As a UK contribution to the World Ocean Circulation Experiment (WOCE), seven PALACE floats were purchased from Webb Research Corporation in 1996. Of these, four were conductivity-temperature-depth (CTD) profilers (S/N 77-80) and three temperature-depth (TD) profilers (S/N 81-83). The CTD profilers were fitted with HACC ("high-accuracy conductivity") sensors by Falmouth Scientific, Inc. Following previous UK interest in the area, it was decided to deploy these floats in the Irminger Basin of the North Atlantic, part of the sub-polar gyre. This was done by one of us (SB) late in October 1996 on RRS Discovery Cruise 223 (Leach and Pollard, 1998). Float 81 expired soon after launch due to damage caused by foul weather during the launch process. Two more expired (79 and 82) early in 1998, leaving four operational at the time of writing (February 1999). All floats were set to cruise at 1500 dbar on a two-week cycle.

The availability of a large quantity of high-resolution, high-quality WOCE hydrographic data from the subpolar gyre over 1996–1997 made possible an evaluation of the performance of the conductivity sensor of each CTD float. We reported the results of this study in a previous publication (Bacon et al., 1998), paper copies of which are available on request from SB; alternatively, it is freely available over the web as a PDF file, the address for which is given with the reference. To summarise: we looked for ship CTD stations which were occupied within 50 days and 100 km of float profiles. There were several such occurrences for each float, distributed over the first 12 months' operation. By comparing ship and float θ/S relationships, we were able to determine salinity offsets for each float, and we showed that salinities derived from all four CTD floats were both stable and accurate to ± 0.005 over the duration of the study. The same procedure was adopted for float–float profile comparisons, of which there were a few. The results were consistent with the comparisons with the ship CTDs. There was one exception, float 80, which had an anomalous offset for roughly the first month after deployment, and was beginning to behave strangely towards the end of the previous study, which covered data from deployment through to early July 1998.

In this note, we provide an update of the earlier results. We consider only the three surviving CTD floats (77, 78 and 80), whose tracks are shown in Fig. 1. Float 80 has spent 27 months wobbling around the Irminger Basin; both 77 and 78 have nearly completed circuits of the Labrador Sea. 77 passed Cape Farewell first, in September 1997; 78 followed it in May 1998. We note that 78 is presently aground (at least it's well inshore of its cruising depth), but this may not be the end for the float because 77 spent much of the winter of 1997/98 (November to January) similarly grounded and yet survived.

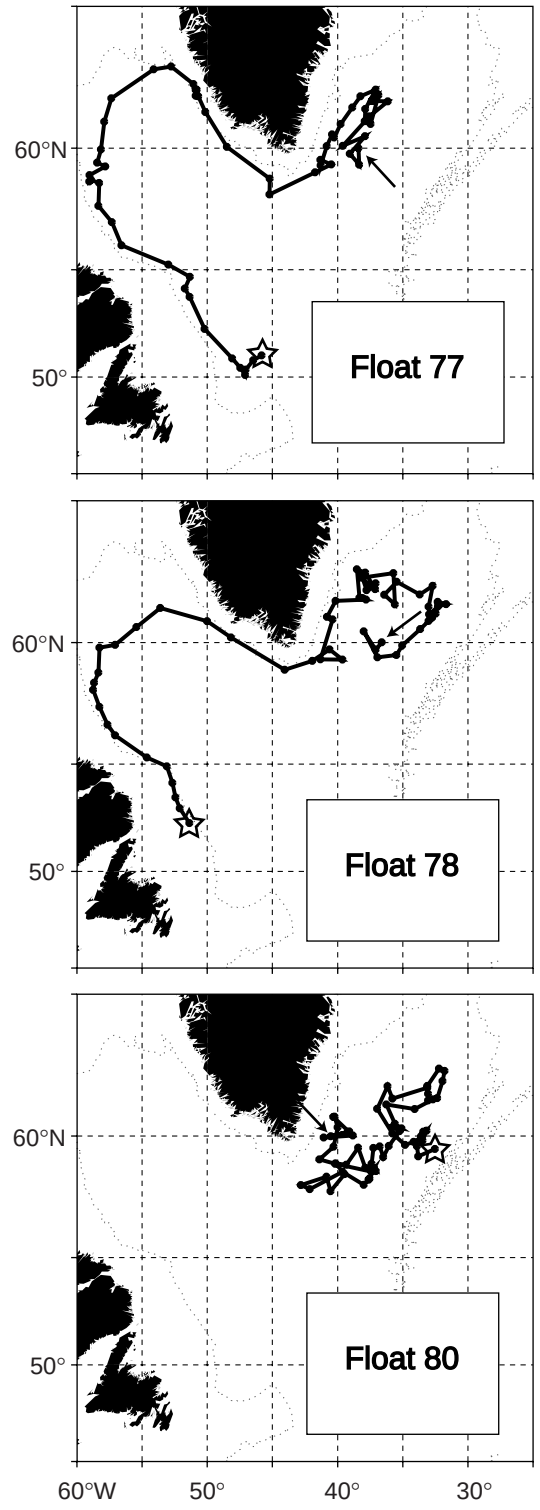

Figure 1. Tracks of float 77, 78 and 80. Bathymetry is illustrated with the 1500 m contour. Deployment positions are marked with an arrow; latest positions (as of February 1999) are marked with a star.

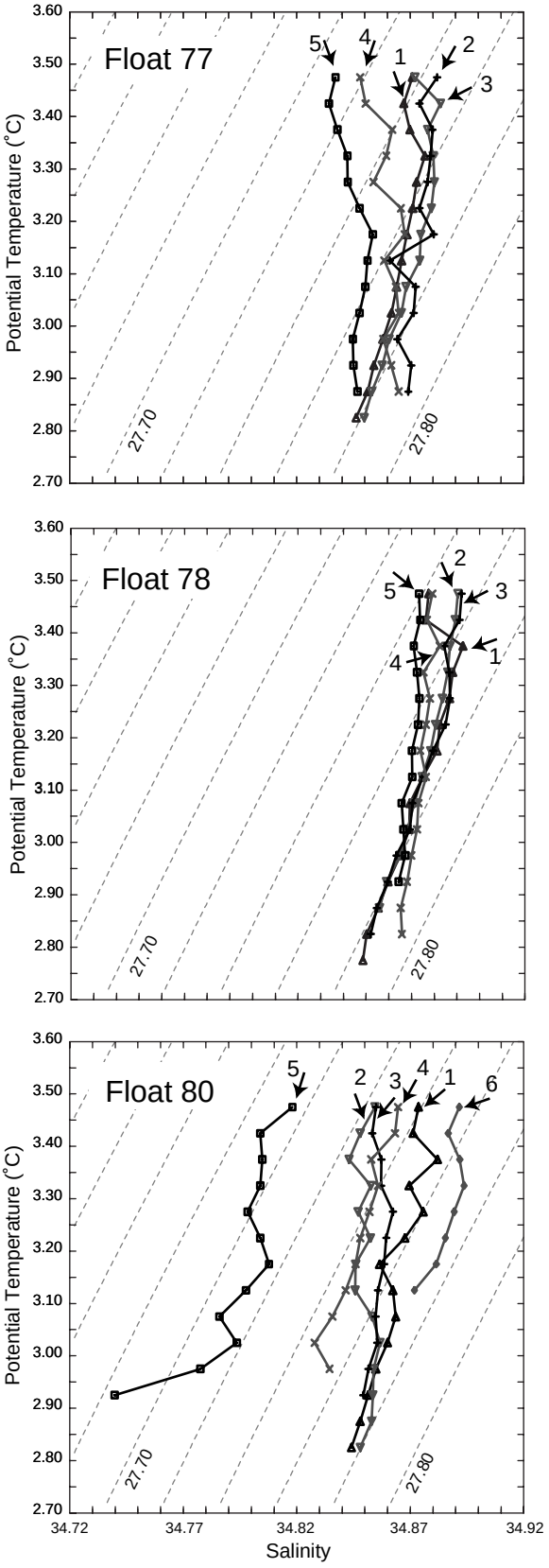

Figure 3. Mean θ/S relationships for floats 77, 78 and 80 in six-month segments. Overlaid are σ_0 contours in 0.02 kg/m^3 increments, 27.8 deepest.

Fig. 2 (page 23) shows contoured salinity time series for floats 78 and 80 (in this context, 77 adds little to the picture from 78). Generally, the pale blue at depth is Labrador Sea Water, the shallow dark blue is the cold, fresh surface waters along the boundary and the darker yellows are encounters with Irminger Current waters, the recirculating warm and salty remnant of the North Atlantic Current. The outstanding patch of apparently erroneous data occurs on float 80 between cycles 42 and 50, which we now analyse further.

Fig. 3 shows mean θ/S relationships for floats 77, 78 and 80, divided into 6-month segments (cycles 1–12, 13–24 etc.). We note firstly the outstanding stability of float 78 salinities: at the deepest common level, 2.9–3.0°C, the salinity range remains ±0.005. The standard error (SE) of the mean salinity in the 0.5°C θ bins is generally 0.001–0.004. The picture is only a little worse for float 77. All but the most recent segment of data fall into a similar salinity range (±0.005) with similar SEs (0.001–0.004), as do the first three segments (18 months, as reported in the previous study) of float 80. The fourth segment of float 80 (cycles 37–42) shows an oddly depth-dependent onset of freshening, and SEs are now in the range 0.004–0.010. By the fifth segment (cycles 43–52), there is a salinity shift of the order of -0.05, and all SEs are ca. 0.010. By the sixth segment (cycles 53–59), some sort of recovery appears to have taken place; all SEs are back to 0.002–0.004. The bias around the fifth segment has been confirmed by comparison with nearby surface (4–5 m) salinity data from the thermosalinograph of the MV Nuka Arctica (Gilles Reverdin, 1999, pers. comm.).

It seems unlikely that this very noisy episode of fresh salinities from float 80 is caused by an oceanic salinity signal. We are probably seeing the consequences of a cycle of biofouling beginning in late spring 1998 and killed off by the following winter. Nevertheless, some of these data might still be usable, albeit with a different offset and larger error bounds.

In conclusion, all four of our CTD floats have produced high-quality salinity measurements for the first 18 months of their lives; one has now expired (79), one has shown a large salinity shift which is probably not environmental (80), and the remaining two (77 and 78) continue, 27 months after deployment, to produce salinity measurements of accuracy 0.005–0.010.

References

Bacon, S., L. Centurioni, and W. J. Gould, 1998: Evaluation of profiling ALACE float performance. SOC Internal Document No. 39, 72 pp., Southampton Oceanography Centre, UK. Available as PDF file (3MB) at: http://www.soc.soton.ac.uk/JRD/HYDRO/shb/posters/BCG.PALACE.Report.pdf.

Leach, H., and R. T. Pollard, 1998: RRS Discovery Cruise 223 28 September–19 November 1996: Vivaldi '96. SOC Cruise Report No. 17, 104 pp., Southampton Oceanography Centre, UK.

Kiel Sound Source Mooring K1/351 Recovered after 5 1/2 Years Deployment in the South Atlantic

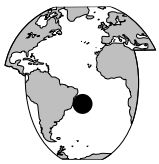

Thomas J. Müller, Institut für Meereskunde an der Universität Kiel, Germany; and Yoshimine Ikeda, Instituto Oceanografico, Brazil. tmueller@ifm.uni-kiel.de

As the WOCE field work is closing, it may be interesting to note that some of the equipment that for logistic reasons stayed at sea much longer than originally scheduled, nevertheless could be retrieved without major technical problems. One such example is the sound source mooring K1/351 of the Institut für Meereskunde, Kiel. It was part of the Deep Basin Experiment (DBE) and was recovered only recently in June 1998 after more than 5 ½ years deployment.

Mooring K1/351 was designed mainly to carry a Webb sound source at 1000 m nominal depth for tracking RAFOS and other floats during the DBE. The sound source was powered with 1023 standard D-cells and programmed to transmit one acoustic pulse of 80 seconds length daily. In this configuration, the sound source was expected to have a life-time of 4 years. At 900 m, a moored RAFOS (MAFOS) float should control any clock shifts of sound sources other than K1/351 using the known mooring positions (König et al., 1991). The uppermost pair of glass spheres (840 m nominal depth) was connected with a stainless steel frame and carried a CB radio transmitter. Also, in one of these spheres, an ARGOS transmitter was implemented that should switch on when sensing light on surfacing (Watchdog); estimated battery life-time was 3 years in sleeping mode. For later recovery, an acoustic release RT 161 (S/N 373) was implemented into the mooring line 60 m above the anchor. The release was powered with Lithium batteries which according to the manufacturer (MORS/Oceano, France) would provide a life-time of 5 years.

Mooring K1/351 was set in the Brazil Basin on 25 November 1992 from FS Meteor during cruise M22/3 at 28°49.7'S, 044°26.3'W and 3705 m water depth (Siedler et al., 1993). Several attempts failed to get ship-time for recovery after 4 years of operation. Finally, the Instituto Oceanografico, Sao Paulo, could make available its Santos based B/Oc. Prof. W. Besnard during one of its cruises. The RT 161 release responded on the first and second attempt to interrogate, with reasonable measurements of its distance to the hydrophone being displayed on the deck unit TT301; when the first release command had been completed, mooring K1/351 started to surface and was taken onboard on 20 June 1998 after more than 5 ½ years deployment. The uppermost pair of glass spheres with the ARGOS and the CB transmitters were missing, and the MAFOS glass tube was damaged.

Earlier experience had shown that the stainless steel frame that connected the uppermost pair of glass spheres with the CB transmitter and the ARGOS watchdog, could be sensitive to corrosion at a welding seam. We may assume that due to corrosion this part was lost, probably after the batteries of the watchdog had ceased after ca. 3 years since its code never was identified by ARGOS. It is also known that some of the early Kiel RAFOS floats could leak water (W. Zenk, pers. comm.). We therefore assume that the moored float (MAFOS) was flooded, and that it then imploded when it was quickly brought to lower pressure after the mooring had been released.

The main parts of mooring K1/351 were in remarkably good condition (Fig. 1, page 23). Although the aluminium housing of the sound source shows some corrosion, the sound source was still operational at the time of recovery as was noted by French colleagues from MARVOR float measurements (M. Ollitraut, pers. comm.). The sound source was connected to the nylon rope with shackles and rings which are made of fire-zinced iron, and a stainless steel swivel to avoid torsion. All these parts are in good condition, too, because in this configuration, corrosion will first attack the shackles and the rings which are chosen to be strong enough to stand it for a long time. The RT 161 housing was greased slightly before deployment and showed no corrosion at all.

When in 1977 on the European side of the Atlantic, John Gould, François Madelain and Gerold Siedler initiated long-term current meter measurements in the Canary and Iberian basins, a one year mooring deployment was the goal, and it was difficult enough to achieve this as some bad experience showed in those days. Some 20 years later at the end of the WOCE field work, electronic equipment, power supplies and mechanical parts seem ready for the challenge to extend mooring deployments to five years on a regular schedule, for certain purposes in the up-coming programmes of CLIVAR and GOOS.

Acknowledgements

It is the careful selection, preparation and on-board handling of all mooring parts which makes successful such long mooring deployments. For this aspect, the work of Dieter Carlsen is particularly appreciated. Financial support came from the Deutsche Forschungsgemeinschaft (M22/3) and the Bundesminister für Forschung und Technologie (Az 03F0157A), both Bonn, Germany; by FASEP (91/0542-7), Sao Paulo; by CNPq (40 3007/91-7), Brasilia; and by the Brazilian-German bilateral programme in marine science and technology (BRA 0033/98 MAR).

References

König, H., K. L. Schultz Tokos, and W. Zenk, 1991: MAFOS: A simple tool for monitoring the performance of RAFOS sound sources in the ocean. J. Atmos. Oceanic Technol., 8(5), 669–676.

Siedler, G., W. Balzer, T. J. Müller, M. Rhein, R. Onken, and W. Zenk, 1993: WOCE South Atlantic 1992, Cruise No. 22, 22 September 1992–31 January 1993. 93-5, Meteor-Berichte, Universität Hamburg, Germany.

Repeat ADCP Survey of the Western Pacific Surface Current by a Commercial Ship

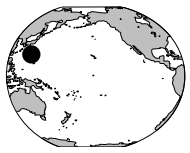

A. Kaneko, N. Gohda, M. Arai, H. Nakajima and Z. Yuan, Hiroshima University, Japan;
T. Sugimoto, University of Tokyo, Japan; and M-H. Radenac, ORSTOM-LODYC, France.
akaneko@ipc.hiroshima-u.ac.jp

The western Pacific is one of the most important regions concerning global climate research. Poleward transport of warm water by the Kuroshio may be part of the coupling mechanism between the tropical and subtropical oceans at the decadal scale. This interaction could also be responsible for modulation of El Niño-Southern Oscillation (ENSO) variability (International CLIVAR Project Office, 1997). The western Pacific is also strongly influenced by the Asian-Australian monsoon system whose interaction with ENSO and especially with its onset phase is still debated. Furthermore, the magnitude of the Indo-Pacific throughflow, which is part of the warm water upper flow of the "conveyor belt" circulation (Gordon, 1986), affects the SST of both the Indian and Pacific Oceans. As the importance of the western Pacific on climate variability is largely acknowledged, recent observational effort is concentrated in regions south of Japan (Imawaki et al., 1997) and in the warm pool of the western equatorial Pacific (Webster and Lukas, 1992; Lukas et al., 1996). Also, operational observations are made along the meridional sections of 137°E and 165°E by the Japan Meteorological Agency (JMA) twice a year (winter and summer). However, there is a major need of enhanced direct velocity measurement in the western Pacific for better understanding seasonal to decadal variability.

An ADCP programme, which started in January 1997, aims at measuring ocean surface currents in the western Pacific on a almost monthly basis. It is intended to run over 10 years. A huge mineral transport ship, the First Jupiter (83,658 t in weight and 289 m in length), equipped with a shipboard RDI-BB 150 kHz ADCP, operates mainly between Japan and Australia (Table 1). The ship routes depend on the situation of international marketing of ore and coal. This is why the third, seventh, and eighth commercial cruises headed for South Africa, Canada, and Europe. During regular cruises, the ship crossing of the Kuroshio south of Japan leads by about five days the crossing of the North Equatorial Current off Philippine, in the source region of the Kuroshio. Time-series of both currents will contribute to monitor the western part of the Pacific Subtropical Gyre. Situated just west of the TAO (Tropical Atmosphere Ocean) array distributed over the tropical Pacific (McPhaden, 1993), meridional distributions of tropical and subtropical surface currents along the ship routes to western Australia provide additional information for prediction of ENSO.

Data quality

In order to accurately measure horizontal velocity, great care is required to process ADCP data from a commercial ship operating at high speed (Hanawa et al., 1996). Although the economical speed of this ship is only 8 m/s (16 knots to be compared to the 24-knot-speed of a ferry), attention is needed to retrieve good quality data and avoid bad measurements. Because the velocity error is proportional to the velocity relative to the ADCP, a major concern during periods of ordinary operation of the ship, is the ship gyro compass error. Therefore, misalignment angles between the ship compass and ADCP transducers, even those smaller than 1°, are specified through a calibration experiment. In this study, it consists in comparing ship velocity data obtained every 20 minutes from the GPS and from the ADCP bottom tracking mode in a shallow-sea operation (Kaneko et al., 1990). Another source of velocity error comes from a rapid change of ship speed and heading in the course of a velocity profile average. Especially rapid

Table 1. Dates and visiting ports for each commercial cruise

	Dates	Visiting Port
1st Commercial Cruise	23 January – 19 February 1997	Port Hedland, Australia
2nd Commercial Cruise	27 February – 2 April 1997	Dampier, Australia
3rd Commercial Cruise	6 April – 31 May 1997	Saldanha Bay, South Africa
4th Commercial Cruise	5 June – 6 July 1997	Port Hedland, Australia
5th Commercial Cruise	10 July – 15 August 1997	Dampier, Australia
6th Commercial Cruise	18 August – 18 September 1997	Dampier, Australia
7th Commercial Cruise	24 September – 21 October 1997	Prince Rupert, Canada
8th Commercial Cruise	31 October 1997 – April 1998 (plan)	Dampier, Australia Rotterdam, Netherlands

changes of ship heading make especially inaccurate velocity data. The standard deviation of ship speed and heading, STD20(VS) and STD20(HD),have been estimated every 20 minutes from initial one-minute data. Velocity data satisfying the conditions STD20(VS) greater than 5 cm/s and STD20(HD) greater than 0.8° are discarded and gaps are filled by applying a linear interpolation. Correlating the above two quantities with the ship velocity difference during the calibration experiment shows that velocity errors greater than 8 cm/s have been filtered out. The separation zone, which develops below the ship bottom from stem to stern, contributes a large bias to the velocity measurement. Because the ADCP transducers are at about 250 m from the stem, the width of the separation zone reaches about 60 m at the transducer position. The separation zone is evidenced because of a rapid increase of vertical velocity (w) from 60 m depth to the surface, while the error velocity (Ve), defined as the difference between vertical velocities obtained from two pairs of ADCP transducers, is nearly zero.

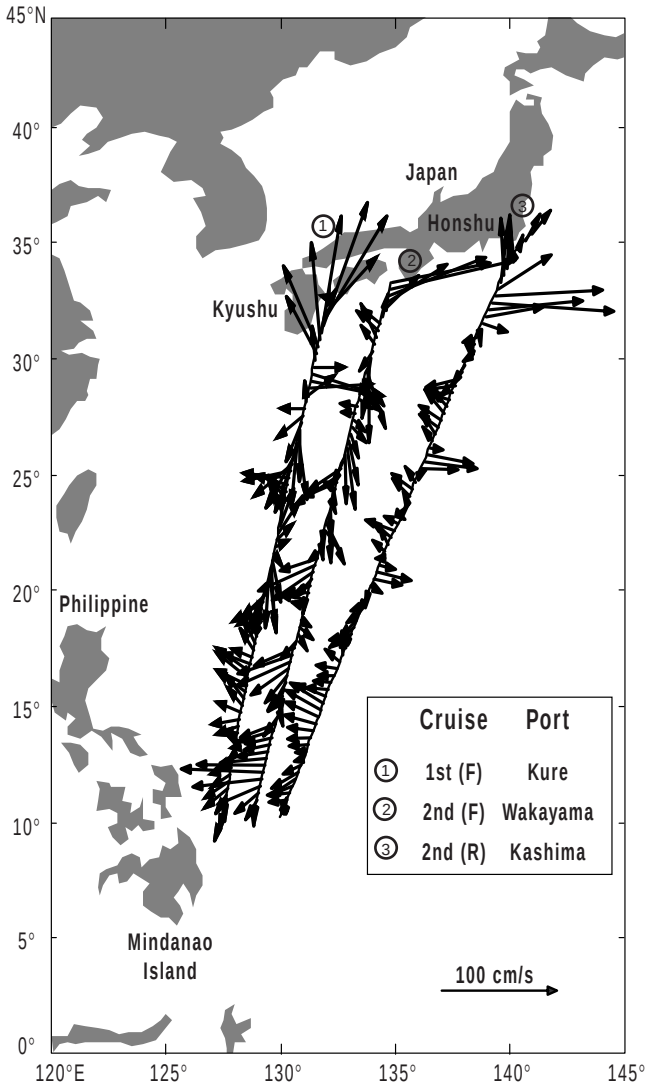

Figure 1. Velocity vectors along the ship routes of the first and second cruises.

Combined with an asymmetric location of the ADCP transducers relatively to the keel, the separation zone induces velocity biases estimated to be greater than 5 cm/s. Thus, considering that the draught of the ship changes from 8 to 18 m, depending on the quantity of cargo, only velocity data at depth greater than 70 m are processed. During the first cruise, an interruption of ADCP measurement occurred accidentally on the way from Japan to western Australia, and the succeeding data were lost. Almost all the return trip data of the sixth cruise have been lost because of writing errors on an optical disk. During other cruises, data have been archived without problems. Analysis of the whole data is still not achieved, and we will comment only the first and second cruises.

Western Pacific velocity variability

The first cruise started from Kure in Japan where the ship was launched. During the second cruise, the ship left Wakayama port and came back to Kashima port because of industrial priorities. All cruises had different routes that merge off Mindanao Island, Philippines (Fig. 1). Horizontal velocity vectors at 100 m depth are also drawn along the ship routes. The Kuroshio south of Japan can be traced as a most prominent, persistent feature. The North Equatorial Current (NEC) shows two westward flowing branches south of 18°N. Note that the separation of the NEC into the Kuroshio and Mindanao Current occurs east of 130°E. The currents directions are highly variable in the region between the Kuroshio south of Honshu and the NEC off Philippine, both with latitude and time. In this region, coherent flow structures have not been observed except the recirculation of the Kuroshio south of Honshu and the variable Subtropical Countercurrent flowing to the east in the zone of 20~23°N (Hasunuma and Yoshida, 1978).

Sections of the zonal and meridional components of velocity along the ship routes are shown in Fig. 2 (page 24) and in Fig. 3 (page 24). The Kuroshio enters the Pacific Ocean at the Tokara Strait and shows a zonal velocity of 80 cm/s at 28°N (Fig. 2a). Approaching the south-east of Kyushu, its direction turns quickly to the north and its magnitude strengthens reaching a maximum velocity of more than 120 cm/s at 31.5°N (Fig. 3a). The meridional velocity decreases rapidly from 110 cm/s at 70 m to 60 cm/s at 200 m, showing a large baroclinicity of the velocity field. The maximum velocity core remains nearly constant downstream (Figs. 2b and c). In contrast, the depth dependent velocity decrease between 70 and 200 m south of Honshu is much smaller than that east of Kyushu. This means that the main stream region of the Kuroshio grows significantly from the east of Kyushu toward the south of Honshu. The NEC is relatively weak during the first cruise and the return trip of the second cruise where the zonal current reaches about 30 cm/s at 16°N (Fig. 2a) and at 14°N (Fig. 2c), respectively. During the outward of the second cruise, the NEC has strengthened remarkably and its maximum velocity is over 70 cm/s at 12°N (Fig. 2b). The NEC weakens when El Niño occurs (Toole et al., 1990;

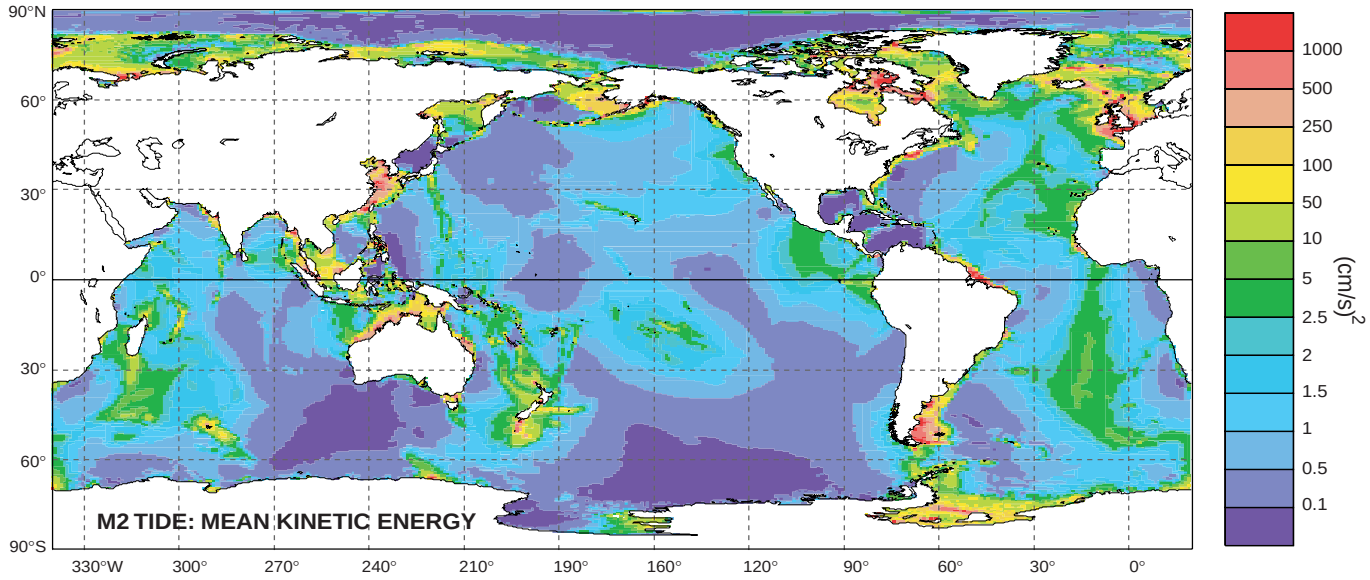

Lyard et al., page 36, *Figure 2. Mean kinetic energy of the M2 tidal currents, in* cm^2/s^2. *The colour scale allows illustratration of both (a) the intensity of deep ocean currents (with typical mean kinetic energy of the order of 1, 2.5, 5, 7.5, 10* cm^2/s^2*) and (b) the shallow water fields (with typical amplitudes of several 100* cm^2/s^2*).*

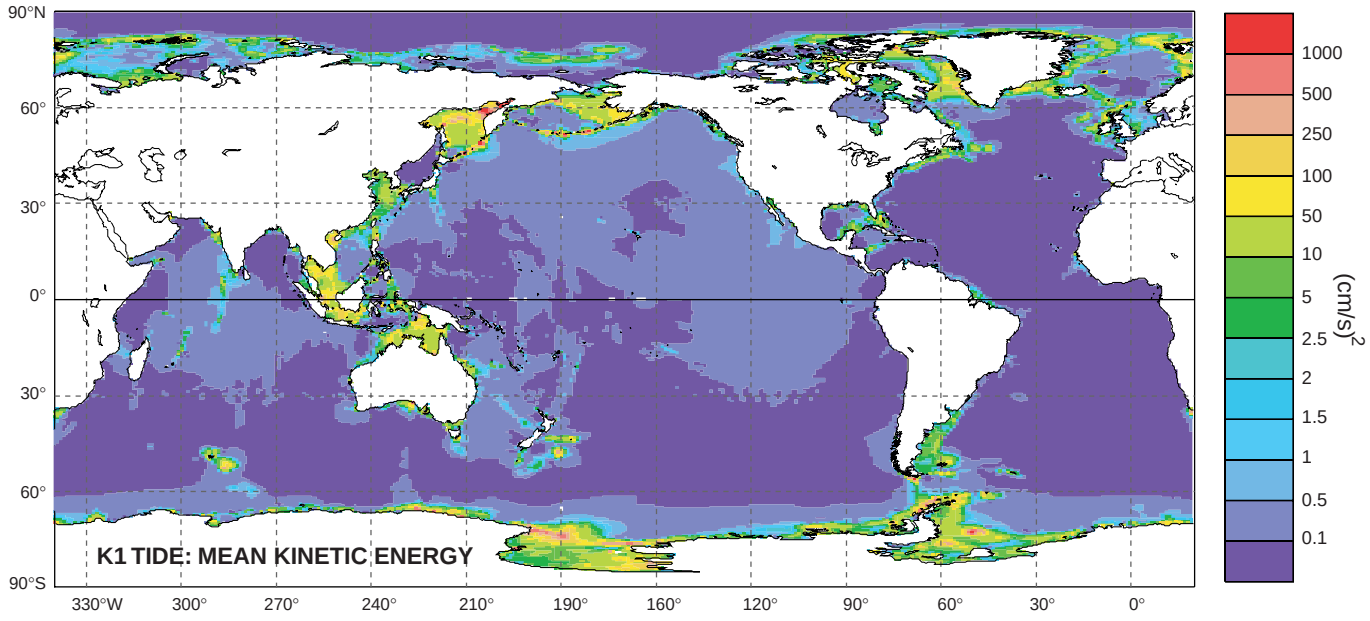

Lyard et al., page 36, *Figure 4. Mean kinetic energy of the K1 tidal currents, in* cm^2/s^2, *with the same scale as for* Fig. 2.

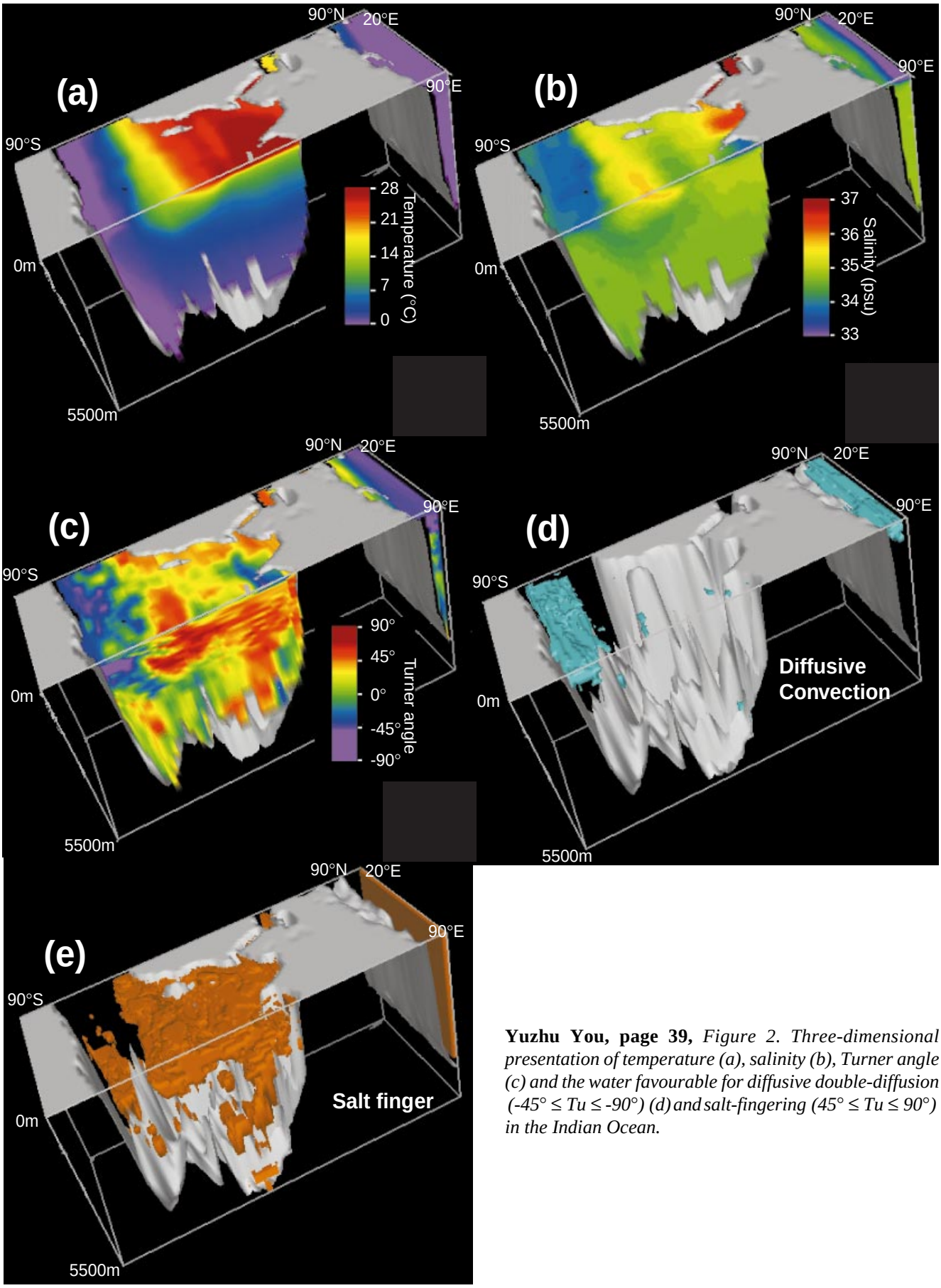

Yuzhu You, page 39, *Figure 2. Three-dimensional presentation of temperature (a), salinity (b), Turner angle (c) and the water favourable for diffusive double-diffusion (-45° ≤ Tu ≤ -90°) (d) and salt-fingering (45° ≤ Tu ≤ 90°) in the Indian Ocean.*

Yuan et al., 1995) and the above variability of the NEC associated with the 1997 El Niño should be considered.

The velocity data of this programme are opened for public use as soon as the processing of individual cruises is achieved. The web site (http://www.ocean.hiroshima-u.ac.jp) gives information to scientists interested to use the velocity data for their own purposes.

Acknowledgements

We express our sincere thanks to Mr H. Miyata, the deputy director of the Ship Division of Daiichi Chuo Kisen Kaisha, for his great support for installing the ADCP on the hull of the huge mineral transport ship First Jupiter. The captain and crew of the First Jupiter are also acknowledged for their assistance in shipboard work.

References

CLIVAR, 1997: CLIVAR – a research programme on climate variability and predictability for the 21st century. ICPO No. 10, 47 pp., International CLIVAR Project Office, Hamburg, Germany.

Gordon, A. L., 1986: Interocean exchange of thermocline water. J. Geophys. Res., 91, 5037–5046.

Hanawa, M., Y. Yoshikawa, and T. Taneda, 1996: TOLEX-ADCP monitoring. Geophys. Res. Lett., 23, 2429–2432.

Hasunuma, K., and K. Yoshida, 1978: Splitting of the subtropical gyre in the western north Pacific. J. Oceanogr. Soc. Japan, 34, 160–172.

Imawaki, S., H. Uchida, H. Ichikawa, M. Fukasawa, S. Umatani, and ASUKA Group, 1997: Time series of the Kuroshio Transport derived from field observations and altimetry data. Int. WOCE Newsl., 25, 15–18.

Kaneko, A., W. Koterayama, H. Honji, S. Mizuno, K. Kawatate, and R. L. Gordon, 1990: A cross-stream survey of the upper 400 m of the Kuroshio by an ADCP on a towed fish. Deep-Sea Res., A, 37, 875–889.

Lukas, R., T. Yamagata, and J. P. McCreary, 1996: Pacific low-latitude western boundary current and the Indonesian Throughflow. J. Geophys. Res., 101(C5), 12209–12216.

McPhaden, M. J., 1993: TOGA-TAO and the 1991–1993 El Niño-Southern Oscillation Event. Oceanogr., 6, 36–44.

Toole, J. M., R. C. Millard, Z. Wang, and S. Pu, 1990: Observations of the Pacific North Equatorial Current bifurcation at the Philippine coast. J. Phys. Oceanogr., 20, 307–318.

Webster, P. J., and R. Lukas, 1992: TOGA COARE – the Coupled Ocean-Atmosphere Response Experiment. Bull. Am. Meteorol. Soc., 73, 1377–1416.

Yuan, G., I. Nakano, H. Fujimori, and A. Kaneko, 1995: Long-term measurement of temperature variability off Mindanao Island by the ocean acoustic tomography. J. Oceanogr., 51, 327–339.

Second International Conference on Reanalyses
on 23–27 August 1999 at Wokefield Park, Mortimer, Reading, UK

Reanalyses of the instrumental atmosphere ocean and land data record, produced by modern data assimilation methods, provide a key resource for many activities of the World Climate Research Programme, in particular for the atmospheric modelling studies of the Working Group on Numerical Experimentation (WGNE), and the investigations being undertaken within the Global Energy and Water Cycle Experiment (GEWEX), the World Ocean Circulation Experiment (WOCE), and the Climate Variability and Predictability (CLIVAR) programme.

Fundamental topics of interest include:

- the deepening of our understanding of low frequency variability,
- the development and validation of coupled atmosphere-ocean-land-ice-chemistry models,
- the assessment of predictability, spanning the medium-range time-scale through seasonal and interannual time-scales to decadal time-scales.

The Second International Conference on Reanalyses to be held on 23–27 August 1999 at Wokefield Park, Mortimer, Reading, UK, will assess progress and problems in exploiting reanalyses for these purposes. It will also identify the main priorities for further work in exploitation of existing reanalyses and for the preparation of new reanalyses.

The subject areas to be considered will include:

- Global reanalysis datasets, Analysis methodology, Impact of data inhomogeneities, Estimation of data bias, Evaluation against independent observation data sets,
- Diagnosis from reanalyses of Global and Regional Aspects of the Hydrological Cycle, the Energy Cycle, and the Angular Momentum Cycle,
- Diagnosis from reanalyses of the mechanisms of atmosphere and ocean phenomena such as the Madden-Julian oscillation, stratospheric variability, inter-annual variability in Monsoons and tropical cyclone frequency, and ENSO variability,
- Use of Reanalyses for driving ocean, land, sea-ice and chemistry models, and for development and validation of Climate System Models and their sub-systems,
- Medium-range, Seasonal-to-Interannual and Decadal Predictability Studies using Reanalyses,
- Future Requirements and Plans.

The format will include two invited talks per day, with normal presentations lasting 15–20 minutes. The poster sessions will be social occasions in congenial surroundings.

Wokefield Park is a modern fully equipped conference centre set in parkland a few miles from Reading and featuring an eighteen hole golf course.

For further information see:

http://www.ecmwf.int/conf.

For specific queries contact the chair of the Local Organising Committee: Dr D. Burridge, ECMWF, Shinfield Park, Reading, RG2 9AX, UK, Tel: +44 118 949 9000, Fax: +44 118 986 9450, e-mail Reanalyses2@ecmwf.int.

The Conference is sponsored by the World Climate Research Programme, European Centre for Medium-Range Weather Forecasts, National Aeronautics and Space Administration and the American Meteorological Society.

A Model for Predicting the Barotropic Component of Ocean Tidal Currents

F. Lyard, C. Le Provost and F. Lefèvre, Laboratoire d'Etude en Géophysique et Océanographie Spatiales, LEGOS, France. Florent.Lyard@cnes.fr

Ocean tides contribute to more than 80% of the sea level variability over the deep ocean. This is the reason why a unique effort has been made over the last 5 years to improve our ability to predict them at the world ocean scale (Shum et al., 1997). This renewed interest for an ancient but still partially resolved geophysical problem has been motivated by the development of satellite altimetry as a major remote sensing technique to observe surface ocean currents in geostrophic balance with the ocean topography slope (Fu et al., 1994). The primary objective of these studies has been to improve prediction of sea level variations due to tides under the tracks of the altimetric satellites. Tides are gravity waves. Then, over the deep ocean, tidal waves of the order of one metre amplitude induce only weak currents, of the order of a few cm/s amplitude: this is the reason why the interest has been focused on tidally induced sea level variations, not tidal currents. However one must keep in mind that the tides are a major contribution to the horizontal movements in the coastal areas, with amplitudes often of the order of 1 m/s and even more.

But nowadays, interest is also focusing on tidal currents. The following three examples can be given to illustrate the reasons of this growing interest: the role of internal tidal wave breaking in controlling the vertical mixing in the ocean (Polzin et al., 1997), the contribution of tidal currents in bottom boundary layer dissipation of the ocean circulation (The Dynamo Group, 1997), the need for open ocean tidal current predictions for the exploitation of acoustic Doppler current profilers (Firing, 1998). Among the many tidal solutions produced recently, only a few of them computed simultaneously sea level and tidal current. Most of these solutions were derived from the analysis of altimetric sea level measurements: tidal currents are deduced from the gradient of the elevation solutions, hence a degraded accuracy. This was already noted by Cartwright and Ray (1991) when computing tidal energy fluxes from their altimetric tidal solutions. The advantage of the solutions deduced from a hydrodynamic model, possibly combined with data assimilation, is that it allows the simultaneous computation of tidal elevations and tidal currents, with the same level of accuracy. Our FES94.1 and FES95.2 solutions are among this class of new tidal solutions. The aim of this paper is to present the tidal current solution associated with the purely hydrodynamic FES 94.1 tidal sea level solution (Le Provost et al., 1994).

The CEFMO model

The approach developed to model the ocean tides at the global scale has been extensively presented in previous papers (see Le Provost et al., 1994, for a recent synthesis). Its major characteristics are the following.

- The basic equations on which the model is built are the fully non-linear barotropic shallow water equations.
- Tides are forced in these equations by the astronomical tidal potential complemented by the secondary effects due to earth tides, ocean loading and self attraction.
- Dissipation is parameterised by (only) bottom fric-

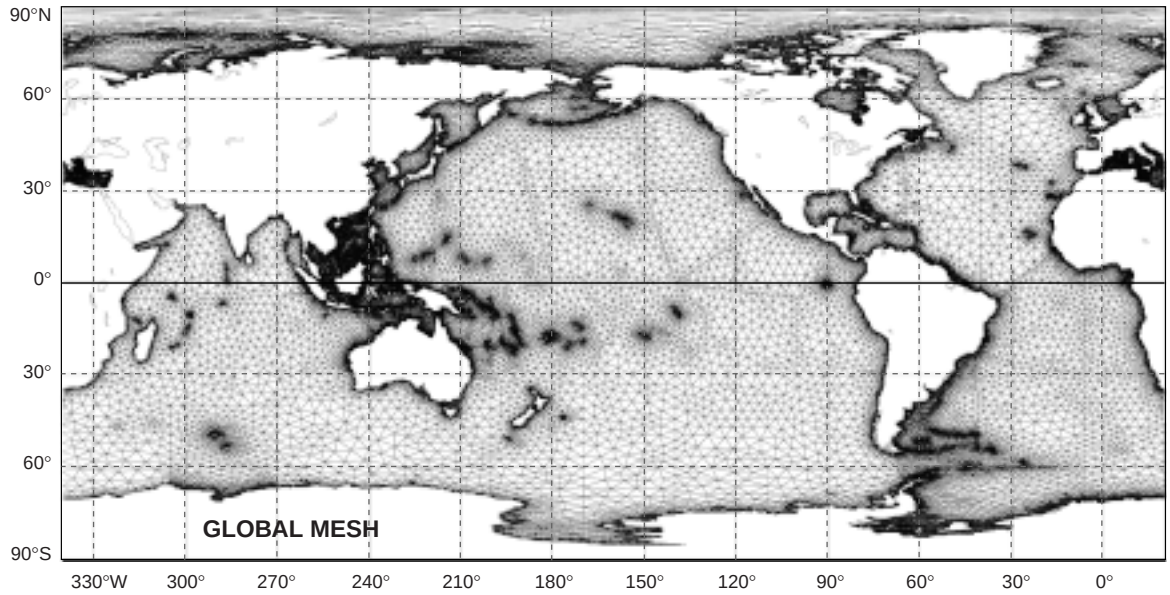

Figure 1. Global mesh of the finite element discretisation used in the FES94.1 solution.

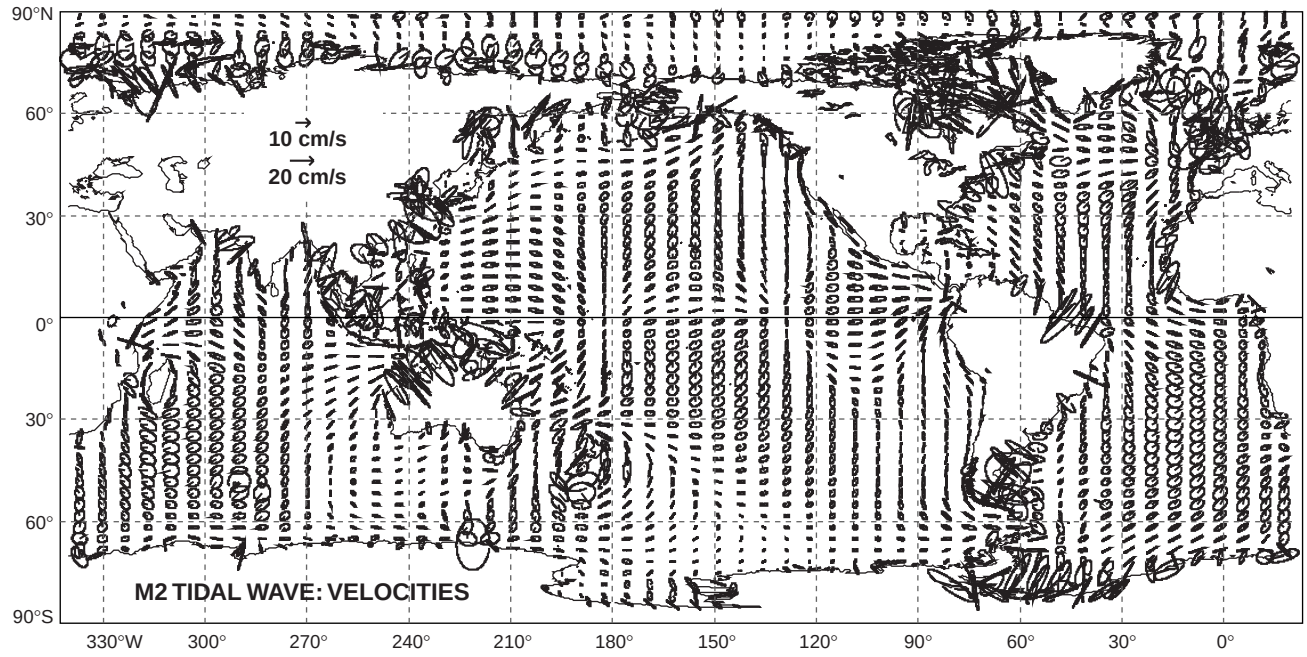

Figure 3. Gridded visualisation of the M2 tidal current hodographs, allowing to illustrate the degree of ellipticity of the velocity field, and the sense of rotation of the current over a tidal cycle. The scale is non-linear, in order to allow representation on the same graph the velocity field over the deep ocean and the shelves.

tion formulated as quadratically dependant on the local velocity field. (It is now clearly recognised as a weak point that the energy sink associated to the generation of internal tidal wave is ignored at the present stage of development of the model).

- The unknowns (sea surface variations and barotropic horizontal velocities) are a priori modelled under a spectral expansion in time, based on the well known spectrum of the tidal potential.
- The non-linearities are taken into account through the use of a perturbation method allowing consideration of the wave-wave interactions, although the resolution for each tidal component is basically reduced to linear systems. A major step in this formulation is a quasi-linearisation of the quadratic bottom friction, where non-linearities are solved in an iterative scheme.
- Loading and self-attraction contributions are estimated a priori, derived from the previous Schwiderski (1980) solution.

One major innovation of this hydrodynamic model has been the use of a finite element technique for solving the problem over the world ocean, with non-structured grids allowing refinement of the computational mesh over topographic features and down to a few kilometres along the coasts, typically 10 km (Fig. 1).

For the production of the FES94.1 solution, the P2 Lagrange approximation of the solution has been used as the basic function on each triangle, for the sea surface elevation alpha. The u and v (West-East, and South-North) components of the mean vertically integrated (or barotropic) velocities have been directly derived from the gradients of alpha. Consequently, they are defined on the basis of a P1 approximation on each triangle, with normal discontinuities at the triangle limits. The velocity solutions delivered in the following are gridded values interpolated on a half degree grid from the initial values taken at the Gauss points. Alternatively one can solve the dynamic equations, taking alpha as a known forcing term deduced from the elevation solution, and seeking for P2 approximation of the velocity field. This approach has been implemented, but is not currently used because of its higher numerical cost plus the difficulty to estimate the gain in accuracy compared to the direct derivation.

Solutions for the M2 and K1 main tidal components

There are several ways to define tidal velocity fields:

(a) complex (amplitude and phase) description of the two orthogonal components u and v,

(b) spatial distribution of the amplitude, direction and phase of the major axis of the current ellipse, and its eccentricity,

(c) graphic visualisation of a discrete distribution of the current ellipses.

We show in the following a graphic display of some of these representations. But the full solutions which are made available on our ftp site are defined under form (a), in the data base associated with the prediction model (see the end of this note).

The M2 velocity field

The M2 tidal current amplitudes are of the order of a few cm/s over the deep ocean, but can reach several m/s over specific areas on continental shelves such as around capes.

Fig. 2 (page 33) gives the spatial distribution at the global scale of the mean kinetic energy of the M2 tidal currents, integrated over one tidal period. These values correspond to the average of the square of the maximum a and minimum b of intensity of the velocity over a tidal cycle, i.e. 0.5 $(a^2 + b^2)$. Amplitudes are typically of the order of a few cm/s in the deep ocean, intensified over some of the mid-ocean ridges, but not everywhere: it is the case in the Atlantic Ocean, but not in the South Pacific for example. As expected, the currents are considerably increased over the continental shelves where they can reach half a metre per second or higher. Fig. 3 allows the visualisation of the degree of ellipsicity of the tidal current, its direction, and its polarisation. Note the main direction of the tidal currents perpendicular to the coast in many areas: the Patagonian shelf break, the Amazonian shelf, where tidal energy is effectively dissipated by bottom friction, as identified for example in Le Provost and Lyard, 1997.

The K1 velocity field

The amplitude of the diurnal constituents are smaller, as expected from what is known for the sea level tidal variations. However, in Fig. 4 (page 33), where the colour scale is the same as for Fig. 2, we can observe the presence of intensified spots of diurnal currents. Some of them correspond to areas where tides are diurnally dominant or at least of mixed character: in the Yellow Sea, China Sea, Arafura Sea. Others are related to topographic Rossby wave features: along most of the continental shelf breaks in the North Atlantic, at latitude larger than the critical latitude (near 30°), over the Arctic and around Antarctica. In particular, such signatures can be seen along the edge of the ice shelves of the Weddell Sea and the Ross Sea.

Validation

It is not easy to validate these numerical solutions. Tidal velocity measurements are sparse over the ocean, and it is not easy to separate within the measurements the baroclinic contributions from the barotropic one. We have started to analyse the WOCE current meter data set, but the results are not yet available. Luyten and Stommel (1991) published a compilation of current meter analysis and checked the validity of the tidal current fields proposed by Schwiderski (1980). The distribution of these data is limited to the North West Atlantic, the Kuroshio, and three clusters in the Agulhas retroflection area, the West Equatorial Indian Ocean, and near 140°W in the Equatorial Pacific. Unfortunately, when referring to Fig. 2, it appears that these data are in areas of weak tidal currents. The comparison of our M2 solution with this data set leads to the conclusion that, over these limited areas, the r.m.s. differences are of the order of 3 mm/s for typical current intensities of 1 to 2 cm/s.

A tidal current prediction code

The FES94.1 solution contains eight components: M2, S2, N2, K2, 2N2, K1, O1, and Q1. The associated tidal elevation prediction code included 13 components, including these 8 constituents, plus 5 others deduced by admittance: Mu2, Nu2, L2, T2 and P1 (Le Provost et al., 1994). For the FES95.2 prediction code, the number of constituents has been extended to 26 (Le Provost et al., 1998).

We have implemented a similar prediction code for predicting the barotropic component of the tidal currents everywhere over the ocean. For the time being, this code relies on a gridded description of the amplitude and phase of the u and v components of the 8 above cited major constituents, completed by admittance by the same 18 minor constituents taken into account in FES95.2. This code allows everywhere, at every time, the computation of barotropic component of the tidal current field. It is available on our ftp site (for further access, please contact techine@pontos.cst.cnes.fr).

It is clear that this model has to be used with caution, because it has not been yet fully validated. However, we have decided to make it available, in response to the inquiry of several scientists of our international community.

References

Cartwright, D. E., and R. D. Ray, 1991: Energetics of global ocean tides from Geosat altimetry. J. Geophys. Res., 96(C12), 16897–16912.

Firing, E., 1998: Lowered ADCP development and use in WOCE. Int. WOCE Newsl., 30, 12–14.

Fu, L. L., E. J. Christansen, C. A. Yamarone, M. Lefebvre, Y. Menard, M. Dorrer, and P. Escudier, 1994: TOPEX/POSEIDON mission overview. J. Geophys. Res., 99(C12), 24369–24381.

Le Provost, C., M. L. Genco, F. Lyard, P. Vincent, and P. Canceil, 1994: Tidal spectroscopy of the world ocean tides from a finite element hydrodynamic model. J. Geophys. Res., 99(C12), 24777–24798.

Le Provost, C., and F. Lyard, 1997: Energetics of the M2 barotropic ocean tides: an estimate of bottom friction dissipation from a hydrodynamic model. Prog. Oceanogr., 40, 37–52.

Le Provost, C., F. Lyard, J. M. Molines, M. L. Genco, and F. Rabilloud, 1998: A hydrodynamic ocean tide model improved by assimilating a satellite altimeter-derived data set. J. Geophys. Res., 103(C3), 5513–5529.

Luyten, J. R., and H. M. Stommel, 1991: Comparison of the M2 tidal currents observed by some deep moored current meters with those of the Schwiderski and Laplace models. Deep-Sea Res., 38, S573–S589.

Polzin, K. L., J. M. Toole, J. R. Ledwell, and R. W. Schmitt, 1996: Spatial variability of turbulent mixing in the abyssal ocean. Science, 276, 93–96.

Shum, C. K., P. L. Woodworth, O. B. Andersen, G. Egbert, O. Francis, C. King, S. Klosko, C. Le Provost, X. Li, J. M. Molines, M. Parke, R. Ray, M. Schlax, D. Stammer, C. Thierney, P. Vincent, and C. Wunsch, 1997: Accuracy assessment of recent ocean tide models. J. Geophys. Res., 102(C11), 25173–25194.

Schwiderski, E. W., 1980: Ocean tides, A hydrodynamic interpolation model. Mar. Geod., 3, 219–255.

The Dynamo Group, 1997: Dynamics of North Atlantic models. Final Scientific Report, Institute für Meereskunde, Kiel, Germany.

Dianeutral Circulation in the Indian Ocean

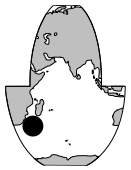

Yuzhu You, Institut für Meereskunde, Kiel, Germany. you@ifm.uni-kiel.de

In a recently held workshop of the Indian Ocean World Ocean Circulation Experiment (WOCE) in New Orleans in September 1998, the topic "meridional overturning of the Indian Ocean" was ranked as the first topic issue to address and discuss. The leading speakers and participants reviewed various updated efforts from observations and models. Large gaps were recognised as existing between different approaches on overturning transport scales and mechanisms. It was still unclear if there was a large overturning component in the deep water of the northern Indian Ocean (below 2000 m). The workshop concluded with a demand for results from high quality WOCE data, now in an intensive analysis phase. This note aims to offer the pre-WOCE information from different angle on dianeutral circulation (an equivalent term to meridional overturning) based on the results of the author's recent studies (published and submitted).

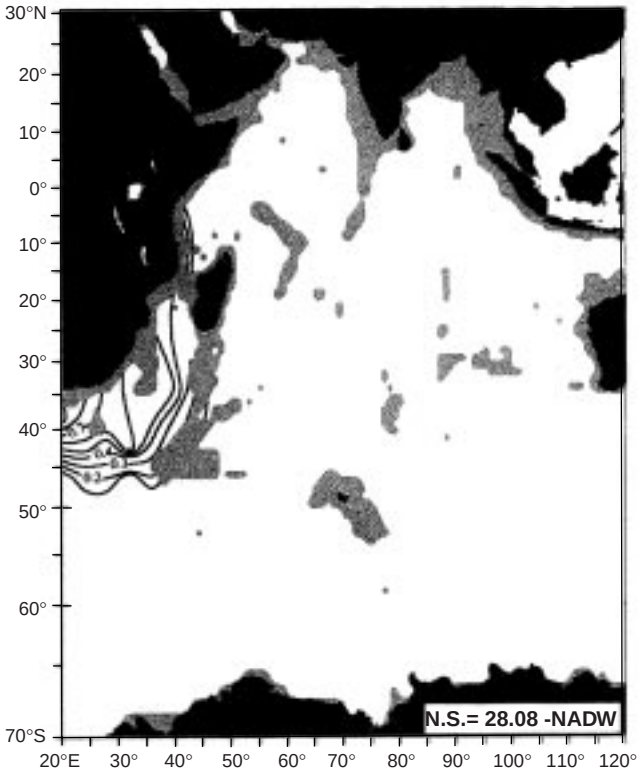

Figure 1. Water mass contribution of North Atlantic Deep Water on neutral surface σ_N = 28.08, in the deep Indian Ocean (at about 3000 m).

Introduction

According to Stommel and Arons' (1960) view of the deep ocean, the deep ocean circulation is driven by sources in the Weddell Sea and North Atlantic, compensated by uniform upwelling over the rest of the world oceans. The North Atlantic part is now often called the "great ocean conveyor" or "thermohaline conveyor belt" (Broecker, 1991; Schmitz, 1996). In the Indian Ocean case, the "conveyor belt" part, i.e., the North Atlantic Deep Water (NADW), only mostly reaches the south-west Indian Ocean west of the Madagascar Ridge and south of Davie Ridge due to the ridge blocking (Toole and Warren, 1993; You, 1998a). Fig. 1 shows the water mass contribution by NADW in the Indian Ocean on the neutral surface $\sigma_N = 28.08$ whose depth is about 3000 m (here σ_N denotes neutral density similar to σ_θ used for potential density). The NADW is confined to only in the Mozambique Basin and Agulhas Basin. The reason is that the NADW core deepens from 1800 m at the equatorial Atlantic (referring to its salinity maximum) to about 3000 m south of Africa which is already below the ridge crest of the Madagascar Ridge (whose depth range is mostly located between 1500–2500 m) (You, 1998a; You and Siedler, 1998). The real contributor to the major deep Indian basin overturning is therefore the Circumpolar Deep Water (CDW) which is injected with NADW characteristics (high salinity and oxygen and low nutrients) by entrainment from south of the Madagascar Ridge. On the other hand, although Fig. 1 indicates that NADW terminates in the western Indian Ocean, it also implies that the continuation of NADW farther into the abyssal Indian and Pacific Oceans is through the CDW by their merging to the south of the Madagascar Ridge.

The Weddell Sea part was recently reported to feed the bottom water of the Indian Ocean from the south-west with a transport of about 1 Sv (Haine et al., 1998).

For discussing overturning transport, I give a brief review of the updated results. From geostrophic calculations, Toole and Warren (1993) determined 27 Sv ($1\,\mathrm{Sv} = 10^6\ \mathrm{m^3\,s^{-1}}$) upward across 2000 m north of 32°S. This estimate is reduced by about half to 13 Sv by Robbins and Toole (1997) after referring to a silicate budget. A large difference also exists in two inverse calculations, 3.5 Sv by Fu (1986) and 16 Sv by Macdonald (1995) below 2000 m. From a general circulation model (Cox/Bryan type), Lee and Marotzke (1997) estimated 14 Sv above 1000 m and only 2 Sv below 2000 m. Schmitz (1996) thus gave a speculative number of 4 Sv at upper intermediate level for NADW replacement.

Conveyor transport

The conveyor transport in the Indian Ocean is achieved through CDW transformation. In a most recent study, You (1999) showed CDW transport across four deep neutral density surfaces, $\sigma_N = 27.95$ (at about 2000 m), $\sigma_N = 28.02$ (at about 2500 m), $\sigma_N = 28.08$ (at about 3000 m) and $\sigma_N = 28.12$ (at about 3500 m) (see Fig. 13 of You (1999)). The dianeutral transport is calculated through the dianeutral velocity e (McDougall and You, 1990)

$$e = D_z + DgN^{-2}\left[aq_{zz} - bS_{zz}\right] + gN^{-2}\left[bF_z^s - aF_z^q\right] - KgN^{-2}\left\{C_b\nabla_n q\cdot\nabla_n q + T_b\nabla_n q\cdot\nabla_n P\right\} \quad (1)$$

where e is the total dianeutral velocity, D and K are dianeutral and epineutral diffusivities, g is the gravitational acceleration, N^2 the square of the buoyancy frequency, a and b are appropriate thermal expansion and haline contraction coefficients, F^θ and F^S are heat and salt fluxes due to salt-fingering, C_b is cabbeling and T_b is thermobaricity. A variety of processes can contribute to the dianeutral velocity e, including the vertical variation of vertical diffusivity (the first term on the right-hand side of (1)), vertical turbulent mixing (the second term), double diffusion (the third term), and cabbeling and thermobaricity (the combined fourth term). Dianeutral motion can cause water parcels to change their density, and as a consequence, the field of isopycnals evolves so that the relative motion between a fluid parcel and an isopycnal is constrained by (1). You (1999) showed predominant dianeutral downwelling transport in the southern Indian Ocean which was well contrasted to the predominant dianeutral upwelling transport in the northern Indian Ocean. A large extent of uniform dianeutral upwelling transport was found in the northern Indian Ocean north of 40°S (north of Antarctic frontal zone), in agreement with the conveyor belt scheme.

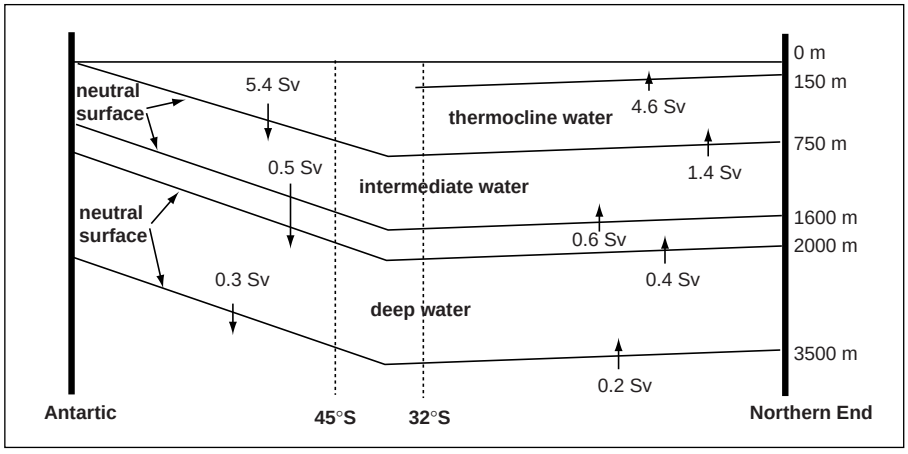

Figure 3. Summarised sketch diagram showing the dianeutral circulation in the Indian Ocean. The given numbers are net integrated transport values in Sv.

Meridional transformation of southern water to the north examined by Turner angle

Meridional circulation and water-mass transformation can also be examined by the Turner angle (after J. Stewart Turner), Tu, which is defined as four quadrant arctangent (McDougall et al., 1988)

$$\mathrm{Tu(deg)} = \tan^{-1}\left(\alpha\frac{\partial\theta}{\partial z} - \beta\frac{\partial S}{\partial z}, \alpha\frac{\partial\theta}{\partial z} + \beta\frac{\partial S}{\partial z}\right). \quad (2)$$

Clear physical meaning contained in Tu was interpreted by McDougall et al. (1988) through a sketch. When Tu is between -45° and -90°, "diffusive" double diffusion is possible, for Tu between -45° and 45° the water column is doubly stable which means that the water column is stably stratified with respect to both potential temperature and salinity and with Tu between 45° and 90° "salt-fingering" double diffusion can be expected. You (1996), You (1998b) and You (1999) has mapped Tu in thermocline, intermediate and deep water layers of the Indian Ocean on neutral surface frame. He found that various deep waters can also satisfy the condition favourable for salt-fingering which has largely been discussed in the past only in Central Water.

In Fig. 2 (page 34), I present the Turner angle in a traditional way on geopotential level to be consistent with the climatological atlas of Levitus data (1994 CD-ROM) which was applied to form the figures. These 3D figures are part of a global ocean atlas of the Turner angle in You (1998c). To best see the Indian Ocean area and the vertical structure at the same time, I choose the vertical section cut at 90°E. The basic temperature and salinity distributions are shown in Figs. 2a and 2b and the Turner angle, Tu (degree), in Fig. 2c. Diffusive double-diffusion ($-45° \le \mathrm{Tu} \le -90°$) is found near Antarctica in the upper layer (the dark blue and mauve colour). Its northward deep extension is characterised by a tongue of doubly-stable condition. The diffusive and doubly-stable structure corresponds to the Antarctic Intermediate Water (AAIW) formation (the low salinity tongue in Fig. 2b). To view clearly the diffusive water near Antarctica, I present the diffusion alone in Fig. 2d in blue colour. The finding of diffusive water near Antarctica by the Turner angle appears to support the traditional idea that AAIW is formed near Antarctica rather than in the south-east Pacific and north of Drake Passage. A series of recent data and model studies considered these two places to be the major AAIW production sites. Perhaps, major pathway points of AAIW is more correct, from a point of view of the flow fields of AAIW. This is because, obviously, the source of low

salinity water of AAIW has to come from the sea surface which can be provided only near Antarctica through precipitation and ice melting during the austral summer. The fresh water feeds AAIW through diffusive convection as cool/fresh water lies at the sea surface. It seems that more discussion is required concerning the conjecture of AAIW production sites in the south-eastern Pacific and north of Drake Passage. A coarse resolution model study cannot resolve the much smaller scale processes of diffusive convection.

The red colour in the Turner angle figure (Fig. 2c) indicates the water favourable for salt-fingering ($45° < Tu < 90°$) which is found extensively in the main thermocline and the deep water of the northern Indian Ocean. The water favourable for salt-fingering is also found in the deep water near the Antarctic which is not from the northern Indian Ocean but is the origin of NADW (You, 1999). To see clearly the salt-fingering water, likewise, I present it alone in Fig. 2e in red colour. It is quite clear that the relatively high salinity found in the deep northern Indian Ocean is from the upper layer carried down by salt-fingering fluxes. The reason is that, in the northern Indian Ocean, the warm and salty water in the upper layer contribute to the salt-fingering in the entire water columns as the temperature and salinity values decrease almost monotonously with the depth. This idea has been put forward by You (1999) and You (1998a).

Dianeutral circulation

Fig. 3 assembles recent dianeutral transport calculations in the Indian Ocean by You (1996) in the main thermocline, You (1998b) in the intermediate layer and You (1999) in the deep water. North of 32°S, an integrated transport of 0.2 Sv was found across the lowermost neutral surface (about 3500 m) and 0.4 Sv across the uppermost neutral surface (about 2000 m) in the deep water layer. In the intermediate layer, You (1998b) found a net upward transport of 0.6 Sv. The transport further increases to 1.4 Sv across the lower thermocline and 4.6 Sv across the upper thermocline (You, 1996). The steady increase of dianeutral upwelling from 0.2 to 4.6 Sv implies the increasing advective transport upward from the Southern Ocean to north of 32°S. This can be examined in the Southern Ocean as follow. As a result, dianeutral transport provides at least 4.6 Sv into the surface layer of about 150 m which returns to the south most likely through Agulhas Current system.

In responding to the rising water in the north, the same process shows a steady sinking water south of 45°S. A strong integrated dianeutral transport of 5.4 is found across the upper intermediate layer downward. However, only a small net transport of 0.5 Sv crosses the lower intermediate layer downward (You, 1998b). The great difference of 10 times more across the upper layer than across the lower layer gives a strong implication for the equatorward advection of AAIW. In the deep water, only 0.3 Sv is estimated to cross the lower layer of the deep water south of 45°S. The concluding result of dianeutral circulation in Fig. 3 suggests a weak deep circulation of the Indian Ocean, consistent with the model study of Lee and Marotzke (1997).

Acknowledgement

I thank Michio Kawamiya for the help to the 3D plots in Fig. 2.

References

Broecker, W. S., 1991: The great ocean conveyor. Oceanogr., 4, 79–89.

Fu, L.-L., 1986: Mass, heat and freshwater fluxes in the South Indian Ocean. J. Phys. Oceanogr., 16, 1683–1693.

Haine, T. W. N., A. J. Watson, M. I. Liddicoat, and R. R. Dickson, 1998: The flow of Antarctic Bottom Water to the southwest Indian Ocean estimated using CFCs. J. Geophys. Res., 103(C12), 27637–27654.

Lee, T., and J. Marotzke, 1997: Inferring meridional mass and heat transports of the Indian Ocean by fitting a general circulation model to climatological data. J. Geophys. Res., 102(C5), 10585–10602.

Macdonald, A., 1995: Oceanic fluxes of mass, heat, and freshwater: A global estimate and perspective. PhD dissertation, 326 pp., Massachusetts Institute of Technology, Cambridge, MA, USA.

McDougall, T. J., and Y. You, 1990: Implications of the nonlinear equation of state for upwelling in the ocean interior. J. Geophys. Res., 95, 13263–13276.

McDougall, T. J., S. A. Thorpe, and C. H. Gibson, 1988: Small-scale turbulence and mixing in the ocean: A glossary. In: Small-scale turbulence and mixing in the ocean, J. C. J. Nihoul and B. M. Jamart (eds.), 3–9, Elsevier, Amsterdam, Netherlands.

Robbins, P. E., and J. M. Toole, 1997: The dissolved silica budget as a constraint on the meridional overturning circulation of the Indian Ocean. Deep-Sea Res., 44, 879–906.

Schmitz, W. J., 1996: The Pacific and Indian Oceans/A global update, on the world ocean circulation, Volume II. Technical Report WHOI-96-08, 237 pp., Woods Hole Oceanographic Institution, Woods Hole, MA, USA.

Stommel, H., and A. B. Arons, 1960: On the abyssal circulation of the world ocean, I, Stationary planetary flow patterns on a sphere. Deep-Sea Res., 6, 140–154.

Toole, J. M., and B. A. Warren, 1993: A hydrographic section across the subtropical South Indian Ocean. Deep-Sea Res., I, 40, 1973–2019.

You, Y., 1996: Dianeutral mixing in the thermocline of the Indian Ocean. Deep-Sea Res., I, 43(3), 291–320.

You, Y., 1998a: Implications of the deep circulation and ventilation of the Indian Ocean on the renewal mechanism of North Atlantic Deep Water. J. Geophys. Res., submitted.

You, Y., and G. Siedler, 1998: Modification of North Atlantic Deep Water in the South Atlantic. J. Geophys. Res., submitted.

You, Y., 1998b: Dianeutral mixing and transformation of Antarctic Intermediate Water in the Indian Ocean. J. Geophys. Res., 103(C13), 30941–30972.

You, Y., 1998c: A global ocean atlas of the Turner angle: Implication for double-diffusion and water mass structure. Deep-Sea Res., I., submitted.

You, Y., 1999: Dianeutral mixing, transformation and transport of the deep water of the Indian Ocean. Deep-Sea Res., I, 46, 109–148.

Second Announcement

WOCE North Atlantic Workshop, Kiel, Germany, 23–27 August 1999

Objectives and structure

The purpose of the Workshop will be to review recent scientific results that have been obtained from observations and modelling on the North Atlantic circulation, pathways and water mass distributions; on thermohaline overturning and flux divergences; and on the important water mass modification processes, and to identify problems and outstanding research requirements.

While the main interest will be on the WOCE period, the decadal variability of the North Atlantic and its relation to the atmosphere and climate as well as conclusions regarding future observational requirements will also be Workshop objectives. The Workshop aims at facilitating scientific collaboration towards achieving WOCE objectives, preparing synthesis products and co-ordinating joint publications.

The workshop will consist of:

- sessions with invited and contributed presentations (see below)
- poster presentations to session topics
- working group discussions

Session structure (tentative)

1. **North Atlantic circulation, pathways and water mass distributions from WOCE observations, altimetry and model results**
   Chair: R. Molinari (molinari@aoml.noaa.gov)
   P. Schlosser (peters@lamont.columbia.edu)
   (a) Gulf Stream and upper-layer circulation
   (b) DWBCs and deep recirculation
   (c) Coupling to the tropics
2. **Thermohaline overturning and flux divergences (of heat, freshwater, carbon cycle) from ocean observations, atmospheric deduction and modelling**
   Chair: H. Bryden (h.bryden@soc.soton.ac.uk)
   C. Wunsch (carl@pond.mit.edu)
   (a) Representativeness of individual sections
   (b) Combining sections with dynamics: inverse analysis problems
   (c) Atmospheric flux divergences
3. **North Atlantic decadal variability and the WOCE period**
   Chair: C. Böning (cboening@ifm.uni-kiel.de)
   G. Reverdin (reverdin@pontos.cnes.fr)
   (a) Analysed decadal variability patterns of large-scale water mass distributions and circulation, and their relation to atmospheric variability and ice import
   (b) Decadal variability mechanism in coupled/uncoupled models and comparison with observations
   (c) The situation of the WOCE period with regard to decadal North Atlantic variability
4. **North Atlantic water mass modification processes: observations and lessons/requirements for modelling**
   (a) Overflows
   Chair: P. Killworth
   (peter.d.killworth@soc.soton.ac.uk)
   R. Kaese (rkaese@ifm.uni-kiel.de)
   (b) Labrador Sea convection
   Chair: M. Visbeck
   (visbeck@lamont.ldgo.columbia.edu
   F. Schott (fschott@ifm.uni-kiel.de)
   (c) Deep mixing/role of topography
   Chair: J. McWilliams (jcm@ncar.ucar.edu)
   N. Hogg (nhogg@cliff.whoi.edu)
   (d) Thermocline ventilation
   Chair: T. Joyce (tjoyce@whoi.edu)
   D. Marshall (d.p.marshall@reading.ac.uk)
   with emphasis on discussing results from recent process studies (e.g., ONR/ACCE, Kiel SFB, VEINS/Nordic WOCE…)

Working Groups

Topics still under consideration, will include:

- Synthesis products on water masses and circulation;
- Conclusions for designing future observations.

Participation

Participants wishing to make oral contributions to session topics are asked to contact respective session chairs (above) about their proposed input. Abstracts for poster presentations which will be grouped by session topics must be submitted by 1 June to the Workshop Secretariat.

Workshop Report

It is planned to publish a Workshop Report with session summaries, abstracts and Working Group reports. Poster abstracts will be available on the web and at the start of the Workshop.

Registration

Registration forms can be obtained through
http: //www.ifm.uni-kiel.de/ro/naws/naws.html
or contact the Workshop Secretariat.

A registration fee will be raised for partial compensation of workshop costs:

Preregistration (before 30 April)	DM 120.
Registration	DM 150.

Registration fees payable by credit card to:

Dietmar Rauter Reisen GmbH
drreisen@t-online.de
Fax: 0049 - (0) 431 - 57 93 61 9

or by bank transfer payable in DM to

Dietmar Rauter Reisen GmbH
Sparkasse Kiel
Lorentzendamm 28
24103 Kiel
account no. 2003945, BLZ: 210 501 70

Local registration times:

Sunday, 22 August, 4–7pm: IfM Kiel, Lobby; Düsternbrooker Weg 20.
Monday, 23 August, 8–9 am: Art Gallery, Düsternbrooker Weg 1.

Organisation

Scientific Organising Committee: C. Böning, H. Bryden, R. Molinari, G. Reverdin, P. Schlosser, F. Schott (chair), C. Wunsch.

Local Organisation: L. Stramma (lstramma@ifm.uni-kiel.de), S. Komander, J. Kielmann, T. Müller, F. Schott.
Workshop Secretariat: K. Maass (kmaass@ifm.uni-kiel.de), Tel/Fax: 0049-431-5973821; S. Komander (skomander@ifm.uni-kiel.de).

Social events

An Icebreaker Party will be held on Monday, 23 August evening, aboard RV Alkor; a Workshop Dinner is scheduled for Wednesday evening (at DM 50).

Hotels

Blocks of rooms have been reserved (until 30 April) at various hotels. Information can be obtained from the website (see above). Participants will be expected to make their own arrangements referring to the North Atlantic Workshop to get special prices.

Limited travel and hotel cost support will be available from the WOCE IPO. Requests for support should be submitted to woceipo@soc.soton.ac.uk together with a short supporting case for attending the workshop and giving estimated costs of economy travel and number of days to be spent in Kiel. It may help if you can find partial support from other sources.

MEETING TIMETABLE 1999

February 22–26	WOCE-AIMS Tracer Workshop	Bremen, Germany
March 15–19	WCRP JSC Meeting	Kiel, Germany
April 13–15	Bottom Pressure Variability: GRACE and other satellites	London, UK
April 13–16	WOCE Data Products Committee Meeting (DPC-12)	Birkenhead, UK
April 19–23	24th General Assembly EGS	Den Haag, Netherlands
April 27–30	TOS: Extreme and Unexpected Phenomena in the Ocean	Reno, USA
May 10–11	GLOSS Workshop on Sea Level	Toulouse, France
May 10–14	CLIVAR SSG-8 Meeting	Southampton, UK
May 31–June 4	AGU Spring Meeting	Boston, USA
July 18–30	IUGG XXII General Assembly	Birmingham, UK
August 23–27	WOCE North Atlantic Workshop	Kiel, Germany
August 23–27	Second Conference on Reanalyses	Reading, UK
September 13–17	Modelling of Global Climate and Variability Conference	Hamburg, Germany
October 4–8	WOCE SSG Meeting (WOCE-26)	La Jolla, USA
October 18–22	Conference on Ocean Observations for Climate	S. Raphael, France
October 25–27	TOPEX/POSEIDON/Jason-1 SWT	S. Raphael, France

WOCE is a component of the World Climate Research Programme (WCRP), which was established by WMO and ICSU, and is carried out in association with IOC and SCOR. The scientific planning and development of WOCE is under the guidance of the Scientific Steering Group for WOCE, assisted by the WOCE International Project Office.

The International WOCE Newsletter is funded by contributions from France, Japan, UK, and WCRP, and is edited by Roberta Boscolo (roberta.boscolo@soc.soton.ac.uk) at the WOCE IPO at Southampton Oceanography Centre, Empress Dock, Southampton, SO14 3ZH, UK, Tel: 44-1703-596789, Fax: 44-1703-596204, e-mail: woceipo@soc.soton.ac.uk,
http://www.soc.soton.ac.uk/OTHERS/woceipo/ipo.html

We hope that colleagues will see this Newsletter as a means of reporting work in progress related to the Goals of WOCE as described in the Scientific Plan.

The editor will be pleased to send copies of the Newsletter to institutes and research scientists with an interest in WOCE or related research.

Printed by Technart Ltd., Southern Road, Southampton SO15 1HG.